Real-time tracking of rectal tumours during colorectal cancer surgery

Master of Science Thesis

Nathalie Versteeg

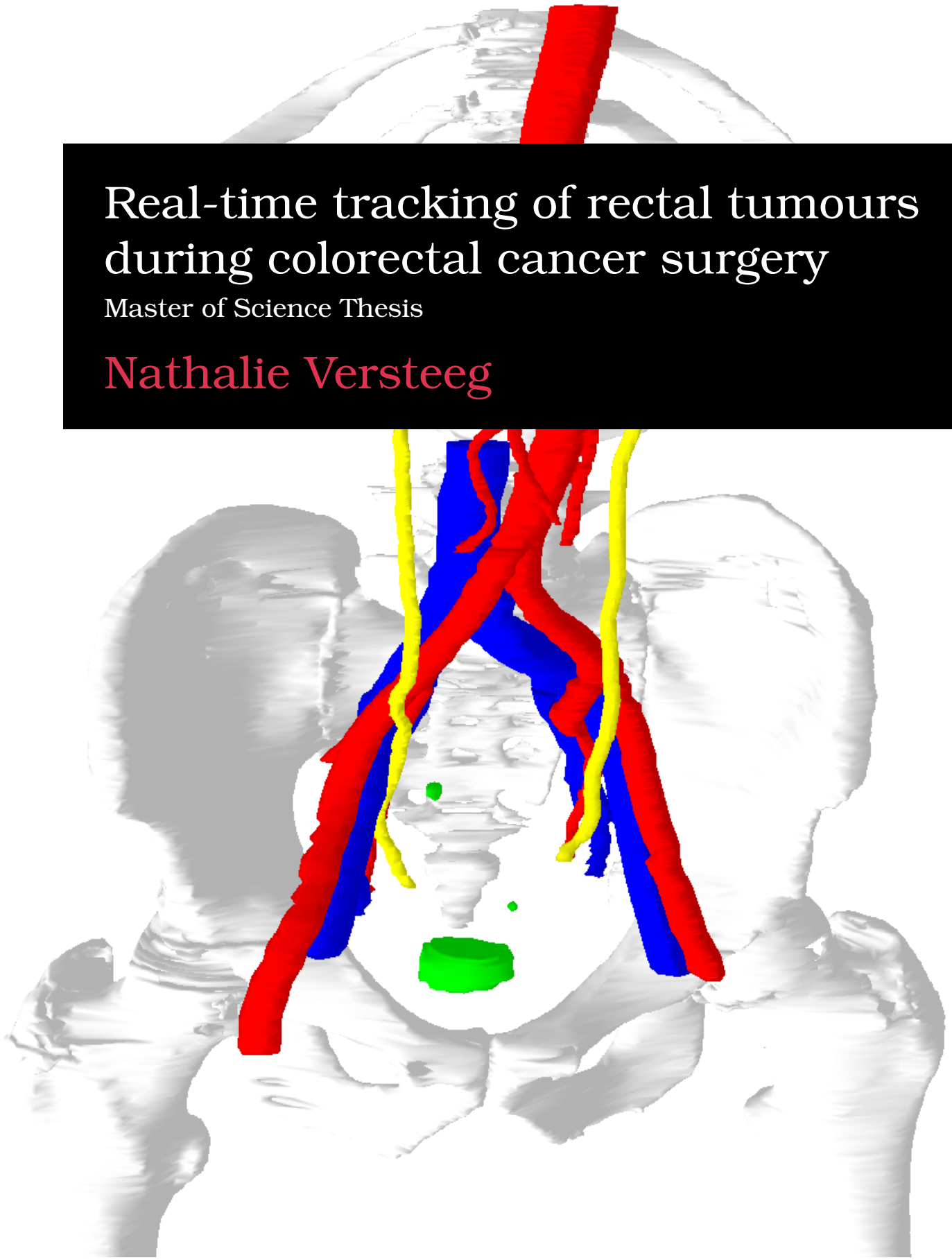

UNIVERSITY OF TWENTE.

ANTONI VAN LEEUWENHOEK
NEDERLANDS KANKER INSTITUUT

Real-time tracking of rectal tumours during colorectal cancer surgery

Master of Science Thesis

For the degree of Master of Science in Technical Medicine with the track Medical Imaging and Interventions at University of Twente

Nathalie Versteeg

January 10, 2017

Faculty of Science and Technology (TNW) · University of Twente

The work in this thesis was supported by the Netherlands Cancer Institute – Antoni van Leeuwenhoek Hospital. Their cooperation is hereby gratefully acknowledged.

UNIVERSITY OF TWENTE.

University of Twente
Department of
Technical Medicine

The undersigned hereby certify that they have read and recommend to the Faculty of Science and Technology (TNW) for acceptance a thesis entitled

Real-time tracking of rectal tumours during colorectal cancer surgery

by Nathalie Versteeg

in partial fulfillment of the requirements for the degree of

Master of Science Technical Medicine

track Medical Imaging and Interventions

Dated: January 10, 2017

Chairman: _____
prof.dr. T. Ruers (NKI-AvL)

Medical supervisor: _____
prof.dr. T. Ruers (NKI-AvL)

Technical supervisor: _____
dr.ir. F. van der Heijden (University of Twente)

Process supervisor: _____
drs. P.A. van Katwijk (University of Twente)

External committee member: _____
dr. J.J. Pouw (University of Twente)

Additional committee member: _____
dr. J. Nijkamp (NKI-AvL)

Abstract

Introduction

In 2014, over 15,000 patients were diagnosed with colorectal cancer in the Netherlands. To achieve optimal oncological outcome, surgery, alone or combined with chemo- and/or radiation therapy, is the primary choice of treatment. The clinical challenge in surgery is to find a balance between radicality of surgery and preservation of function. Imaging is an important decision making tool in the treatment plan. Pre- and intraoperative images can be used to create 3-dimensional (3D) anatomical maps delineating vital structures, tumour and malignant lymph nodes. Continuous localisation of surgical tools related to the patients anatomy visualised in a 3D map provides guidance during surgery. The aim of this study is to implement a surgical image-guided electromagnetic (EM) navigation procedure in which a moving tumour can be traced to provide the surgeons with real-time information on the tumour location and orientation.

Material and methods

The window field generator (WFG) was incorporated into the workflow and the accuracy of the WFG was evaluated. Four 6-DOF sensors, micro 0.8 * 9 mm rod, were placed parallel on a sensor-plate at 5 cm distance from each other and measured at 126 (=x*y*z=2*7*9) positions parallel to the WFG (in the x-y-plane), using stackable boxes up to a distance of 52 cm (z-axis) from the table. For each position 40 samples were acquired. In a test setting absolute errors were determined with respect to the NDI Polaris Spectra Hybrid system and in the operation room (OR) the relative distance between the individual sensors was evaluated. The jitter, defined as the standard deviation (SD) over 40 measurements and the root-mean-square error (RMSE) were determined. A sensor implantation and fixation method was designed. A chain test was designed to test the entire workflow and an in-vivo study was implemented. The main study parameter was to evaluate feasibility of the navigation system during real-time tumour tracking in rectal surgery. Accuracy during surgery was validated with anatomical

landmarks. To verify the tumour matching process, the tumour of the included patients was matched by 4 different observers to determine the reproducibility of the registration.

Results and discussion

The WFG was successfully incorporated into the navigation setup by placing it on the table in a custom made matrass that was designed. The vector jitter was approximately 0.02 cm within 45 cm from the WFG in both settings, this is sufficient. In test setting the position vector RMSE increased up to 1.10. cm at 45 cm distance from the WFG. In the OR setup the difference in distance between sensor 1 and 4 measured by the WFG is between 14.8-15.6 cm up to 35 cm from the WFG. De accuracy decreased further from the field generator (z-axis) and when the sensors were further apart, the measurement error increased. Sensor implantation and fixation was done by using entering the anus with a proctoscope and using the tissue glue PeriAcryl90. Implantation was successful in ex-vivo testing and in one of three patients that was operated on. Sensor fixation needs further development. Image registration shows a large inter-observer variability, making the registration method not yet accurate enough for clinical use.

Conclusions

The workflow seems feasible in terms of extra time needed. The navigation system in the current setup is not accurate enough for clinical use. The field generator itself is not accurate enough and the current sensor implantation method does not deliver interpretable data. Further, the image registration method is not yet accurate enough for clinical use. The use of wireless sensors should be evaluated, since this would solve many problems.

Contents

List of Figures

List of Tables

Acknowledgements

This thesis report is the result of my MSc graduation internship for Technical Medicine at the university of Twente started January 2016 at the Netherlands cancer institute - Antoni van Leeuwenhoek hospital. The past year I have faced the challenges of implementing a patient study protocol and all the research necessary for a successful implementation.

I would like to thank my supervisors for all their help and guidance. First of all, I would like to thank Jasper for his daily supervising. Thanks for the feedback and discussions during the weekly meetings to keep me focused. Thanks for all the moments you made time to help me in between and of course thanks for the much needed coffee. Theo, always wanting to go one slide back. Thanks for the enthusiasm and keeping a clinical eye on the subject. Ferdi, thanks for monitoring my progress during our meetings and thanks for always making time for feedback on my writing. Paul, you have a way of immediately putting your finger on the sore point. Thanks for also giving the handle to deal with it and for the mental support during our group meetings.

Further I would like to thanks Annemijn, Eliane and Michelle for all the group meetings. Not only for being a wonderful support, but also for all the fun and laughter! Last, but certainly not least, I would like to thank my family, and especially my boyfriend Jelmar, for all the support. Jelmar, thanks for all the lovely food you cooked for me when I was stressed, for always finding a way to cheer me up and for all the faith in me!

Utrecht
January 10, 2017

Nathalie Versteeg

Chapter 1

Introduction

In 2014, over 15,000 patients were diagnosed with colorectal cancer in the Netherlands. To achieve optimal oncological outcome, surgery, alone or combined with chemo- and/or radiation therapy, is the primary choice of treatment. The clinical challenge in surgery is to find a balance between radicality of surgery and preservation of function. Imaging is an important decision making tool in the treatment plan. However, the available images are not optimally utilized during surgery. If they can be used for intraoperative guidance, the value of these images is greatly increased.

The goal of this chapter is to provide clinical and technical background information about colorectal cancer and surgical navigation. Section 1-1-1 provides clinical aspects of colorectal cancer and Section 1-1-2 goes into more detail about treatment, surgical approach and clinical challenges in rectal cancer. Section 1-2-1 provides information about surgical navigation, next previous research and technical challenges are covered in Section 1-2-2 and Section 1-2-3 respectively. In Section 1-3 the goal of the study defined and the objectives are determined and Section 1-4 provides the outline of this thesis.

1-1 Clinical background

1-1-1 Colorectal cancer

Epidemiology

Colorectal carcinoma (CRC)[1] is the second most common cancer in females and the third most common cancer in males worldwide, [1]. In 2012 the number of CRC deaths for both sexes was 693,933, based on data from GLOBOCAN 2012 from the International Agency for Research on Cancer (IARC). Population forecasts for 2020 are that there will be 853,550 deaths, this is 159,617 more than in 2012, [2]. The incidence of CRC increases strongly with

[1] All acronyms can be found in the glossary.

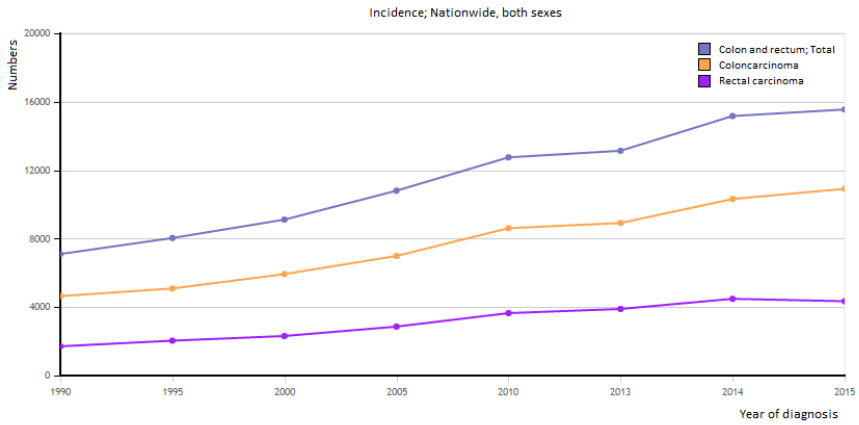

(a)

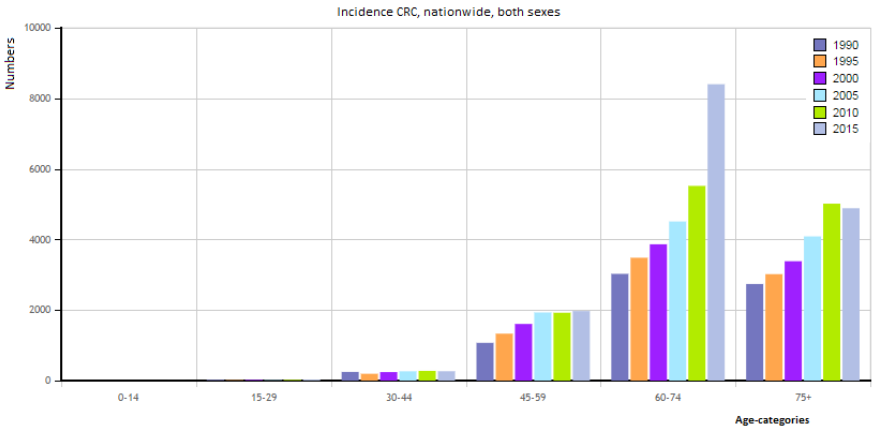

(b)

Figure 1-1: Incidence of colorectal carcinoma in the Netherlands for both sexes is seen in the upper image (a), and the incidence of colorectal carcinoma in the Netherlands for both sexes divided in 15-year age categories is seen in the lower image (b), adopted from [3].

age and, in this aging society, incidence in the Netherlands has more than doubled since 1990 (see Figure 1-1), [3]. In 2014, over 15,000 patients werediagnosed in the Netherlands. Annually, CRC causes over 4,000 deaths, [4].

Early stage CRC has a good prognosis opposed to advanced stages of CRC. When the cancer is limited to the mucosa (stage 0) the 5-year survival rate is over 95% of patients. With increasing involvement of deeper layers prognosis decreases. When the tumour cells have penetrated the submucosa (stage 1) or the muscle layer or serosa is also involved (stage 2) the 5-year survival is 90% and 55-85% respectively. Nodular involvement (stage 3) gives 20-55% survival after 5 years and this decreased to less than 1% for distant metastatic disease (stage 4), [5], [6].

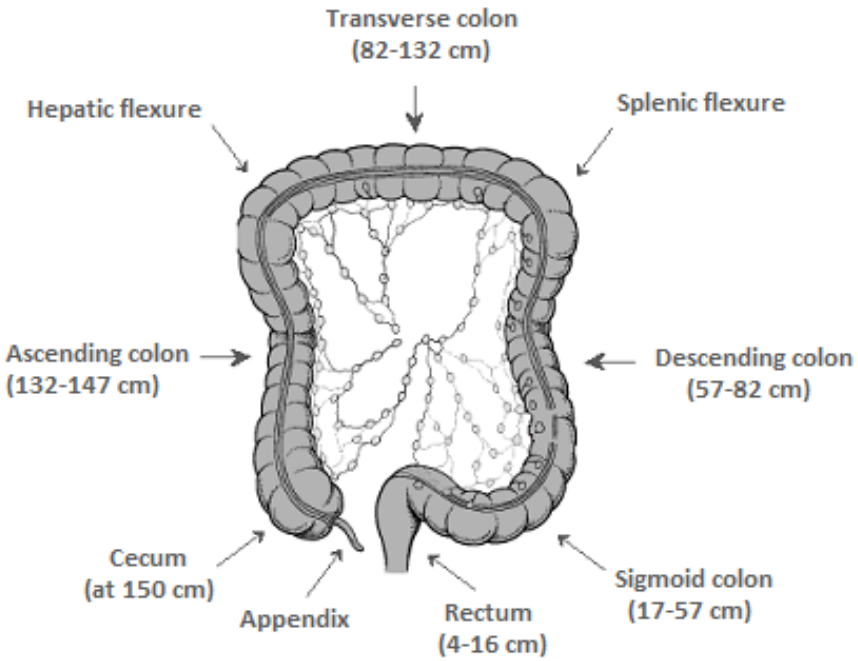

Figure 1-2: Parts of the colon and rectum and distance from the anal verge, edited from [6].

Anatomy of the Colon and Rectum

The entire large intestine is about 150 cm long and consists of the cecum, appendix, colon, rectum and anal canal (Figure 1-2). The large intestine is characterized by omental appendices, tenia coli, and haustra, these are sacculations of the colon wall between the tenia coli, [7], [8].

The wall is build up in different layers displayed schematically in Figure 1-3. The interior surface of the lumen is a mucosal layer, with a surface epithelium, a lamina propria and muscularis mucosae. The next layer is submucosa, containing mucosal glands, vessel and nerves of the submucosal plexus (Meissner's plexus). Next, a layer of muscularis propria is formed by circular muscle cells and longitudinal muscle cells, the latter in three bands called taeniae coli. The myenteric plexus (plexus of Auerbach) between both muscularis propria layers provides motor innervation. The next layer is either serosa, for intraperitoneal regions and adventitia for retroperitoneal regions, [7], [8].

The peritoneum is a serous membrane covering the abdominal cavity and most of the abdominal organs. Retroperitoneal parts, are attached to the surrounding structures with connective tissue, making them rather rigid. Intraperitoneal regions are only covered in a layer of peritoneum and are more mobile, [7], [8].

The colon consists of four parts, namely the ascending-, transverse-, descending- and sigmoid colon. The ascending colon lies retroperitoneal on the right side of the bowel, the transverse colon lies intraperitoneal and crosses from right to left between the hepatic flexure to the splenic flexure, the descending colon, also retroperitoneal, lies on the left side starting from

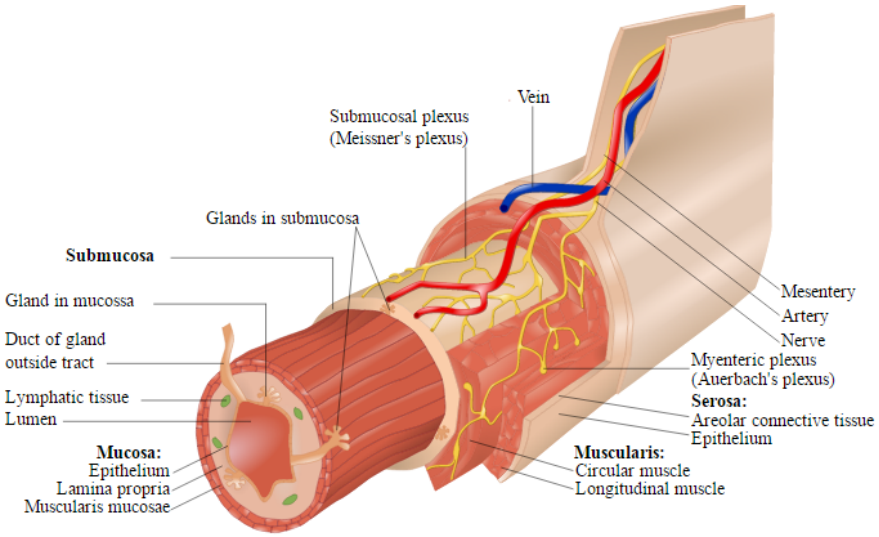

Figure 1-3: Layers of the wall of the large intestine, adopted from [9].

the splenic flexure. The s-shaped sigmoid colon lies intraperitoneal and links the descending colon and the rectum. The rectosigmoid junction, the transition between sigmoid and rectum, is recognized by the union of tenia coli into one continuous layer of smooth muscle. The terminal part of the intestine, the rectum, lies almost entirely in the pelvis following the curve of the sacrum and coccyx. The upper third of the rectum lies in the peritoneum, while the remainder lies beneath the peritoneal reflection, the lower lining of the peritoneum, outside the peritoneal cavity. When the rectum penetrates the levator ani, the pelvic diaphragm, it ends and becomes the anal canal, [7], [8].

Pathophysiology and pathogenesis

Most colorectal carcinomas originate from adenomatous polyps arising from the colorectal mucosal epithelium. Adenomatous polyps are premalignant lesions and eventually develop into carcinomatous tissue over the course of years or even decades. About 90-95% of all tumours in the large intestine are adenocarcinomas, [6], [8], [10], [11]. The stages of CRC carcinogenesis are shown in Figure 1-4.

Most CRCs are not hereditary and develop after multiple mutations changing the normal mucosa to invasive cancer. In 85% of cases it takes at least 8-10 mutations in several growth regulating genes before invasive cancer develops. Deactivation of the adenomatous polyposis coli (APC) gene is described as the 'gatekeeper' gene. It occurs in the early development of an adenoma and is usually followed by multiple other mutations that facilitate adenoma growth (K-ras) and the adenoma-carcinoma transition (DCC and p53), [10], [11].

Age is the most important risk factor for CRC development. Before the age of 40 the risk is low, only about 3%, but the risk gradually increases towards the age of 50 after which it doubles each decade. Next to age, family history is the most common risk factor for CRC, though only 5% of CRCs are hereditary. Other risk factors are prior CRC, inflammatory diseases such as colitis ulcerosa and Crohn's disease, genetic factors and dietary factors.

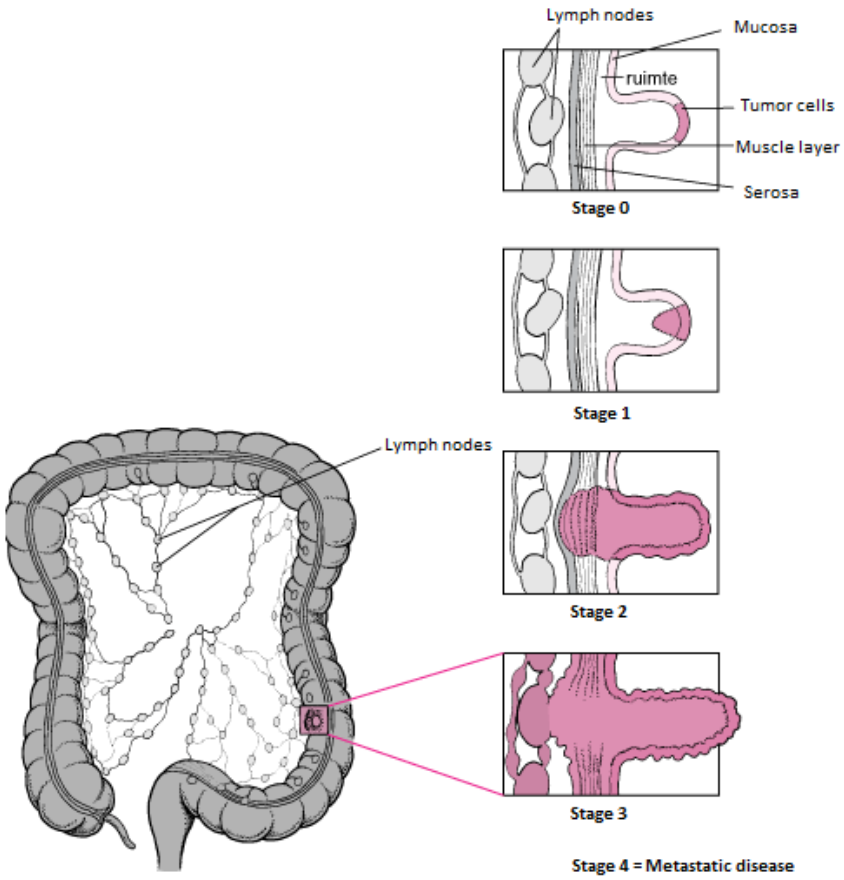

Figure 1-4: Stages of colorectal cancer, edited from 6. In stage 0 the tumour cells are limited to the mucosa. When the tumour cells have penetrated the submucosa the cancer is in stage 1. If serosa or muscle is involved the cancer is in stage 2. In stage 3 loco regional lymph nodes are involved and in stage 4 the cancer developed distant metastases.

A diet high on fat, especially animal fat, is linked to the formation of polyps, a precursor of cancer. Carcinogens formed by bacteria in the bowel during fat metabolism can irritate the bowel and polyps could form in response to this irritation. Fibres reduce the exposure of the bowel to carcinogens by speeding up the passing of fat through the bowel or diluting the concentration of fats. The importance of dietary factors is clearly visible in more evolved countries. In western countries the incidence is about three times higher than in less developed countries. Western diets often lack fibres and are high in fat, both implicated for higher risk of colorectal diseases, [2], [8], [10], [11].

Diagnosis and screening

In early development CRC is often asymptomatic. Alarming symptoms are unexplained persistent diarrhoea, difficulty passing faeces or faecal incontinence, narrow or ribbon shaped stool, weight loss and blood or mucous in the faeces. With an increasing tumour bulk, faecal blood loss is a common sign of CRC. Proximal tumours often present themselves with occult blood loss, while both occult and bright blood loss occurs in distal tumours, [8], [10], [11].

The golden standard for diagnosis of CRC is a colonoscopy, since this allows biopsies and polypectomies for histological examination of the tissue. However, faecal occult blood tests have been widely introduced in screening programs for detection of early stage CRC and when positive this predicts a 50% chance of adenoma or carcinoma, [10], [11]. Several studies in European populations show that CRC mortality rates have dropped 14-18% with the introduction of CRC cancer screening. In screening programs colonoscopy is performed when the faecal occult blood test is positive. For high risk patients, those with inherited syndromes, endoscopic screening is the examination of choice, [10], [11], [12], [13].

In 2014, colorectal cancer screening in the form of a biannual faecal occult blood test (FOBT), followed by a colonoscopy when the FOBT is positive, was introduced in the Netherlands. Screening is aimed at early detection of CRC for all persons between 55 and 75 years old. Almost 2,500 out of the 15,000 new cases were discovered through the screening program, [4]. In 30% of the new cases it concerns rectal carcinoma, [3]. A tumour located in the rectum is a challenging field due to the difficult to reach location deep in the pelvis.

1-1-2 Rectal cancer

Of the approximately 15,000 new cases of CRC in the Netherlands, in nearly 5,000 cases it concerns rectal carcinoma. The 5-year overall survival rate of patients diagnosed in the Netherlands between 2008 and 2012 is 65%, [3].

Rectal cancer differs from colon cancer in embryological origin, anatomy and physiology. The proximal part of the colon, up to the splenic flexure, has the embryological origin from the midgut. The distal colon and rectum originate from the hindgut. A mesentery hangs the primitive gut dorsally, extending as the mesentery to the small bowel and proximal colon for the midgut and as the mesorectum for the hindgut.

The blood supply and drainage for the 3 gut-segments are separate, though there are some anastomoses present. The rectum is supplied from the inferior mesenteric artery, venous drainage is to the inferior mesenteric vein. The portal system ensures venous drainage from

the large intestines, therefore the liver is the primary site of metastatic disease for colonic cancer. The rectal artery drains directly into the inferior vena cava, thus for distal rectal tumours the lungs are the initial site of metastatic disease. Hence, treatment for colon and rectal cancer is different, [14], [15], [16].

Treatment

To achieve optimal oncological outcome, surgery, alone or combined with radiation- and/or chemotherapy, is the primary choice of treatment for rectal cancer, [10], [11], [14], [17], [18]. Due to the position in the pelvis and the relation to vital structures, rectal cancer surgery is challenging,[14], [15], [16]. Several research groups showed a decreased percentage of local recurrence, from 25% down to 5-9%, with the introduction of total mesorectal excision (TME) for rectal cancer, [19], [20], [21]. The TME procedure envelopes the entire mesorectum, leaving the visceral lining of the mesorectum intact, while preserving the hypogastric plexus, [18], [22].

TME has become the standard surgical procedure in many countries. Besides the introduction of TME, (neo)adjuvant radiation- and/or chemotherapy has improved local recurrence as well. The Dutch colorectal cancer group shows a reduction in 5-year local recurrence risk from 10.9% in patients with TME alone and 5.6% in TME preceded by radiotherapy, [18]. The radiation procedure depends on the size and extent of the tumour and involved lymph nodes. If the size and extent is limited, a short scheme of radiation is adequate. A dose of 25 Gray is administered during 5 days in portions of 5 Gray per day. If the tumour is extensive, a long scheme of radiation therapy is given supplemented with chemotherapy. Over the course of 5 weeks patients receive 25 times 2 Gray, in combination with a daily intake of oral chemotherapeutics, [23].

Principles of surgical approach

Total mesorectal excision is the gold standard to achieve a curative resection. The TME procedure can be done with a sphincter sparing procedure, e.g. (very) low anterior resection (LAR), or by abdominoperineal resection (APR). In the LAR procedure an anastomosis is made resulting in the preservation of sphincter function, meaning the preservation of intestinal continuity since no permanent colostomy is needed. Sometimes a temporary colostomy or ileostomy is placed to prevent anastomotic leakage. The main principle of TME is sharp dissection between the visceral and parietal fascia. Removing the mesorectum, including lateral and circumferential (radial) margins. The terminal branches of the inferior mesenteric artery and draining loco regional lymphatics should also be removed, [17].

A sphincter sparing procedure is only possible when a negative distal resection margin can be achieved. For most rectal tumours the acceptable negative distal margin is 2 cm. The proximal margin should be at least 5 cm. The circumferential margin is important to decrease mesorectal spread. About 3 to 5 cm around the primary tumour should be excised. More proximal tumours should have a distal margin of about 5 cm to decrease chance of anastomosis leakage, [17].

1-1-3 Clinical challenges

Although the outcome of surgery greatly improved with the introduction of TME with or without radiation- and/or chemotherapy, local recurrence and mortality still pose major problems in management of rectal cancer, [24]. Nagtegaal and Quirke show that circumferential resection margin (CRM) is a strong predictive factor of local recurrence, [24]. In 2014, 5.2% of patients with a resection of a primary rectal carcinoma still had positive resection margins in the Netherlands, [25].

Several factors are of influence in CRM positivity. Tumour related factors are Tumour-Node-Metastasis (TNM) stage, size of the tumour, degree of stenosis, ulcerative growth and histological factors such as infiltrating margins, poor differentiation and vascular invasion. The surgical technique also has a substantial effect on radicality of the excision and prognosis of the patient. Nagtegaal and Quirke show that there is a direct relation between the quality of surgery and positivity of the CRM, [24]. Also the location of the tumour is vital. More distal tumours show higher rates of CRM positivity, due to the difference in surgical technique and local anatomy in very distal tumours. Besides, the normal anatomy may be disturbed due to radiation effects or fibrosis, also making it more challenging to attain negative resection margins, [24].

In the attempt to attain negative margins, functional structures may be damaged. This can lead to faecal incontinence in LAR or even in urinary incontinence. Preservation of function is very important for the quality of live for the patient after surgery, [26]. Finding a balance between radicality of surgery and preservation of function is very challenging. Rectal cancer surgery is associated with up to 43% overall postoperative morbidity, [17], [27].

There is much to be gained with the improvement of surgery. Imaging provides a surgeon with much wanted information about the anatomy of the patient. However, this imaging is not being used to its maximum potential. Nowadays the surgeon uses his knowledge of the patients anatomy, based on available imaging, to determine the surgical strategy. However, these images are barely used during surgery. Better intra-operative guidance by using the available imaging during surgery could improve the surgical results.

1-2 Technical background

1-2-1 Surgical navigation

Imaging is an important decision making tool in the treatment plan. Though a decision for resection of the tumour is based on imaging, the available images are not optimally utilized during surgery. If they can be used for intraoperative guidance, the value of these images would greatly increase. Intraoperative guidance could be used for assessment of resection planes and to avoid vital structures such as vessels, ureters and nerves, [28], [29]. To integrate the preoperative images into the surgical procedure, image guided navigation systems can be used. Pre- and intraoperative images can be used to create 3-dimensional (3D) anatomical maps delineating vital structures, tumour and malignant lymph nodes. Continuous localisation of surgical tools related to the patients anatomy visualised in a 3D map provides guidance during surgery.

Surgical navigation is widely researched in many surgical fields. Initially, neurosurgery was the main playing field of surgical navigation. Navigation in neurosurgery originated from frame-based stereotactic procedures (Greek; 'stereo' = 3-dimensional and 'taxis' = to move toward) developed at the beginning of the previous century. However it was not before the invention of intracranial imaging, several decades ago, that neurosurgeons started performing stereotactic surgery to navigate towards targets in the brain based on the individual patient's image data, [30], [31]. A wide range of navigation procedures is integrated successfully into the clinical routine of neurosurgery. It is used for biopsies, to place pedicle screws and stabilize the spine and for intracranial tumour resections. The navigation helps to visualize the tumour borders and minimize the skull opening (craniotomy), decreasing operation time and the risk of postoperative complications, [32]. Navigation is also used in orthopaedic surgery or for resection of bone tumours. It can be used in joint replacement, as a precise measurement tool to accurately place and align the implant to restore function, or for determination of sacral screw position to reduce malposition rate and radiation exposure, [32], [33], [34].

Surgical tracking systems

There are two main surgical tracking options, optical- and electromagnetic tracking. Optical tracking is based on a set of cameras, with a known spatial relation to each other, that are able to detect infrared-reflecting spheres attached to a patient or instrument. If at least 3 reflective markers are placed on a rigid frame with known geometry, such as a surgical instrument, the orientation of the instrument can be determined. Optical tracking devices have a sub-millimetre accuracy, but the key limitation is that they require a direct line-of-sight to be able to detect the sensors. In most part of pelvic surgery a direct line-of-sight cannot be realised, limiting the possibilities of optical tracking, [35], [36].

Electromagnetic (EM) tracking is based on an electromagnetic field generator that can detect the position and orientation of EM sensitive sensors in the EM field. The magnetic field induces a current in the sensors and they can be localised with 1-2 millimetre accuracy, [36]. Since the EM tracking is based on magnetic induction, a direct-line of sight is not necessary, making it more accessible for pelvic surgery, [35], [36], [37].

A challenge in EM tracking is the influence of ferromagnetic materials that are present during surgery, these can influence the stability of the magnetic field. The ferromagnetic materials are magnetised in the presence of an EM field, causing distortions of the field and thereby affect the accuracy, [36], [38], [39].

Principles of electromagnetic tracking

EM tracking uses a magnetic field of known geometry to determine the position and orientation of sensors located within this magnetic field, [36], [39]. These sensors can be incorporated in a medical device to track the device during surgery. To determine the position of these devices relative to the patient, sensor patches can be taped on the patients skin within the range of the field generator.

A magnetic field is generated by moving electric charges in a magnetic material. When all the electrons in a metal object are given the same spin, the same intrinsic magnetic moment, a magnetic field is created. Electromagnetic tracking systems (EMTSs) are based

on a magnetic field produced by a current flowing through a wire. The wires can have different shapes producing different magnetic fields. The EMTS contains transmitting and receiving coils, helical structured wires, to create the magnetic field. The field can be strengthened by adding a metal core inside the coil.

There are three categories of EMTSs available. EMTSs have a constant orientation of the current, i.e. the current flows in one direction. A sequence of direct current (DC) pulses is emitted, comparable to turning the transmitter on and off. In EMTSs driven by alternating current (AC) the flow is continuous and the magnetic field varies in direction and intensity. Frequency ranges between 8-14 kHz. Last, passive or transponder systems track by localising implanted transponders or a permanent magnet, [39], [40].

The main difference between AC and DC systems is their interaction with metallic materials. In AC systems eddy currents are induced in conductive materials that are brought into the magnetic field, interfering with the magnetic field. The advantage of a DC system is that it is not as much affected by conductive materials. Since DC systems are not continuous, the eddy currents can decay in between the pulses reducing the distortion, [39].

1-2-2 Previous research

In 2013 an observational pilot study was started to gain experience with an in-house developed navigation setup for image guided navigation, the Navigation 1 study (N13NAV).

25 patients underwent navigation guided surgery based on EM tracking. All patients underwent a contrast-enhanced computed tomography (CT) scan prior to surgery. Electromagnetic marker patches were placed on bony parts of the pelvis before the CT scan was made and the location of the patches was marked. The contrast CT scan is used to reconstruct the vital structures in a 3D image. If magnetic resonance images (MRIs) are also available, these can contribute to a more accurate 3D reconstruction of the tumour tissue. The mesorectal plane mostly contains soft tissue including the tumour and this is best imaged using magnetic resonance, [28]. In the operating room operating room (OR) the patient is placed on a mattress with an incorporated field generator. The marker patches were placed on the marked area and used to match the navigation system to the preoperative images. The 3D reconstructions are loaded into the navigation software and the procedure is started.

In 2015 an intra-operative cone-beam CT (CBCT) imaging system was installed (Philips Allura FD20) in our hybrid OR. The image made with this system are referred to as XperCT images. The introduction of the hybrid OR led to a change in the protocol, in which marker patch locations are now derived from intra-operative imaging, instead of from the CT scan acquired a day in advance. With intra-operative imaging, accuracy of the navigation system increased with a factor 10. Thus with the introduction of the hybrid OR all marker patches are placed in the OR. The patient is in the right position for operation when the scan is made, reducing the risk at sensor displacement and increasing the accuracy.

All participating surgeons (n=12) were positive about navigation guided surgery. They indicate that their orientation during surgery has greatly improved. They can quickly locate lymph nodes and they improved the assessment of tumour borders in cases with complex anatomy surrounding advanced tumours and recurrences. The pilot study was very successful and expanded to 75 patients.

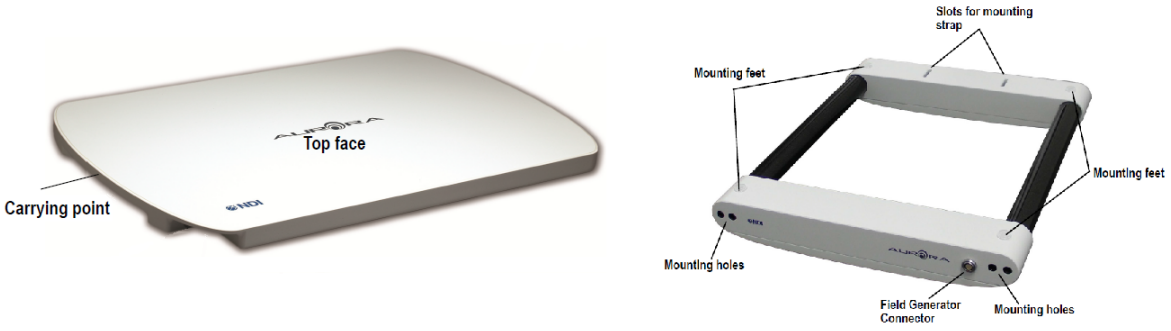

Figure 1-5: Table top field generator of the left and the window field generator on the right, adopted from [41].

The developed navigation system assumes that the anatomy of the patient is not changing between pre-operative imaging (when the 3D map is made) and actual surgery. Therefore, the N13NAV study is only applicable for tumours and lymph nodes which were deemed rigid. For example, locally advanced tumours attached to the sacrum or local recurrences and lymph node metastasis along the iliac vessels.

1-2-3 Technical challenges

The abdomen is a more challenging field for surgical navigation. Organs within the peritoneal cavity do not have a fixed position and move due to breathing, peristalsis or deformation of the organs during surgery. Organs deep in the pelvis are also a challenge for surgery. Most rectal tumours do not have a fixed position. This makes it difficult to maintain an accurate anatomical representation during the procedure, [28]. To realise real-time surgical navigation of moving targets a novel surgical tracking and navigation setup needs to be developed.

The needs for tracking of mobile tumours during surgery are to have a sensor in or near the tumour and to know where the sensor is with respect to the tumour in the 3D model. To derive the sensor position with respect to the tumour in the 3D model, the intra-operative image needs to be of sufficient quality to register the tumour itself.

In previous studies, a table top field generator (TTFG) was used (Figure 1-5) for sensor tracking. The TTFG has the advantage that it can be placed below the patient, and there is shielding such that metals and electronics in the table do not influence the accuracy. The TTFG is accurate in the order of 1 mm within a clinical environment, [37], [42]. However, the coils in the field generator distort the intraoperative image quality, introducing streak-artefacts, and noisy images.

Recently, a new field generator was developed by Northern Digital Inc. (NDI) (Waterloo, Ontario, Canada) to circumvent this problem. The window field generator (WFG) has an imaging window in the middle and the EM coils placed on the sides of the field generator, supported by carbon sidebars (Figure 1-5). According to NDI, the WFG has an accuracy of 0.5 mm and 0.3° for sensors with 6 degrees of freedom (DOF). These values are based on measurements in an ideal environment and is comparable to the TTFG (0.8 mm and 0.7°), [41]. However, the WFG is less protected to surrounding influences, which might hamper the

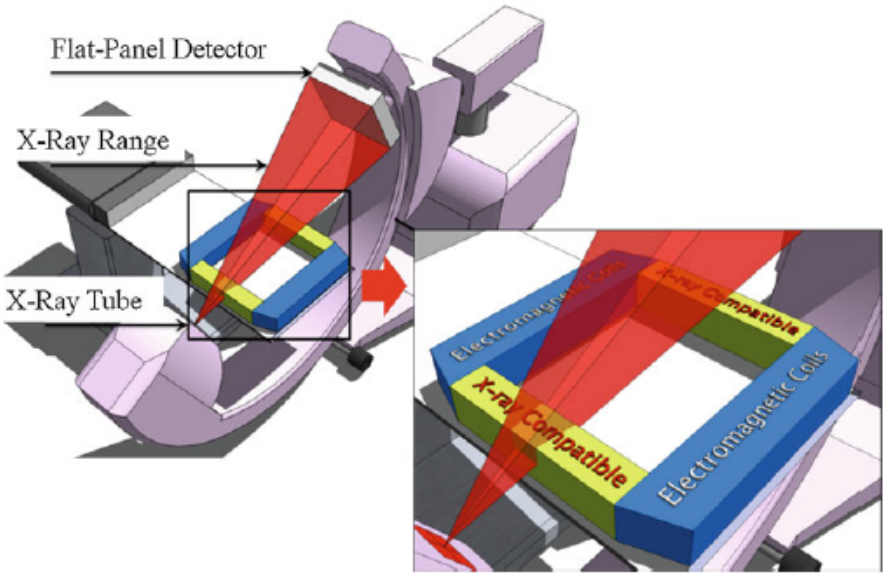

Figure 1-6: Schematic of WFG and intraoperative CT scanner, adopted from [44].

accuracy in the OR. Imaging quality with the WFG should improve in comparison to the TTFG since the coils are not in the imaging field. A schematic is shown in Figure 1-6, [43].

1-3 Objectives

The clinical challenge in rectal cancer surgery is to find a balance between radicality of surgery and preservation of function. Better intra-operative guidance by using the available imaging during surgery could improve the surgical results.

The technical challenge is that rectal tumours are not rigid, thus the navigation setup used for rigid navigation is not sufficient.

The aim of this study is to implement a surgical image-guided EM navigation procedure in which a moving tumour can be traced to provide the surgeons with real-time information on the tumour location and orientation. In order to achieve real-time tracking of a moving target, a traceable sensor is attached on or near the tumour. There are wired sensors readily available, approved for in-vivo use.

Several steps have to be taken towards realising the implementation of the navigation procedure. A patient study needs to be designed and approved by the medical ethics committee. A method for sensor placement needs to be developed. With the introduction of intraoperative imaging and the implementation of placing the sensor the current navigation setup and workflow need to be evaluated.

1-3-1 Primary objective

In-vivo study: The aim is to evaluate the feasibility of an in-house developed electromagnetic navigation system with real-time tumour tracking in rectal cancer surgery. Feasibility in the

study protocol is defined as the successful completion of the whole investigational workflow resulting in continuous delivery of interpretable navigation data for rectal surgery. Evaluation of the accuracy of the system and handling during surgery will be evaluated.

1-3-2 Secondary objectives

Before implementation of the study several steps have to be taken.

Navigation setup and workflow: A sub-goal is to evaluate the current workflow and setup of the navigation procedure, and if needed adaptation are done to the workflow and setup.

Accuracy of the EM field generator: A sub-goal is to verify the accuracy of the window field generator in test and OR setting.

Implantation and fixation method design: The third sub-goals is to design a placement and fixation protocol for implantation of the sensor to the tumour or surrounding tissue to be able to track the tumour real-time.

Image registration accuracy: After placing the sensor in the tumour, intra-operative imaging is used to link the 3D tumour model to the actual tumour location. To link the data, a registration between the intra-operative and the pre-operative CT scans is acquired. The fourth sub-goals is to verify this registration.

1-4 Outline thesis

In Chapter 2 the materials and methods are elaborated on. The navigation setup, the hardware and software and the workflow are explained. Section 2-3 to Section 2-7 are the methods towards obtaining the primary and secondary objectives of this research. In Chapter 3, the results of the topics in methods Section 2-3 to Section 2-7 are stated. In Chapter 4 the primary and secondary objectives are discussed. The discussion is build up differently than Chapter 2 and Chapter 3. All results are intertwined to be able to discuss the objectives and the structure is based upon the main goal and sub goals. Chapter 5 shows the conclusions that are drawn from the results and lists several recommendations for future research.

Chapter 2

Material and methods

The goal of this chapter is to show the materials and methods needed to reach the primary and secondary objectives. First the navigation software and hardware are elaborated on. To reach the first sub goal the workflow is evaluated and the updated. The workflow for the new navigation procedure is listed in Section 2-2. and the requirements for the incorporation of the field generator into the setup is shown in Section 2-3. To attain the second sub goal, Section 2-4 describes how the accuracy of the field generator is tested. For the third sub goal, the sensor implantation and fixation method design is shown in Section 2-5. A chain test design to evaluate the whole workflow is shown in Section 2-6. Finally the in-vivo study design is shown in Section 2-7. The fourth sub goal is elaborated on in this section.

2-1 Navigation setup

The navigation system used for this research is a combination of components from the Aurora Electromagnetic Measurement System from Northern Digital Inc. (NDI) (Waterloo, Ontario, Canada) together with in-house developed navigation and visualisation software.

2-1-1 Hardware

The navigation setup consists of several hardware components. The electromagnetic window field generator (WFG) (see Figure 1-5), the blunt tip trackable probe, reference marker patches and a wired tumour sensor for in-vivo tumour tracking (Figure 2-1), the sensor interface unit (SIU), system control unit (SCU) and a computer that processes the input and visualizes the navigation. Figure 2-2 shows an overview of the navigation hardware and interconnections. The WFG has a cylindrical work field with a radius of 25 cm from the origin of the field generator and a height of 60 cm (z-direction). The measurement offset is 4.1 cm from the top of the WFG (Figure 2-3).

The Electromagnetic (EM) field will generate a current in small EM sensors located within the EM field that can be measured through a sensor interface. To determine the exact position

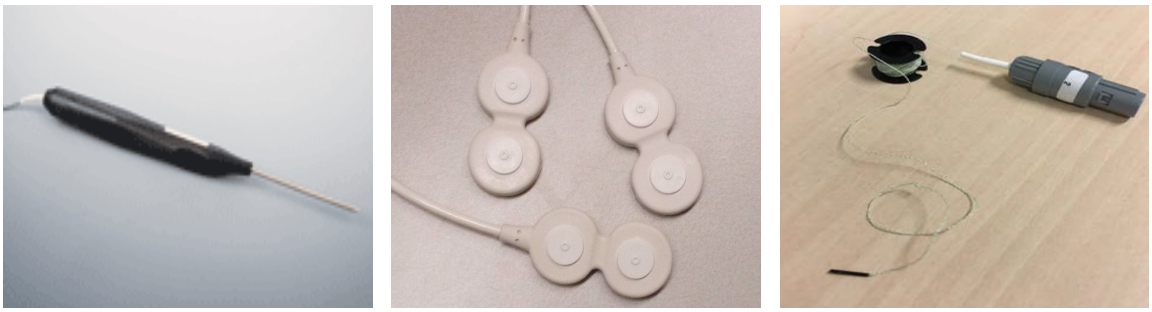

(a) (b) (c)

Figure 2-1: Hardware components used in surgical navigation. Left (a) is the Aurora standard straight tip 6DOF probe, the middle image (b) shows the reference sensor patches (2x5DOF per patch) and right (c) is the in-vivo tumour tracking sensor (6DOF).

and orientation of the sensor within the EM field, 6 degrees of freedom should be known. The 6 degrees of freedom are three positional values (x-, y- and z-coordinates) and three rotational values (for instance, orientation around the x-, y- and z-axis, respectively pitch, yaw and roll). The tumour tracking sensor is a 6DOF measuring sensor containing 2 coils at a known angle from each other, the sensor patches contain two 5DOF sensors under a fixed angle from each other creating 6 degrees of freedom as well. The EM sensors are typically 1 mm in diameter and 8-10 mm long. Sensors can easily be embedded in surgical tools, such as a blunt tip probe, a laparoscopic camera, or a surgical knife, [37], [42].

The SCU provides power to the field generator, so it is able to produce a series of varying magnetic fields. This creates a known volume of varying magnetic flux. Whenever sensors, connected to the SIU, are placed within the measurement volume of the field generator a voltage is induced within the sensor. The characteristics of the voltage induced in the sensors are dependent on the position and orientation of the sensor and on the strength and phase of the varying magnetic fields. The SIU converts the analogue signals coming from the sensors to digital signals. The SCU collects the digital sensor data and can communicate these with the host computer [41].

2-1-2 Software

The navigation software consists of 2 different executables *SurgicalNavigation.exe* and *Plusserver.exe*. The latter is part of an open source initiative and is the standard for communication in image guided surgery, [45]. *Plusserver.exe* is used to communicate with the Aurora Electromagnetic tracking system (EMTS). The *SurgicalNavigation* executable is developed in-house in Embarcadero Delphi XE8 and uses dynamic link libraries (DLL) developed in C++. The program is able to read and visualise Digital Imaging and Communications in Medicine (DICOM) data from the Picture Archiving and Communication System (PACS) and execute affine registrations between scans. Through communication with the *Plusserver* executable and with an opensource DLL, OpenIGTLink, *SurgicalNavigation* can receive tracking information from the Aurora system, as well as from other tracking systems. The tracking information can be linked to the imaging that is loaded from PACS.

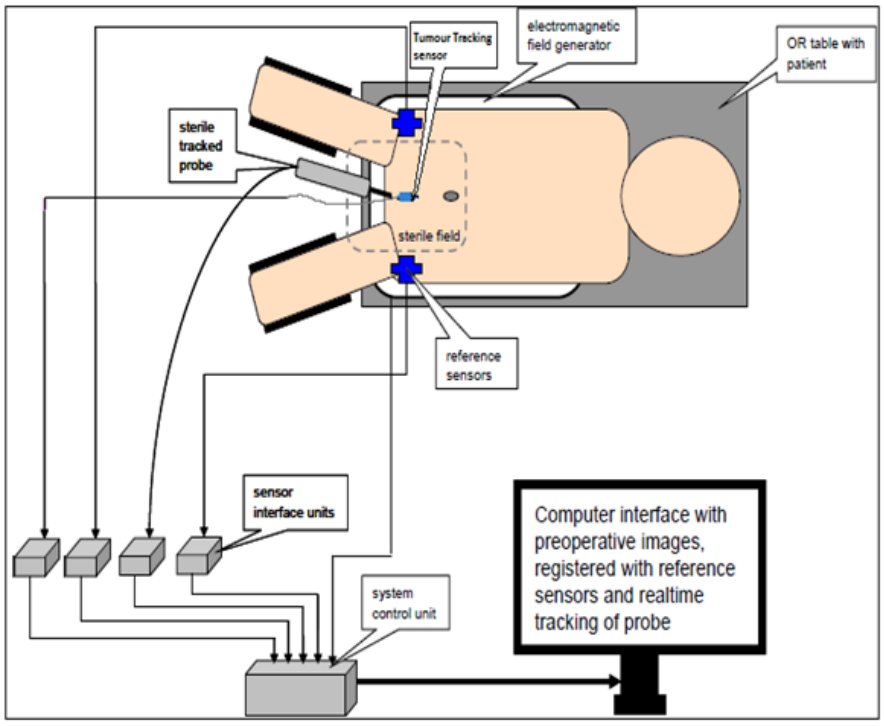

Figure 2-2: Overview of the navigation hardware components and the interconnections between the components.

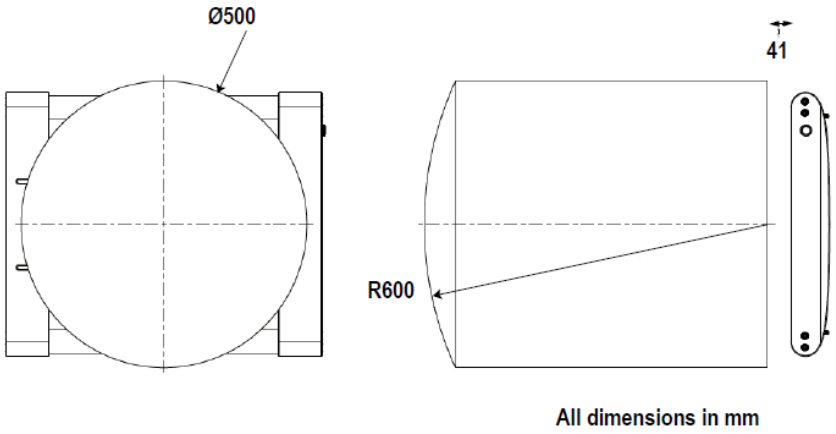

Figure 2-3: Measurement volume of the WFG. The range over the x- and y-axis has a radius of 25 cm from the origin of the field generator. In the z-direction the field ranges up to 60 cm. The measurement offset is 4.1 cm from the field generator.

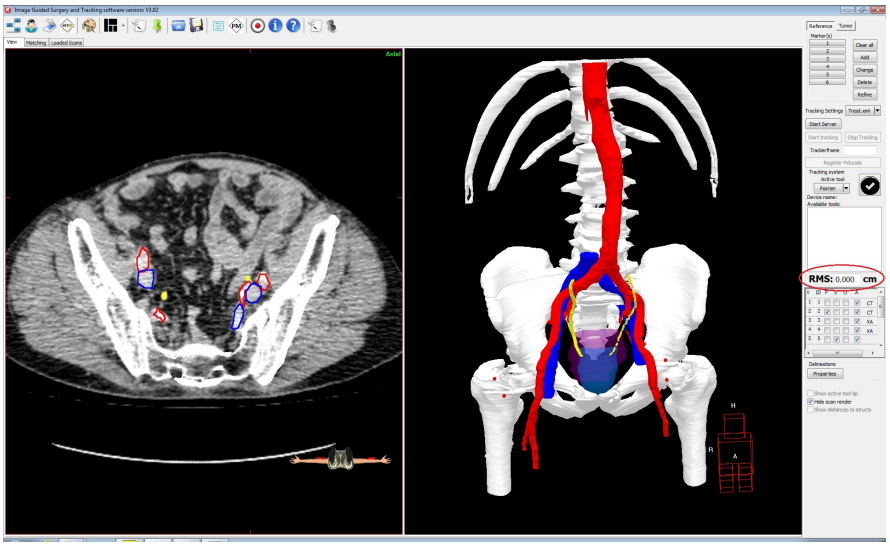

Figure 2-4: Overview of navigation seen on the computer screen during surgery. Delineation of vital structures in the preoperative contrast enhanced CT scan (left), 3D rendering(right). The RMSE is calculated and shown continuously (red circle).

2-2 Workflow

With the implementation of the WFG and sensor implantation into the workflow of the navigation procedure, the current navigation setup is not sufficient. The mattress currently used for navigation was custom made for the table top field generator (TTFG) and not compatible with the WFG. How the WFG should be incorporated into the navigation setup was part of this study and shown in Section 2-3. A full chain test was developed to evaluate the entire workflow of the new navigation setup. The design of the chain test is shown in Section 2-6.

The entire workflow of the previous navigation study is evaluated and adapted to the new navigation setup. Before surgery the new workflow is as follows:

- A CT scan with contrast is made of the patient.
- The images (CT/MRI) are loaded from the DICOM server into registration and segmentation software (Worldmatch).
- The available images are registered based on the bony anatomy. (chamfer match for CT-CT registration, mutual information grey-value registration for MR-CT)
- Vital structures and the tumour are delineated in all slices of the images. (see Figure 10)
- The matched scans and delineations are saved and send to the PACS.
- The XperCT is planned for the day of surgery.
- Involved parties should be informed on the navigation procedure.

- The day before surgery the surgery bed is prepared.

On the day of surgery the workflow will be:

- Make sure the EM pointer is in the operating room (OR).
- The scans and delineations are loaded from the PACS into SurgicalNavigation software.
- The sensor patches are placed on the skin of the patient, two on the back of the patient, left and right from the spinal cord, and one at the level of pubic bone.
- After being anaesthetised, the patient is positioned for surgery.
- The tumour tracking sensor is placed on or near the rectal tumour (implantation approach is part of this study).
- An intraoperative XperCT scan is acquired of the patient in surgery position.
- Directly after the XperCT scan, the location of all EM-sensors is saved to later correlate the actual sensor positions and orientations with the intraoperative image.
- A bone match is done between the preoperative scans and the intraoperative scan.
- The sensor patch locations are derived from the intraoperative image.
- The tumour contour of the preoperative scan is registered to the intraoperative scan to derive the actual tumour position in the OR and linked to the tumour sensor position that was saved earlier.
- Navigation can be started and the real-time tumour position can be tracked. (see figure 10 for overview on navigation trolley)
- During surgery several measurements are done to measure accuracy (measurements are part of this study).

2-3 Incorporation of the field generator into the navigation setup

To incorporate the WFG into the navigation setup there were two possibilities. Placing it on the operating table or placing it under the operating table. Based on the requirements below a setup was designed.

Requirements of the navigation setup are as followed:

- The table setup should be suitable to do rectal surgery by abdominoperineal resection (APR) or low anterior resection (LAR), i.e. the surgeon should not be hindered in performing the usual surgery.
- The table should be compatible with intraoperative imaging, since an intraoperative CT scan is mandatory.

- The anatomic site for navigation should be within reach of the field generator, to be able to do an accurate navigation procedure.
- The anus should be accessible for rectal toucher and for sensor implantation.
- The navigation system and all components need to be protected from fluids or other substances that can damage the field generator.
- The navigation system needs to be protected from displacement, deformation and excessive pressure.
- The measurement offset of 41 mm of the field generator should be taken into account when incorporating the field generator.
- The field generator must be able to connect to the navigation trolley.

2-4 Accuracy of the window field generator

The aim of this study was to evaluate the feasibility of an in-house developed electromagnetic navigation system with real-time tumour tracking in rectal surgery. To perform tumour registration, image quality should be high. The TTFG should be replaced by the WFG since the TTFG is not sufficient in terms of imaging quality. In intraoperative images made during a navigation procedure with the TTFG soft tissue structures cannot be differentiated. The WFG improved the image quality so the soft tissue in the abdomen could be recognized and used for registration (see Figure 2-5).

According to NDI the accuracy of the WFG is equivalent to the accuracy of the TTFG, [41]. The accuracy measurements at NDI are performed in an ideal test environment. The navigation system will be used during surgery, where many surrounding equipment can hamper the accuracy of tracking. Therefore accuracy measurements were performed in an ideal environment and in the OR setting.

To test the accuracy of the field generator the position accuracy of four 6DOF sensors, micro 0.8 * 9 mm rod, for the WFG in a test- and OR setup were measured. To measure the EM field an in-house built measurement setup with stackable boxes was used. Four sensors were placed parallel on a sensor-plate at 5 cm distance from each other and measured at 126 (= x * y * z = 2 * 7 * 9) positions parallel to the WFG (in the x-y-plane) up to a distance of 52 cm (z-axis) from the table. For each position 40 samples were acquired.

In the test setup the measurements from the WFG were compared to measurements with the NDI Polaris Spectra Hybrid system with passive reflective markers, placed on the sensor plate as well as the field generator (see Figure 2-6). The calibration of the two systems was done by placing the sensor plate on different heights and rotated 4 times a quarter. In-house developed software determined the transformation and calibrated the systems. This optical tracking system is known to have an accuracy of less than 0.025 cm RMSE, [36], [37], [38].

For each measured position the jitter was defined as the standard deviation (SD) over the 40 measurements. For the position accuracy the RMSE was used. For each position the average of the 40 measurements using the Aurora system were compared with the average predicted sensor position from the optical tracking system.

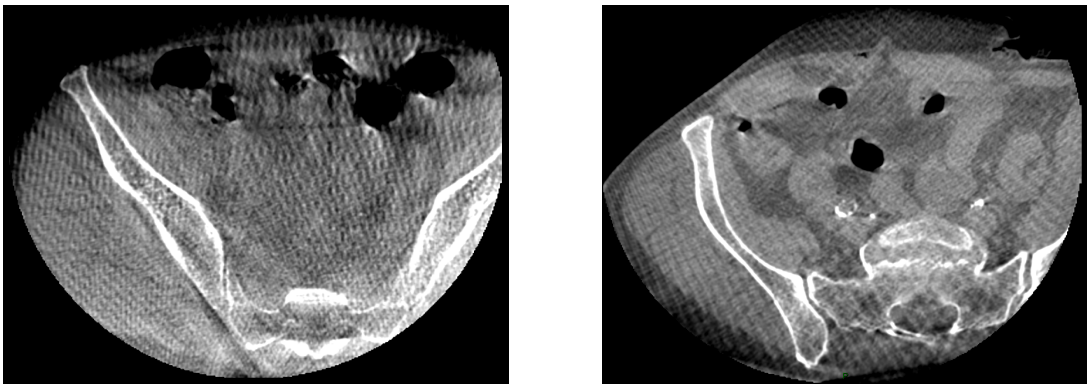

(a) (b)

Figure 2-5: XperCT made in the OR for two different patients. On the left (a) the navigation procedure was done using the TTFG and on the right (b) the WFG was used.

In the OR setup the field generator is placed in the mattress, therefor optical markers cannot be placed on the field generator. In order to determine the accuracy in the OR setup, relative errors were determined, where the distance between the individual sensors was evaluated. The jitter is independent of the optical tracking system, and was therefore also determined.

2-5 Sensor implantation and fixation method design

Operable rectal tumours are often mobile and therefore more difficult to localize. To be able to take positional changes of the tumour into account wired tracking sensors are available. This sensor should be delivered and fixed to the tumour or its surrounding tissue to be able to track the tumour real-time.

2-5-1 Sensor delivery

To deliver the sensor the physician needs to enter the body. Rectal tumours are the target, so entering the body through the anus was the chosen approach.

There are several devices available for delivery of the sensor. The device should provide an appropriate working channel to be able to place the sensor with surgical forceps. It should provide direct sight at the tumour and the device must be able to be withdrawn without dislocating the sensor. In the hospital endoscopic devices, a rectal speculum, a vaginal speculum and a proctoscope are available. The boundary of the distance to the tumour was set at 10 cm from the anus. On forehand, the endoscopic devices were excluded, as extra personnel is needed to control the device, and the remaining devices were expected to suffice. The remaining three devices were tested on a specimen excised in an abdominoperineal resection. This specimen contained an intact anal sphincter and at least 10 cm of bowel tissue. If all three devices prove to be insufficient, the use of an endoscope can be reconsidered.

Figure 2-6: Test setup for accuracy measurements of the WFG with respect to the NDI Polaris optical tracking system. Red box shows the sensor plate with 4 6DOF sensors and optical reflective markers.

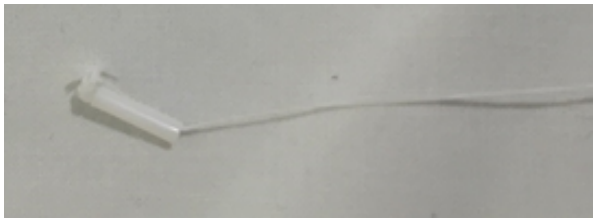

Figure 2-7: Substitute sensor for fixation tests.

2-5-2 Sensor fixation

Previous in-house research, [46], showed that anchoring, plugging or gluing the sensor to the rectum wall or tumour are the most valid fixation methods. Anchoring and plugging will pierce the rectal wall to fixate the sensor. Glue will merely fixate the sensor on the surface of the rectal wall or tumour making it the less invasive choice. Second, anchoring and plugging will probably require a special device, currently not available, so in this research the primary choice for the fixation method is gluing the sensor to the tumour or rectal wall near the tumour. The glue should be biocompatible and have a short polymerisation time.

Three glues frequently used for tissue repair were selected for testing, namely blue Histoacryl (B. Braun Medical B.V. Oss, Nederland), PeriAcryl90 (GluStitch Inc., Canada) and Dermabond topical skin adhesive (Ethicon US, LLC). Blue Histoacryl is a n-butyl-2-cyanoacrylate monomer that hardens when it comes in contact with physiological liquids. It should take 60-90 seconds until polymerisation is finished. PeriAcryl90 is a combination of two cyanoacrylate monomers n-butyl and 2-octyl and also hardens when it comes in contact with physiological liquids. It is available in a normal and high viscosity variant. The high viscosity variant is 9 times thicker than the normal variant and is evaluated in this research. Polymerisation times are not available, but were expected to be within 5 minutes,[47]. Dermabond is a 2-octylcyanoacrylate monomer and contains a chemical initiator to ensure polymerisation. Polymerisation should take place within 3 minutes, [48], [49].

In the first test a handmade substitute for the sensor was used (Figure 2-7), since the actual sensor is too costly to use for these experiments. All three types of glue were tested on a chicken breast and the easiness of gluing, time of polymerisation and the stiffness/hardness of the glue were reported and evaluated. The glue was deemed inadequate and eliminated from further testing, if it was not easy to glue, polymerisation took longer than 5 minutes or it did not stick to the tissue properly. Next, the glues were tested ex-vivo on intestinal tissue. A piece of bowel tissue was used to glue the sensor on and the above stated criteria were evaluated.

Finally, the full procedure was tested in an APR specimen. The chosen device to gain access to the tumour was used to provide the working channel. Surgical forceps were used to correctly place the sensor on the tumour. A syringe was be used to aspirate and apply the glue. Both substitute sensors and actual wired sensors were used in this test phase. To distribute the forces on the sensor, the glue and tumour tissue, the wire should be stitched to the anus to minimalize the chance of tearing the sensor loose.

2-6 Chain test

To validate the workflow of the navigation procedure a chain test was designed. The validation of software and hardware were validated at once. A phantom was designed to give a realistic representation of a patient's pelvis, the phantom is seen in Figure 2-8. The case was designed such that the whole workflow around the surgery was represented. To cover the entire chain from preoperative imaging to actual navigation with tumour tracking in the OR the test started with acquiring a preoperative CT scan of the phantom.

The 3D model of the phantom was made, delineations were stored in the DICOM server and uploaded on the navigation trolley. On the day of the 'surgery' the bed with the designed

mattress was prepared and placed in theOR. The phantom was placed on the bed and external markers were placed on the outside, similar to the patient setup. The phantom should be placed above the field generator and the markers should be within the magnetic field. The tumour sensor was placed and an intraoperative XperCT scan was acquired. The CT scan, delineations and the XperCT scan were registered. It was validated that the delineated structures were correctly linked to the CT scans.

The tumour sensor was linked to the tumour delineation in the 3D model. The navigation system was connected and the sensors were registered. Connection should be established within a minute. The RMSE between the actual position and the scanned position was reported, the RMSE should be under 0.8 cm.The navigation accuracy should be visually validated by pointing out visual landmarks. In the 3D model the pointer should be within 0.3 cm from the landmark. The tumour was moved and the update in the 3D model was evaluated. Visual findings of the update were reported. A landmark on the tumour is pointed at with the pointer and visually validated with the 3D model, the pointer should be within 0.3 cm from this landmark.

2-7 In-vivo study

A research proposal for an in-vivo study was submitted with the Medical Ethics Committee (MEC) and approved to start. The aim of the in-vivo study is to research the feasibility of the real-time sensor tracking in rectal surgery. Secondly, it aims at determining the accuracy of the navigation system relative to anatomical landmarks during surgery. The study was designed as a single centre observational feasibility study. Before start of the study the field generator was incorporated into the OR setup, a sensor fixation protocol was designed and a chain test was done to evaluate the workflow. The outline of the study is described in the following subsections.

2-7-1 Inclusion of patients

Eligible patients are patients of the Netherlands Cancer Institute (NKI-AvL), who are scheduled for rectal surgery by LAR or APR of tumours within 10 cm from the anal verge.

Patients included in this study will undergo one additional contrast enhanced planning CT scan within 3 weeks before surgery. The planning CT, and other available images such as magnetic resonance image (MRI), will be used to create a 3D anatomical model, including the pelvic bones, the iliac vessels, ureters, tumour and any suspicious lymph nodes (see Figure 2-11). The resulting 3D reconstructions are evaluated by the surgeon who will perform the surgical procedure.

The inclusion criteria for the study are as followed:

- The patient is planned for LAR or APR.
- The tumour should be within 10 cm of the anal verge (based on preoperative imaging).
- Patient should be suitable for contrast enhanced CT scanning.

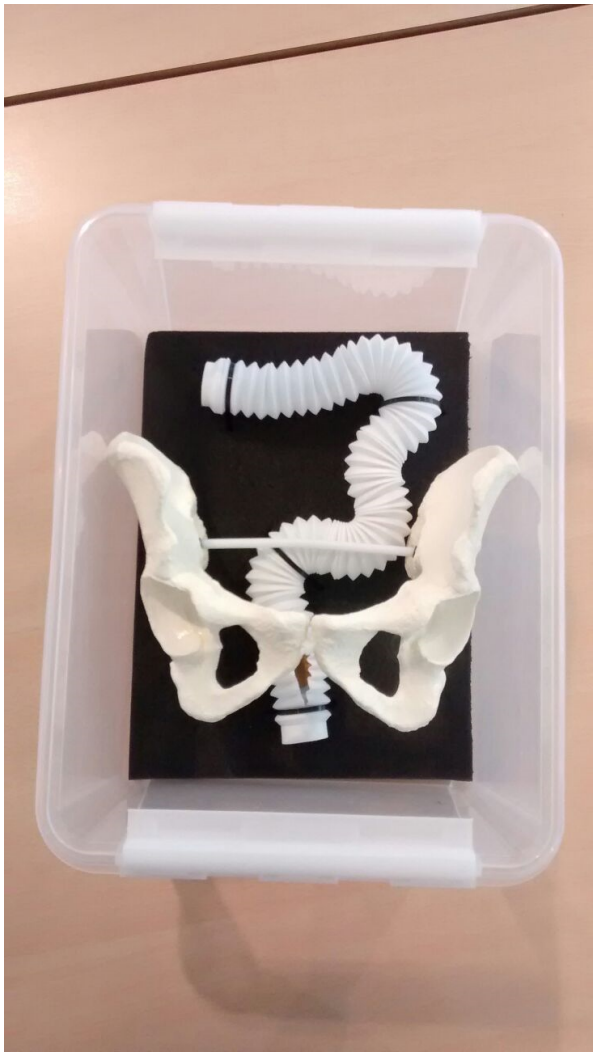

Figure 2-8: Navigation chain test phantom.

- Signed informed consent.
- Patients $\geq$ 18 years old.

Exclusion criteria are:

- Patients with metal implants in the pelvic area.
- Patients for which it is impossible to do a rectal examination.

2-7-2 Study parameters

Main study parameter

In this pilot study we aimed to evaluate feasibility of the navigation system during real-time tumour tracking in rectal surgery. Feasibility was primarily evaluated by judging the successful delivery of interpretable navigation data per procedure. In addition, the extra time needed and the easiness to glue the sensor to the tumour was recorded. The additional time should not be more than 30 minutes.

Secondary study parameters

To determine the calibration position accuracy during surgery, between the measured sensor position and the position determined from the XperCT scan, the RMSE was continuously calculated. This RMSE should at least be under 1 cm for the navigation procedure to proceed.

Next, optical identification of anatomical landmarks were used to validate this accuracy. By hovering the blunt tip probe over the landmarks, post processing can determine the error of the navigated probe tip and the segmented landmarks.

The accuracy was also correlation with ultrasound. The outcome measure is a difference in distance (mm) between where the navigation system measured the location of the tumour border from the sutures/clips on the rectal tissue and the same distance measured with ultrasound on the excised rectal specimen.

Measurements

To realise the endpoints several measurements were done during surgery.

During surgery a measurement was performed to get an estimate of the registration and navigation accuracy. To assess correctness, in supine position the surgeon pointed at the pubic bone, and also moved the pointer over the curvature of the promontory and in prone position the surgeon points out the coccygeal bone. In supine position the surgeon also indicated the iliac vessels and ureter crossings. Correct positioning of the navigation data was verified by visual inspection.

These actions were recorded, and if needed, adaptations in anterior-posterior, cranial-caudal and/or left-right direction were done to improve accuracy. To do these adaptations the

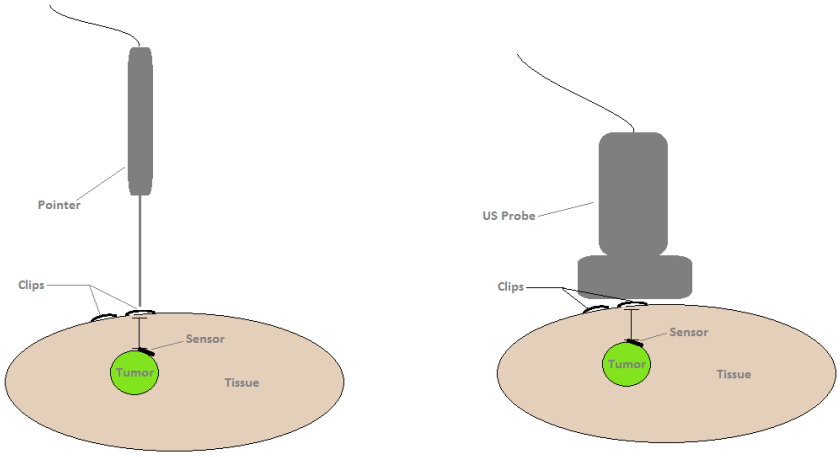

Figure 2-9: Distance between pointer tip and tumour (left) correlated with distance measurement done with US (right).

surgeon pointed out a landmark and if this did not correlate with what was seen on the 3D model, the pointer tip position as seen on the screen was displaced towards the landmark.

Next, the surgeon used the navigation system and the probe to localize the tumour. If the tumour was visible or palpable, the tumour border was followed with the blunt tip probe and the positions on the navigation system were logged. The resulting location of the tumour was assessed by the surgeon in terms of trueness.

The surgeon hovered the blunt tip probe over the tumour border and placed sutures or clips at the measured location of the tumour border. For each pointed position the estimated position of the pointer relative to the tumour border was stored. This position was also assessed on the resected specimen directly after removal, using ultrasound as gold standard (Figure 2-9).

2-7-3 Tumour registration accuracy

After having placed the sensor on the tumour, intra-operative imaging was used to link the 3D tumour model to actual tumour location. To link the data, a registration between the intraoperative and the pre-operative CT scans was acquired. To verify the tumour matching process, the tumour of the included patients was matched by 4 different observers to determine the reproducibility of the registration.

The centre of mass of the tumour on the preoperative CT scan was determined and set as the origin. After registration of the tumour on the XperCT scan the new position of this centre of mass is determined once again. The difference between the origin and the new position between the observers was compared. The mean displacement was calculated and the standard deviation of the displacement was determined to quantify the amount of variation between the observers.

The amount of overlap between the observers was determined by using the Dice similarity coefficient (DICE). DICE is defined as the common volume divided by the encompassing volume (see Figure 2-10 for a schematic overview).

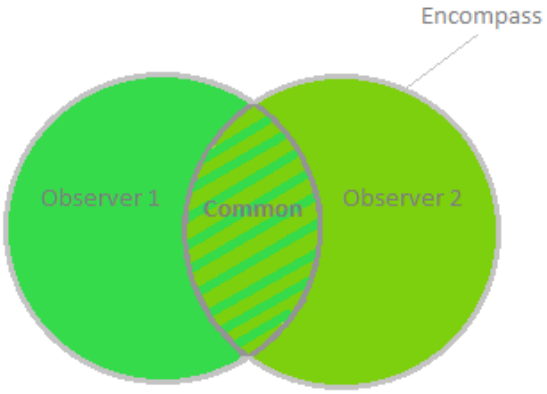

Figure 2-10: The amount of overlap between two observers of the new tumour position in the tumour matching process. DICE = common/encompass.

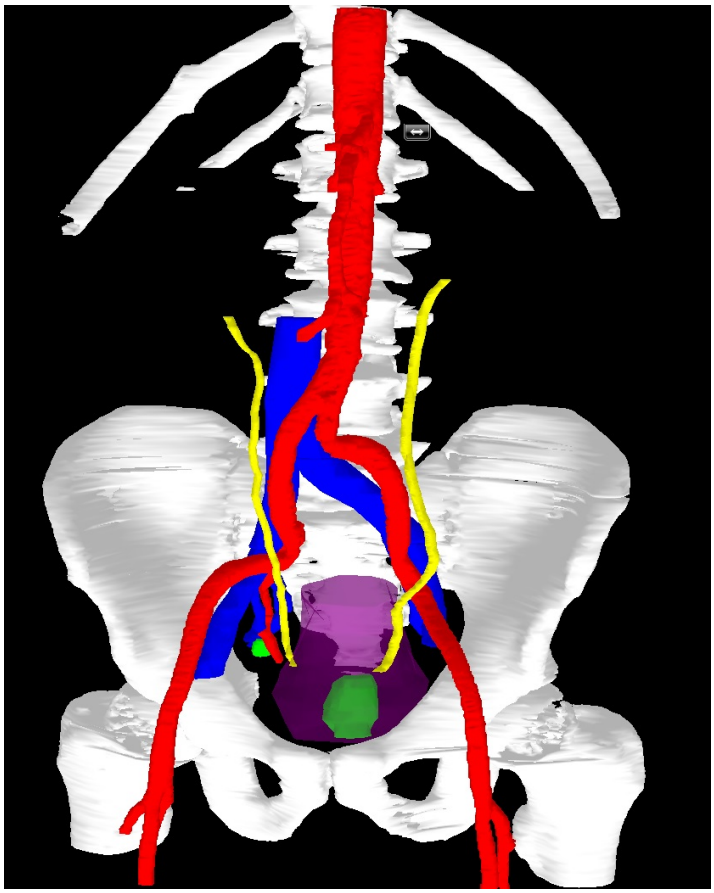

Figure 2-11: 3D reconstruction based on a contrast enhanced CT-scan. Bony structures (white), arteries (red), veins (blue), ureters (yellow) are delineated together with the tumour(green) and any suspicious lymph nodes (green). In this image the mesorectum (purple) is also delineated.

Chapter 3

Results

The current setup of the navigation procedure and workflow was evaluated and adapted. The electromagnetic field generator and the navigation materials were integrated into the operating room (OR) workflow. When a patient was suitable for the navigation procedure, and the patient gave his/her consent, the preoperative planning was initiated. A contrast enhanced CT scan was planned and, after scanning, the 3D model was created. Before the patient arrived in the OR the navigation setup was prepared. The incorporation of the field generator is addressed in Section 3-1 and accuracy of the window field generator (WFG) in Section 3-2. When the patient was in the OR, the markers were placed on the skin. After general anaesthesia the tumour sensor was placed according to the implantation and fixation method that was designed in this study, results are shown in Section 3-3. The chain test designed to evaluate the workflow is addressed in Section 3-4. Navigation accuracy measurements during surgery and measurements concerning tumour localisation are addressed in Section 3-5. A schematic of the workflow is seen in Figure 3-1.

3-1 Incorporation of the field generator into the navigation setup

For rectal cancer surgery with intraoperative imaging, a dedicated OR table is used with a carbon fibre imaging part and leg blades. The patient can be placed in both supine and prone position. The necessary table setup used in rectal surgery turned out to be incompatible for placement of the WFG under the table. The configuration to attach the leg blades to the imaging compatible part of the bed obstructed the proper placement of the WFG under the table (see Figure 3-2). This made it impossible for the field generator to hang straight and stable under the table. Also, with the field generator under the table it was not possible to change the leg blade positions without dispositioning the field generator.

Therefore placing the WFG on the table was the chosen approach. To place the WFG on the table a custom made matrass was designed that incorporates the WFG (see Figure 3-3). The matrass was designed according to the requirements stated in the methods Section 2-3. The field generator is placed directly above the imaging compatible part, at the lower edge of the

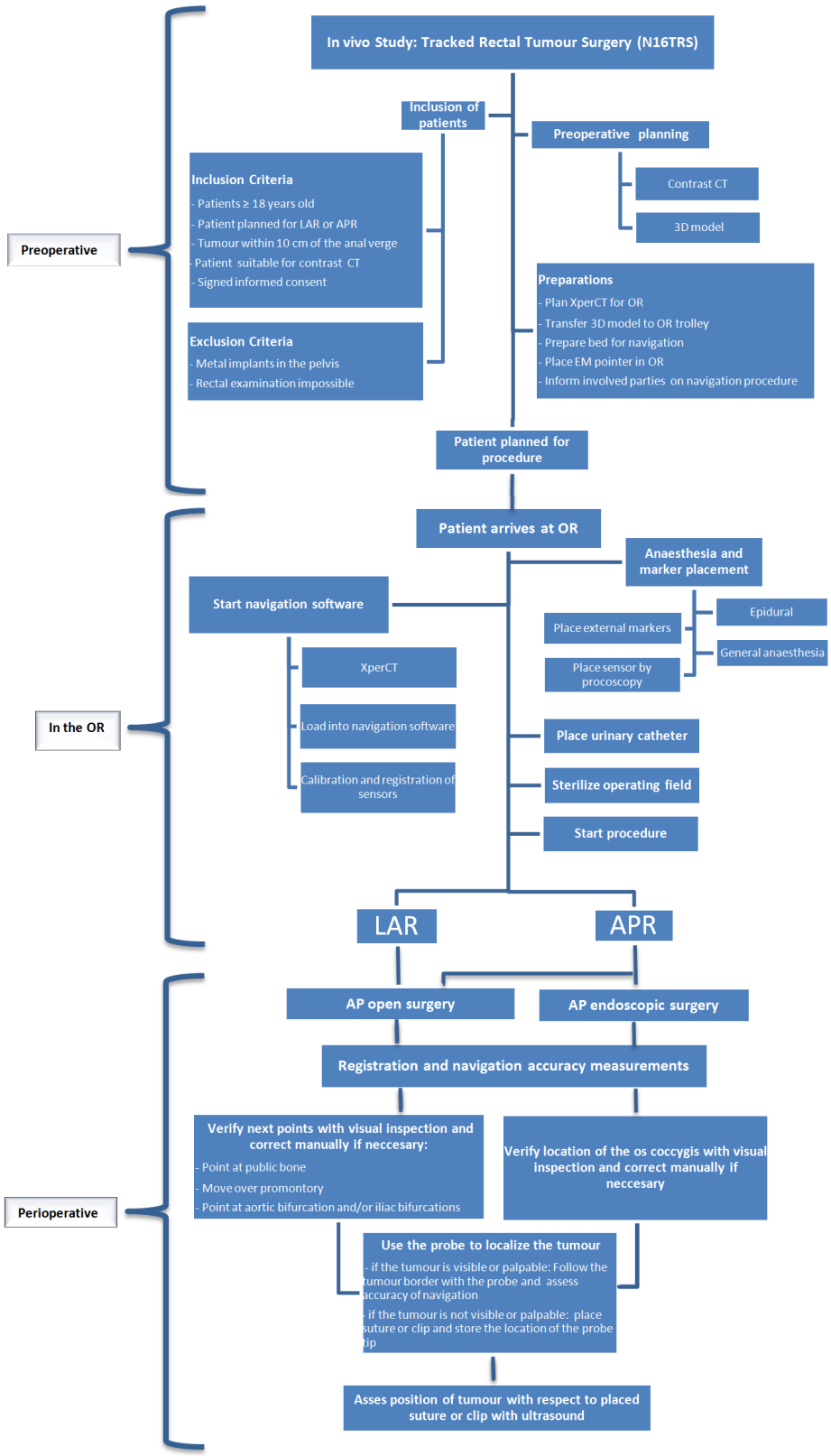

Figure 3-1: Complete workflow from inclusion to surgery.

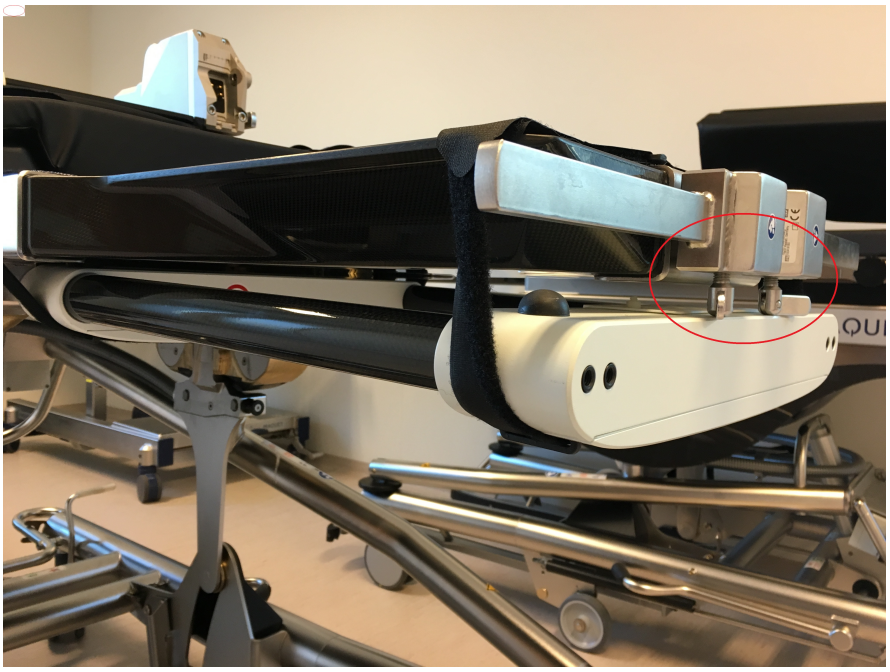

Figure 3-2: WFG mounted under imaging compatible table.

bed. The patients bottom cannot be placed entirely on the lower edge of the bed since the magnetic field that is created starts a few centimetres cranial from the edges and the pelvis cannot be placed outside the magnetic field.

To be able to reach the anus for rectal toucher and sensor implantation, a semi-circular opening was created in the matrass. To protect the field generator and the cable from fluids and also from displacement, deformation and excessive pressure, the field generator and cable are completely embedded in the matrass. The matrass is surrounded by a custom made matrass cover, that is resistant from fluids, and that can be opened with a zipper to insert and to remove the field generator. The cable exits the matrass on the side of the navigation trolley. The mattress's top layer, above the field generator, is 4 cm. This was chosen to account for the offset of the field generator.

SeeFigure 3-4 for the final result of the mattress. In Appendix A the mattress design dimensions of all components are shown.

3-2 Accuracy of the window field generator

Four 6DOF sensors placed parallel on a sensor-plate were measured in a test- and OR setup. The position accuracy was determined up to a distance of 52 cm from the table (z-axis).

In the test setup the measurements from the WFG were compared to measurements with the Northern Digital Inc. (NDI) Polaris as a reference. To calculate the position vector root-mean-square error (RMSE) the 40 measurements for each position were averaged, this was done both for the data from the field generator as the data from the optical tracker. Next, the difference between the positions (x-, y- and z-axis) was determined and the Euclidian distance

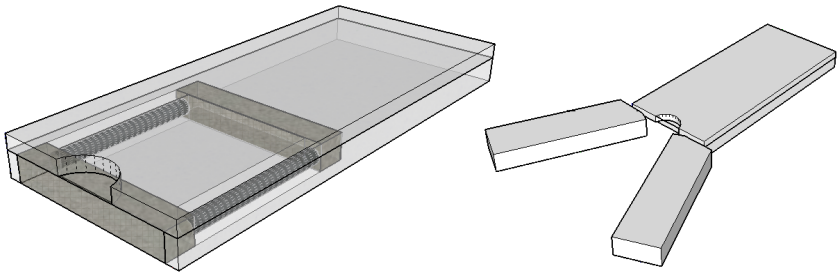

Figure 3-3: Drawings of mattress design. Left a transparent top layer shows how the field generator is placed in the mattress. Right shows an overview of the mattress including the leg blade cushions.

(a) **(b)**

Figure 3-4: Final developed mattress with WFG and cable incorporated (a). The cable exits the mattress on the side (red circle) (b).

was calculated resulting in a position vector. The position vector RMSE is the RMSE of the position vectors in each height layer from the field generator.

The vector jitter was approximately 0.02 cm within 45 cm from the WFG and position vector RMSE was approximately 0.36 cm up to 30 cm from the WFG increasing to 1.10 cm at 45 cm distance from the WFG. The jitter and RMSE are shown in Figure 3-5 and Figure 3-6, respectively. Table 3-1 shows the RMSEs for the x-, y- and z-direction individually as well as the vector RMSE as a function of the distance from the WFG.

The vector errors versus the distance from the field generator are shown in Figure 3-7 and Figure 3-8, respectively. The largest difference occurred in the z-direction. When looking at the error in the z-direction (see Figure 3-9 and Figure 3-10), it can be seen that the points measured with the WFG were above the projected positions determined by optical tracking. Further from the field generator the difference became larger. There was also a slight deviation in the x- and y-directions. The error in the x and y-directions was also increasing with increasing distance from the WFG. The RMSE at 45 cm from the field generator in the z-direction was 0.97 cm, in the x-direction this was 0.39 cm and in the y-direction 0.36 cm. Appendix D contains additional figures showing the deviation in the x- and y-directions.

In the OR setup, the relative distances between measurement locations were measured to determine the accuracy. The distance between the sensors on the sensor plate is exactly 5 cm. So sensor 1 and 2 are 5 cm apart, sensor 1 and 3 are 10 cm apart and sensor 1 and 4 are 15 cm apart. The vector jitter was approximately 0.02 cm within 45 cm from the WFG (see Figure 3-11). The difference in distance between sensor 1 and 2 measured with the WFG was between 4.85-5.1 cm up to 35 cm from the WFG. Above this distance, measurements were between 4.85-5.3 cm. When the sensors were further apart, the measurement error increased (see Figure 3-12 and Figure 3-13). Between sensors 1 and 3 this resulted in a distance measurement between 9.8-10.4 cm at 35 cm from the WFG. For the distance measurement of sensors 1 and 4 this resulted in distance measurements between 14.8-15.6 cm at 35 cm from the WFG. Appendix E shows additional figures for the distance between sensors 1 and 2 and sensors 1 and 3.

Table 3-1: RMSEs for the x-, y- and z-direction as well as the vector RMSE, at each measured layer, as a function of the distance from the WFG.

Distance from WFG		**5 cm**	**10 cm**	**15 cm**	**20 cm**	**25 cm**	**30 cm**	**35 cm**	**40 cm**	**45 cm**
Position RMSE [cm]	**x-error**	0.082	0.110	0.131	0.145	0.153	0.162	0.178	0.255	0.392
	y-error	0.064	0.061	0.070	0.088	0.112	0.153	0.210	0.290	0.357
	z-error	0.058	0.070	0.066	0.102	0.172	0.285	0.465	0.702	0.965
	vector-error	0.119	0.144	0.162	0.198	0.256	0.362	0.541	0.801	1.101

3-3 Sensor implantation and fixation method design

3-3-1 Sensor delivery

A rectal speculum, vaginal speculum and a proctoscope were tested on a specimen excised in an abdominoperineal resection. This specimen contained an intact anal sphincter and at least 10 cm of bowel tissue (see Figure 3-14). All three devices were tested by sensor placement

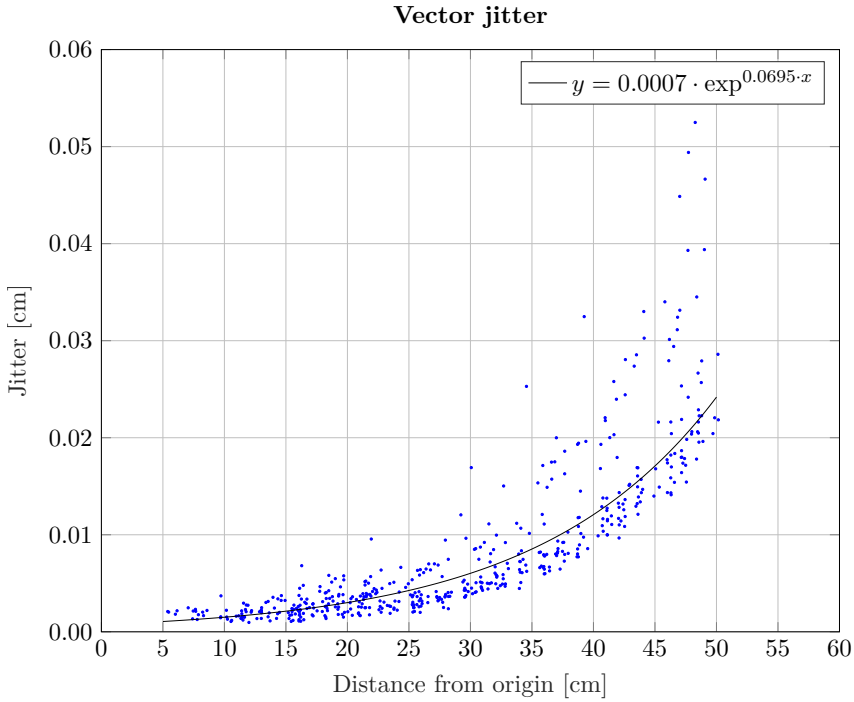

Figure 3-5: Vector jitter in test setting.

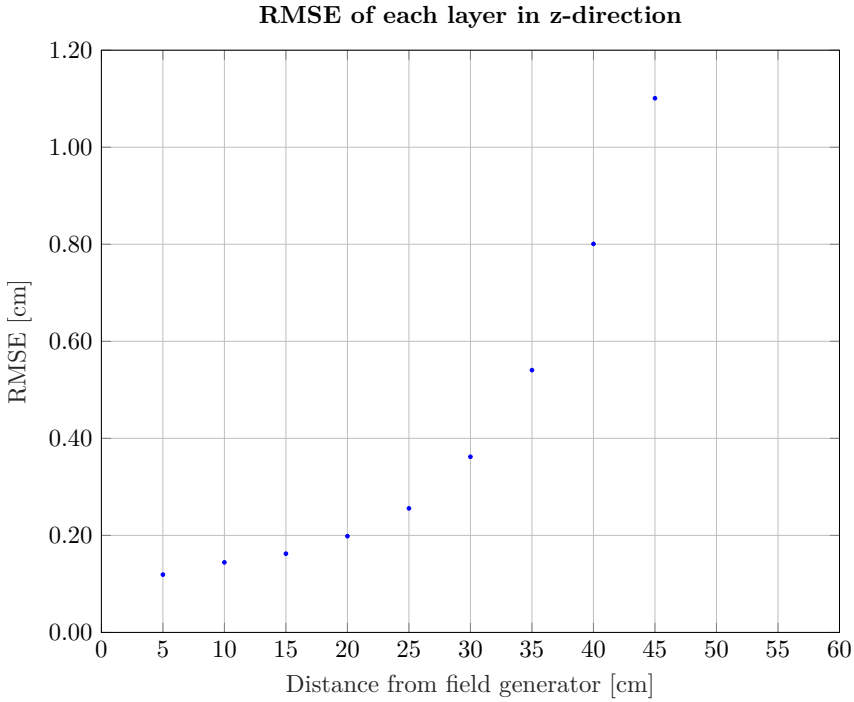

Figure 3-6: RMSE in test setting.

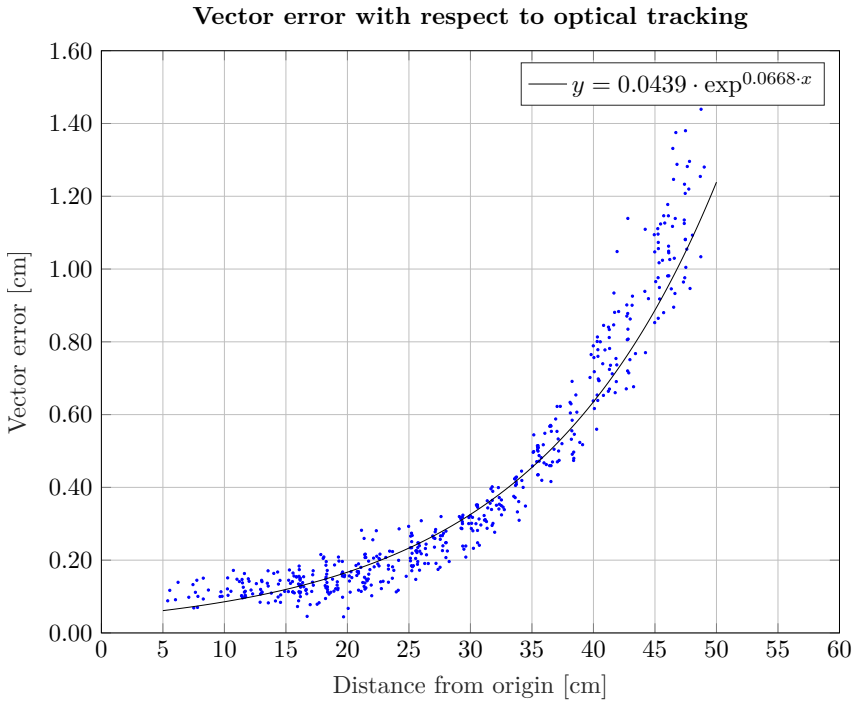

Figure 3-7: Vector errors in the z-direction.

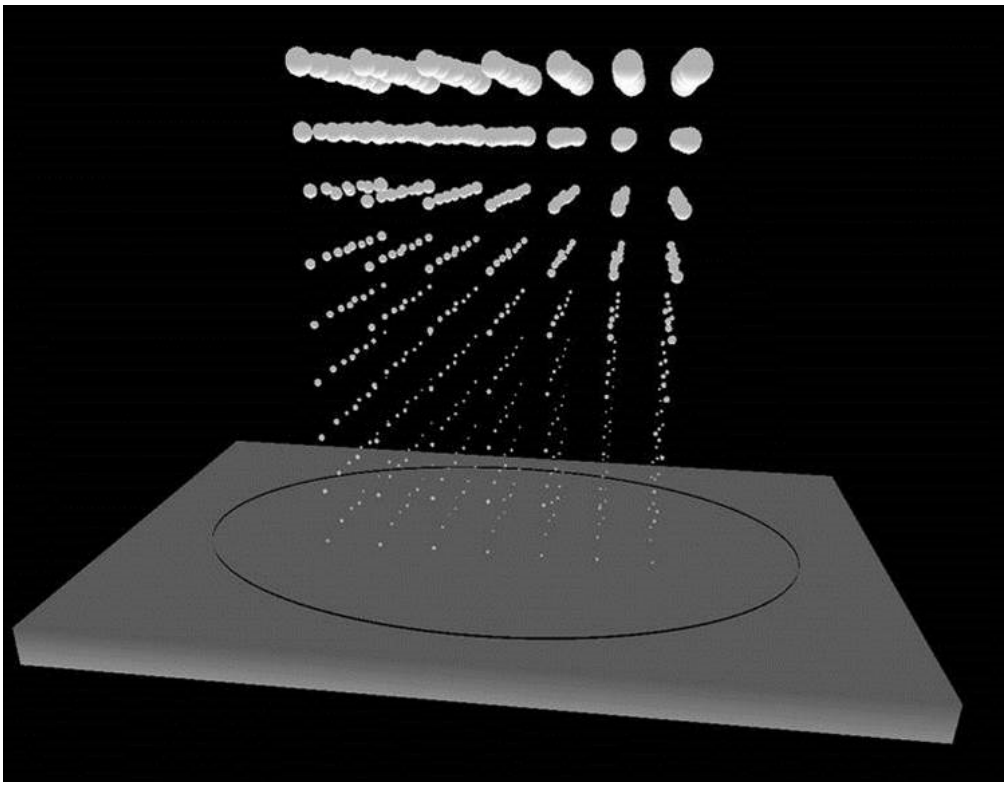

Figure 3-8: 3D visualisation of the vector errors in the z-direction.

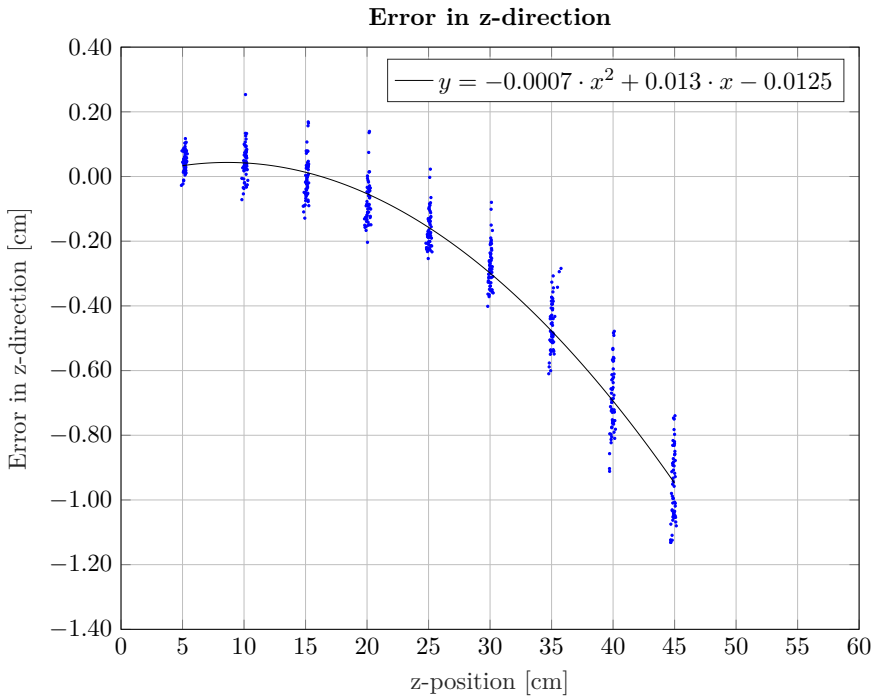

Figure 3-9: Error z-direction.

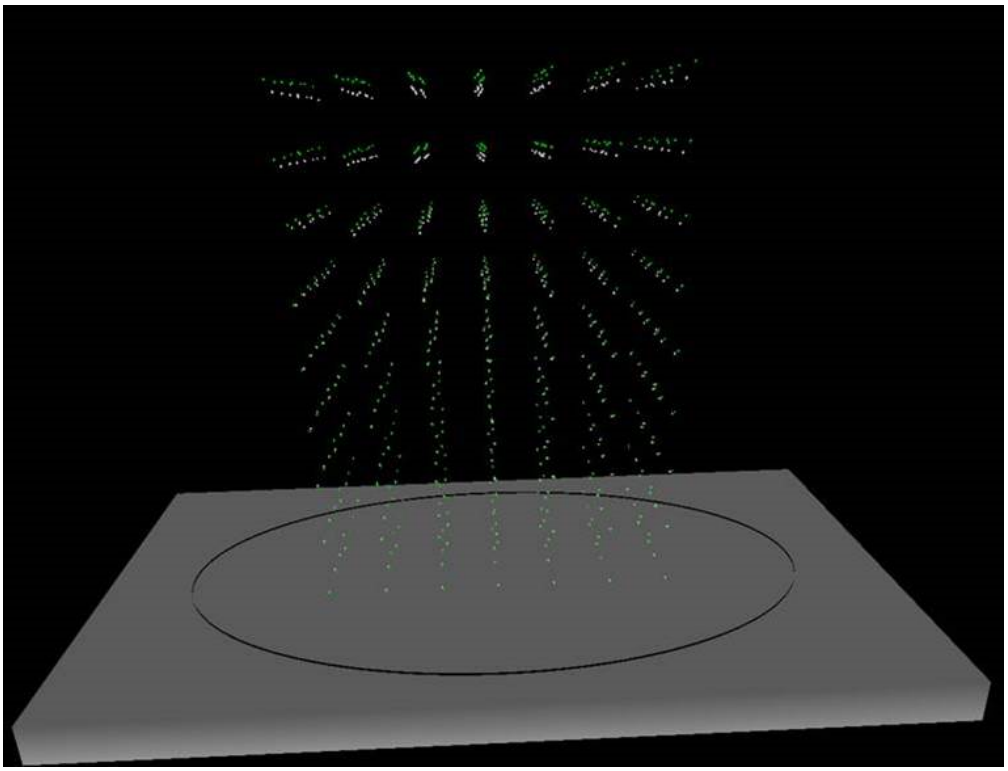

Figure 3-10: Error z-direction with the points measured with the WFG (lime) and with NDI Polaris (grey).

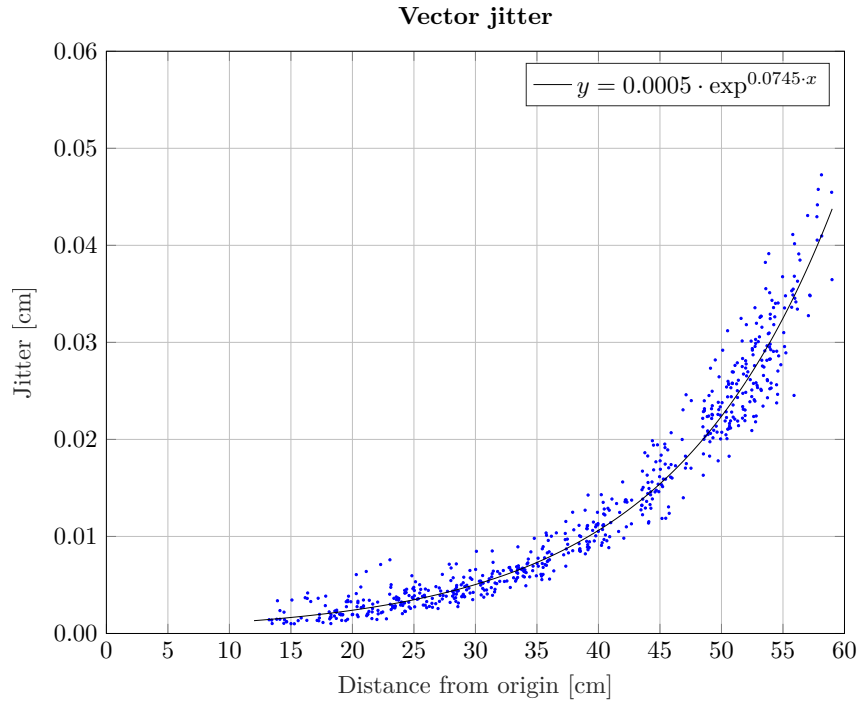

Figure 3-11: Vector jitter in OR setting.

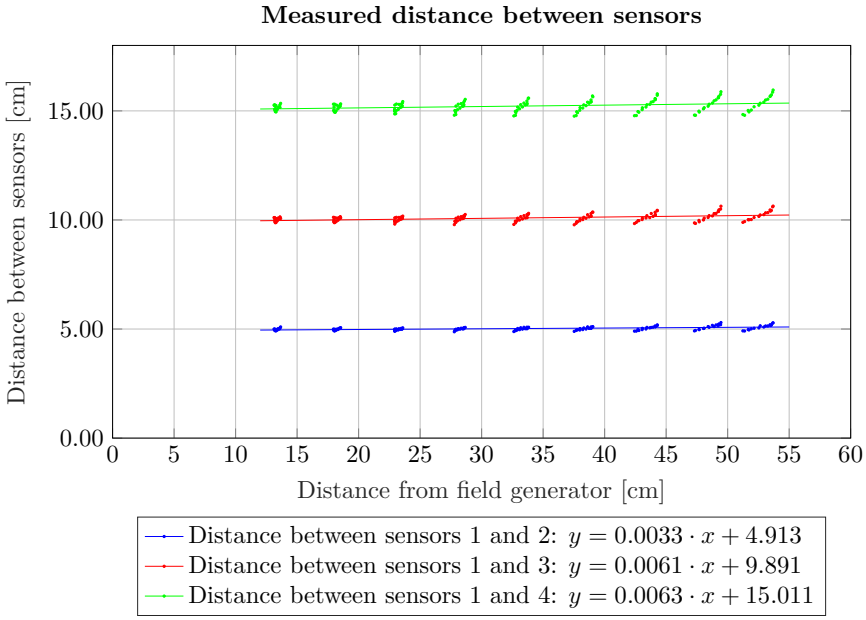

Figure 3-12: Distance measurements between sensors.

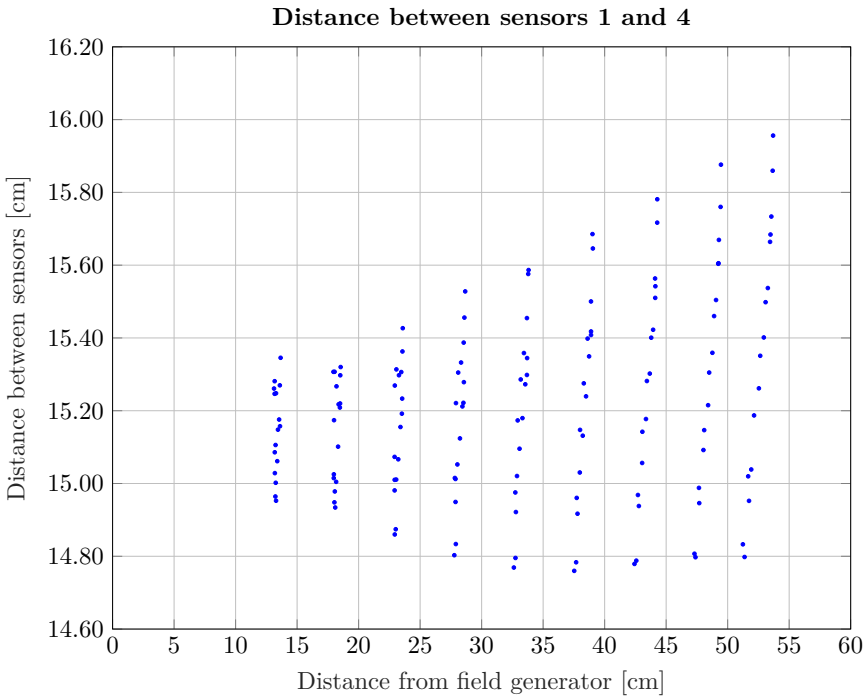

Figure 3-13: Distance measurements between sensors with the distance between sensor 1 and 4 in more detail.

with the fixation method that is elaborated on in Section 3-3-2. Both the rectal and vaginal specula immediately proved unfit. When they were extracted from the anus the blades were closed entirely. This caused the entrapment of the sensor and wire between the blades so the sensor was pulled out with the extraction of the device. The proctoscope has an opening on the end of the device. The sensor could be placed at the opening and when the proctoscope was extracted the sensor stayed in place. This was tested by re-entering the anus with the proctoscope and checking if the sensor was still in place.

3-3-2 Sensor fixation

The three glues, blue Histoacryl, PeriAcryl90 and Dermabond topical skin adhesive were tested on a chicken breast. The easiness of gluing, time of polymerisation and the stiffness/hardness of the glue were tested. To apply the glue, it was aspirated into a syringe and applied with a needle. A spinal needle was used for this since the sensor could be placed at as far as 10 centimetres from the anus. The first test showed that blue Histoacryl and PeriAcryl90 have similar properties. However the blue Histoacryl is less viscous. This caused more leakage from the blue Histoacryl before the polymerisation process had finished. Since the properties of blue Histoacryl and PeriAcryl90 are quite similar, but the higher viscosity of the PeriAcryl90 is advantageous, blue Histoacryl was eliminated for further testing.

Between Dermabond and PeriAcryl90 the tested properties differ. Dermabond had a higher stiffness than PeriAcryl90. Dermabond had a polymerisation time of maximum 3 minutes after breaking the original applicator. The polymerisation process started immediately when

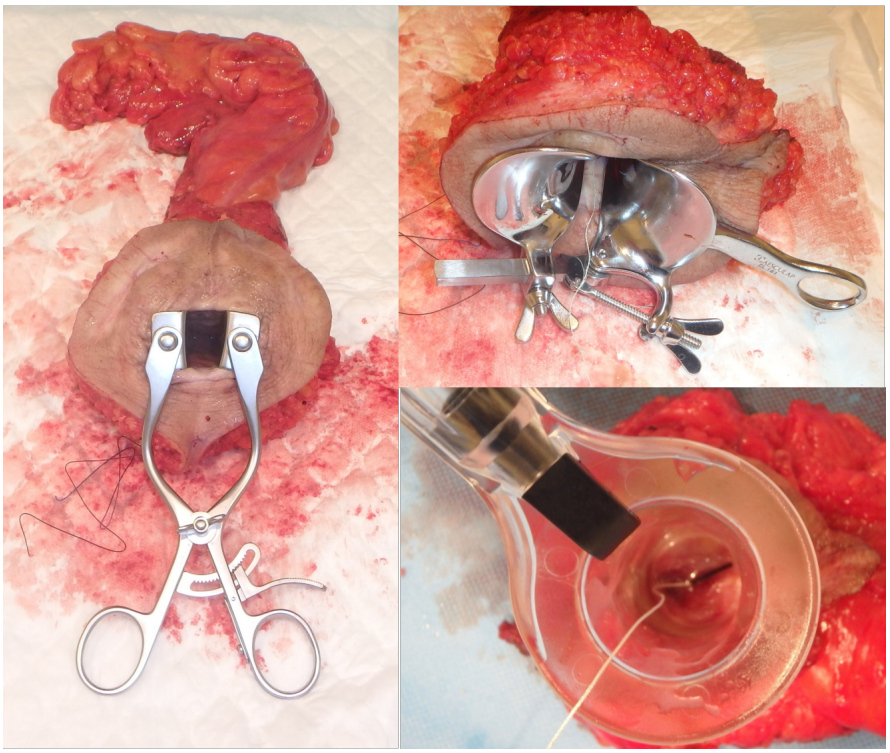

Figure 3-14: Three tested devices for sensor delivery. Left image is the rectal speculum, right upper image the vaginal speculum and right lower image the proctoscope.

breaking the applicator, limiting the time for application of the glue. The polymerisation time for PeriAcryl90 was 3-5 minutes after contact with physiological fluids. The possible advantage of PeriAcryl90 is that the glue can be kept outside the original container until it comes into contact with physiological fluids. PeriAcryl90 was easy to apply, the glue could be aspirated beforehand and saved until needed for application. For Dermabond, the quick polymerisation time after breaking the applicator makes it challenging to aspirate the glue and apply it before the glue has set.

Next, Dermabond and PeriAcryl90 were tested on intestinal tissue (see Figure 3-15). PeriAcryl90 filled the folds of the bowel wall and enlarged the grip on the surface. The high stiffness of Dermabond prevented this from happening. The slightest pull on the sensor glued with Dermabond detached the sensor from the bowel wall. For this reason Dermabond was eliminated for further testing.

Next, the full procedure was tested in an abdominoperineal resection (APR) specimen. The proctoscope was used to gain access to the tumour. Surgical forceps were used to correctly place the sensor on the tumour. A spinal needle was used to aspirate and apply the PeriAcryl90 glue on the sensor. After a polymerisation period of 5 minutes, the proctoscope was retracted. First, the fixation of the sensor was tested by manually by putting tension on the sensor wire. To further test the strength of the fixation a forceps was clamped to the wire and the bowel was held upright with the forceps hanging free on the wire (see Figure 3-16). This was tested in 2 different specimens and both held the weight of the forceps. The weight was approximately 80 grams. So there was about 0.8 N pulling on the wire.

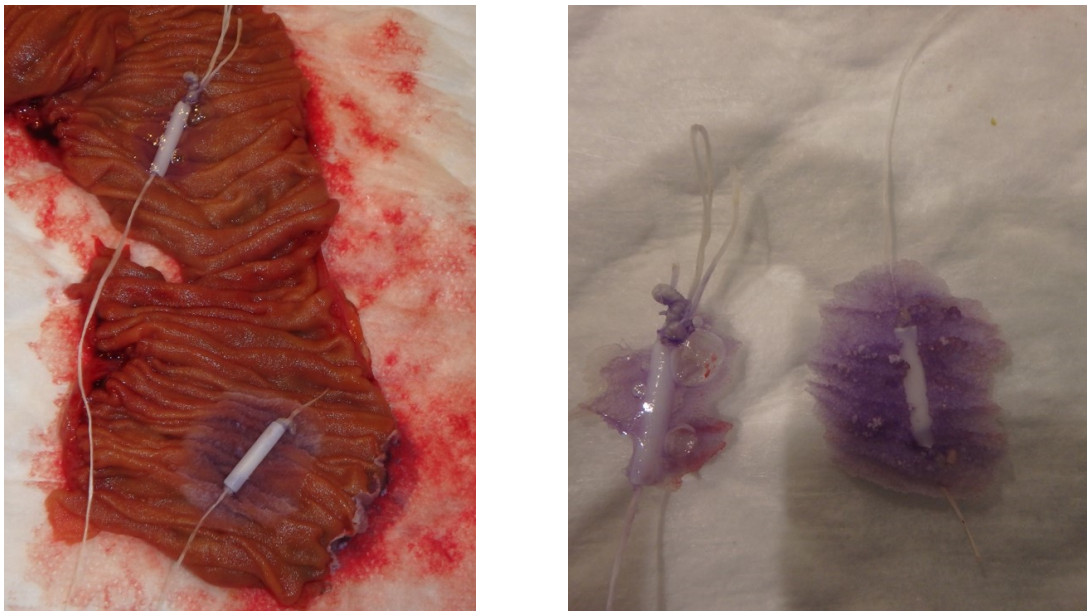

(a) (b)

Figure 3-15: In both images on the left side (a) the Dermabond glue is seen and on the right side (b) PeriAcryl90.

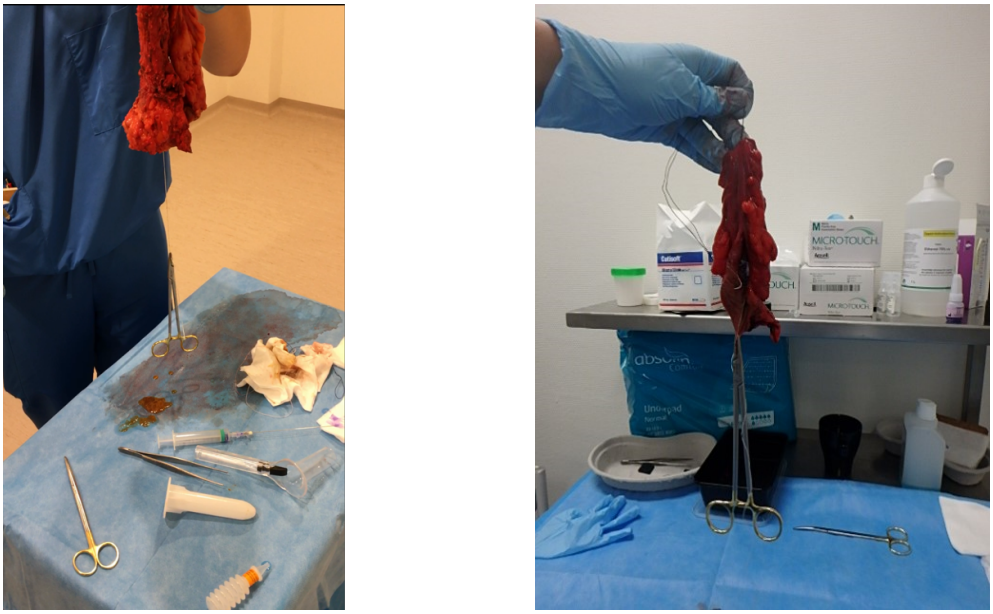

(a) (b)

Figure 3-16: Testing the strength of the glue fixation.

This lead us to believe that the fixation method with PeriAcryl90 is sufficient and this resulted in the following sensor implantation protocol for the in-vivo study:

1. Glue for fixation: PeriAcryl90 high viscosity.
2. Applicator: Spinal needle.
3. Polymerisation time: 3 - 5 minutes.
4. Apply on dry surface.
5. Attach wire to anus with a suture.

To distribute the forces on the sensor, glue and tumour tissue the wire should be stitched to the anus to minimize the chance of tearing loose the sensor.

3-4 Chain test

To validate the workflow of the navigation procedure a chain test was designed. For the chain test a phantom was designed to give an accurate representation of a patient's pelvis. The phantom was build up from a 3D pelvis model and a tubular structure that represents the bowel. In the lower end of the bowel a simulated tumour made of beeswax was placed. The tumour can be moved to attach a tumour sensor during the chain test. All components were placed in a crate that represents the external of the patient. Figure 2-8 shows the phantom and Figure 3-17 shows the setup during the chain test in the OR. A chain test form was designed and shown in Appendix B.

Next, everything was prepared for 'surgery'. A 3D model was created beforehand. The bed was prepared with the designed mattress. The bed was placed in the OR and the phantom placed on the lower part of the mattress just on the edge of the semi-circular opening in the mattress. The navigation software was started, two markers were placed on the bottom of the crate and one was placed on the pubic bone (see Figure 3-17). The tumour sensor was attached to the tumour and the position of the phantom with respect to the magnetic field was evaluated. All sensors were located within the magnetic field. An intraoperative computed tomography (CT) scan was made, loaded into the software and registration of all the scans was performed. The connection to the navigation system was established within a minute. Next all the sensors were registered and the tumour sensor was linked to the tumour segmentation. Detailed information about how to match the tumour delineation to the sensor is found in Appendix C. The found RMSE for the accuracy of the external sensor registration was 0.25 cm. This is lower than the set maximum of 0.8 cm, so the registration was accurate enough. The pointer was used to visually validate the navigation accuracy. The accuracy was visually evaluated and within 0.3 cm. When the tumour was moved to a new location the update was very quick and accurate according to visual assessment. When the tumour was pointed out on the updated position the accuracy was within 0.3 cm. A detailed manual to use the navigation software for navigation of mobile tumours was designed, and is seen in Appendix C.

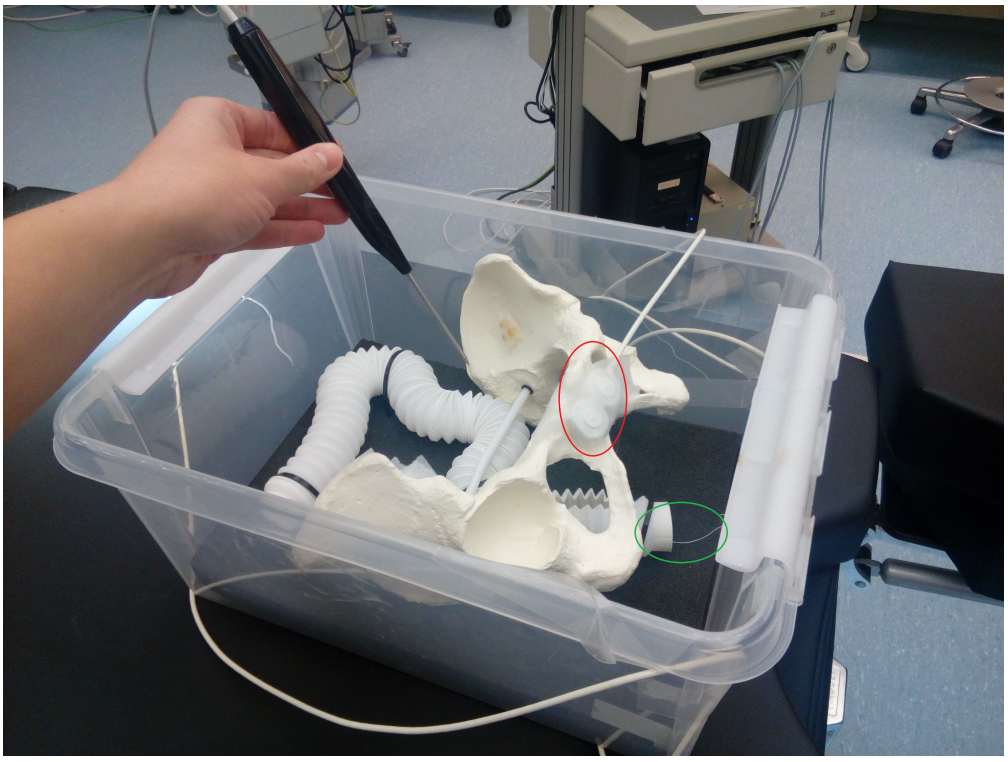

Figure 3-17: The navigation setup during the chain test. The navigation trolley is placed right next to the bed, at a safe distance and outside the sterile field. The reference sensors are placed on the back and pubic bone (red circle) and the tumour sensor is placed (green circle). The crate is placed directly at the edge of the semi-circular opening in the mattress.

3-5 In-vivo study

The workflow and navigation setup was ready before starting the in-vivo study. The new mattress was ready for use and the developed method for sensor implantation was successful in ex-vivo tests. The chain test to evaluate the workflow had a positive result. The timing of the procedural steps was good. The RMSE determined for the registration accuracy in the chain test was within the set boundary of 0.8 cm and the tumour localisation updated very quickly and looked accurate. The navigation system was not as accurate as expected due to the use of the WFG, nevertheless the patient study was started. The surgeon only used the navigation system for measurements and did not rely on the system to be able to perform the surgery.

3-5-1 Included patients

Currently 3 patients have been included in the study (see Table 3-2). The 3D models that were created for patients 1-3 are found in Appendix F. The sex, age, procedure type and distance from the anus to the tumour were registered. There were 3 types of procedures registered. 'LAR', 'APR, AP open' meaning that both the abdominal and the perineal part of the procedure were open surgery and 'APR, AP laparoscopic' meaning that the abdominal part was laparoscopically done and the perineal part was open surgery. In principle, when the procedure was entirely open, the navigation was used during both the abdominal and the perineal part of the surgery. However, for patient 3 it was chosen to only navigate in prone position.

The first patient underwent a low anterior resection (LAR) and the tumour was located at 9.5 cm from the anus, on the outer reach of the proctoscope. It was attempted to glue the sensor twice. The glue kept hardening quite fast, making it difficult to glue the sensor. Slowly dripping out of the needle, the glue hardened into the needle, disabling it. The glue also stuck to the proctoscope and the surgical forceps. After 20 minutes, two attempts with a new needle and new glue, the decision was made to clip the sensor to the tumour. One clip was on the wire and one was on the sensor. After a few attempts the sensor was successfully clipped to the tissue. After clipping, the navigation system was not able to detect the sensor and the navigation procedure could not proceed. An XperCT was made, since the patient navigation was still used for lymph node navigation. After the procedure, the sensor was taken for testing. It appeared that the sensor could be detected by the navigation system, but could not give reliable data. The wire was still intact, but the sensor was slightly bent. After trying to straighten the sensor, it was broken. After this first patient it was discussed that gluing needed some extra ex-vivo testing.

The second patient was planned one week after the first and underwent an APR with a laparoscopic abdominal procedure. Ex-vivo testing of the glue was not possible beforehand, so it was decided that the sensor would be clipped (or stitched if possible) instead of glued. To be able to clip the sensor to the tissue without damaging the sensor, it was sewn into a vicryl mesh. Through 2 holes, made in this mesh, it should be clipped to the tissue. A surgeon performed the sensor fixation. Clipping proved to be difficult, so the vicryl mesh was stitched to the tissue. This was possible since the tumour was 3 cm from the anus and it could easily be reached. The sensor fixation procedure took 10 minutes and acquisition of the XperCT took

5 minutes. Navigation accuracy measurements during surgery and measurements concerning tumour localisation could be done in this patient and results are shown in Section 3-5-2.

Between the procedures of patient 2 and 3 an ex-vivo specimen was available to do another sensor fixation test. The approach was changed, a pipette was used to apply the glue instead of the spinal needle, and an experienced surgeon performed the fixation. Fixation was good and the glue did not harden into the pipette, so this approach would be used in the third procedure.

Patient 3 underwent APR with open surgery on the abdominal part during which navigation without tumour tracking was used. The sensor was placed after the abdominal part of surgery, when the patient was already in prone position. Sensor fixation was difficult, since the patient did not receive proper bowel preparation before the surgery. The surgeon was able to glue the sensor to the tissue, without the glue sticking to the pipette, surgical forceps or the proctoscope. The fixation process took about 10 minutes after which an XperCT was made. However, before the surgery started the sensor came out with an excrement, so the navigation procedure could not proceed.

3-5-2 Study parameters

The main study parameter was to evaluate the feasibility of the navigation system during real-time tumour tracking in rectal surgery. Feasibility is primarily evaluated by judging the successful delivery of interpretable navigation data per procedure. So far, successful sensor fixation resulted in obtained data in only one of the three patients. Additionally, the extra time needed was recorded together with the easiness to glue the sensor to the tumour. During all procedures the extra time needed stayed within the set boundary of 30 minutes. The easiness of gluing in each patient was elaborated on in Section 3-5-1. All study parameters are summarized in Table 3-3.

Secondary study parameters were the determination of the accuracy of the navigation towards anatomical landmarks and the correlation of the navigation data with ultrasound. Both were only performed in patient 2, since sensor placement was only successful in this patient.

The position RMSE of the sensor registration accuracy for the external sensors is continually calculated while the navigation program is running. The mean RMSE during a part of the navigation procedure was calculated. During 7:30 minutes of navigation 3000 frames were taken and every 500 frames the RMSE was determined. The mean RMSE during these minutes was 0.515 cm.

The optical identification of anatomical landmarks were used to validate navigation accuracy. In this case the coccygeal bone was uses to verify accuracy. The pointer tip was visually not close enough to the coccygeal bone in the 3D model. Adaptations were done manually to improve the accuracy. While the surgeon held the pointer at the coccygeal bone, the location of the tip in the 3D model was manually adapted so that it was within 0.3 cm of the coccygeal bone. In retrospect, the coccygeal bone was not delineated properly, and resulted in a overestimation of the navigation error during surgery.

The correlation of navigation with ultrasound did not result in useful data. The difference in distance (mm) between the pointer location and the sensor location with respect to the WFG was calculated from the positional data and the distance between the pointer location

Table 3-2: Data included patients.

Patient	Sex	Age	Procedure	Tumour distance from anus
1	M	60 year	LAR	9.5 cm
2	M	62 year	APR, AP laparoscopic	3.0 cm
3	M	65 year	APR, AP open	5.0 cm

Table 3-3: Results primary study parameters.

Patient	Interpretable navigation data obtained	Extra time needed		Easiness to glue the sensor
		XperCT	Sensor placement	
1	NO	-	20 min	Sensor failure after clipping
2	YES	5 min	10 min	Not glued but stitched
3	NO	20 min(2x10)	10 min	Sensor glued (patient had no bowel prep so sensor was pulled out with large excrement)

on the specimen and the tumour border were measured with ultrasound. This data cannot be compared to each other.

The pointer was located at (x1, y1, z1) = (0.832, 15.432, -27.117) with respect to the WFG and the sensor was located at (x2, y2, z2) = (2.593, 15.321, -27.945). The distance from pointer to sensor was 1.95 cm. The distance between the pointer location and the sensor could not be determined with ultrasound, since the sensor itself could not be identified with ultrasound.

According to a distance measurement on ultrasound, there was about 5 cm between the stitch placed on the specimen and the tumour border. Figure 3-18 shows the distance from the location of the stitch that was placed and the tumour. During the ultrasound a finger was placed on this location resulting in a bright spot. The tumour looks darker than the surrounding healthy tissue.

3-5-3 Tumour registration accuracy

To verify the tumour matching process, the tumour of two included patients, patients 1 and 2, was matched by 4 different observers to determine the reproducibility of the registration.

The centre of mass of the tumour on the preoperative CT scan was determined and set as the origin. After registration of the tumour on the XperCT scan the new position of this centre of mass is determined and shown in Table 3-4. The difference between the origin and the new position between the observers was compared. The mean displacement for patient 1 was 0.39 ± 0.14 cm in LR direction, -1.21 ± 0.52 cm in CC direction and 0.13 ± 0.10 cm in AP direction. For patient 2 this was 0.21 ± 0.20 cm, -0.53 ± 0.33 cm and -0.14 ± 0.23 cm in LR, CC and AP direction respectively.

The amount of overlap between the observers was determined. The amount of overlap is defined as the common area divided by the encompassing (see Figure 16 for a schematic).

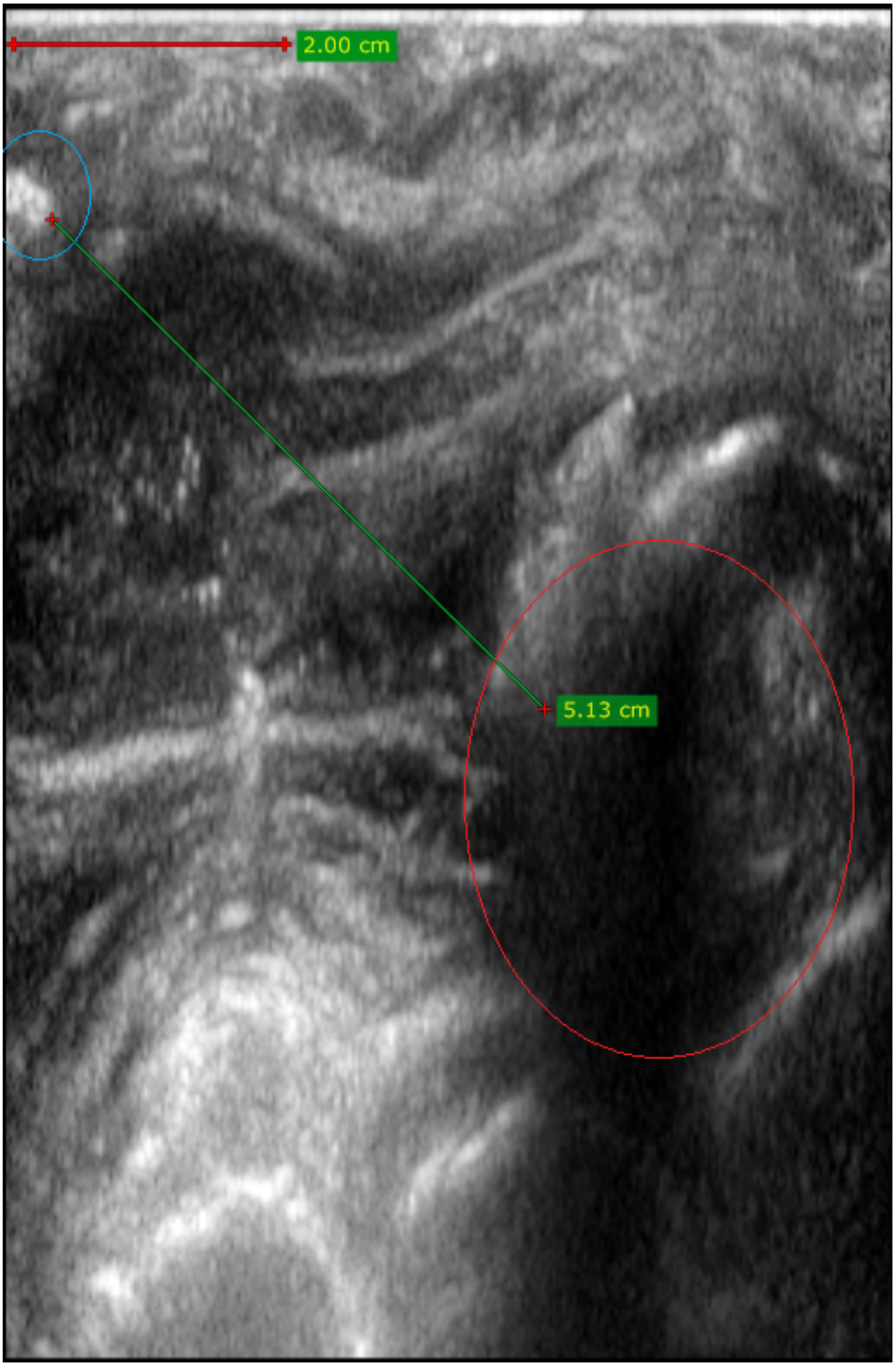

Figure 3-18: Distance between the location of the stitch (blue circle) and the tumour (red circle). The image is seen at 200% of the original size.

Table 3-4: Differences in displacement [cm] between the original tumour position and the new position between the observers.

	Patient 1			Patient 2		
	LR	CC	AP	LR	CC	AP
Observer 1	0.44	-2.10	0.18	0.16	-0.07	0.04
Observer 2	0.55	-0.90	0.23	-0.02	-0.79	-0.20
Observer 3	0.41	-0.95	0.14	0.16	-0.35	0.08
Observer 4	0.16	-0.88	-0.04	0.54	-0.90	-0.49
Mean displacement	*0.39*	*-1.21*	*0.13*	*0.21*	*-0.53*	*-0.14*
SD displacement	*0.14*	*0.52*	*0.10*	*0.20*	*0.33*	*0.23*

Table 3-5: The amount of overlap (DICE) between observers. Values between 0 and 1, where 0 is no overlap and 1 is complete overlap.

	Patient 1			Patient 2		
	Observer 2	Observer 3	Observer 4	Observer 2	Observer 3	Observer 4
Observer 1	0.00	0.00	0.00	0.31	0.63	0.19
Observer 2		0.60	0.33		0.38	0.45
Observer 3			0.40			0.23

The tumour of patient 1 was small, the volume was about 0.5 cc. The tumour of patient 2 had a volume of 5 cc.

The amount of overlap (Dice similarity coefficient (DICE)) is defined as a value between 0 and 1, where 0 is no overlap between the matches and 1 is complete overlap between observers, meaning that the match is exactly the same. For patient 1, observer 1 did not have any overlap with the other observers. Observers 2 and 3 showed the most overlap between the tumour matches. The amount of overlap between the observers is shown in Table 3-5. A visual rendering of the displacements in tumour matching between the different observers for patient 1 is shown in Figure 3-19 . Appendix G shows a table with all values of the common area and the encompass that resulted in the values for the overlap between observers stated in Table 3-5. Appendix H shows the rendering of tumour matching between the observers of patient 1 in sagittal view and of patient 2 in coronal and sagittal view respectively.

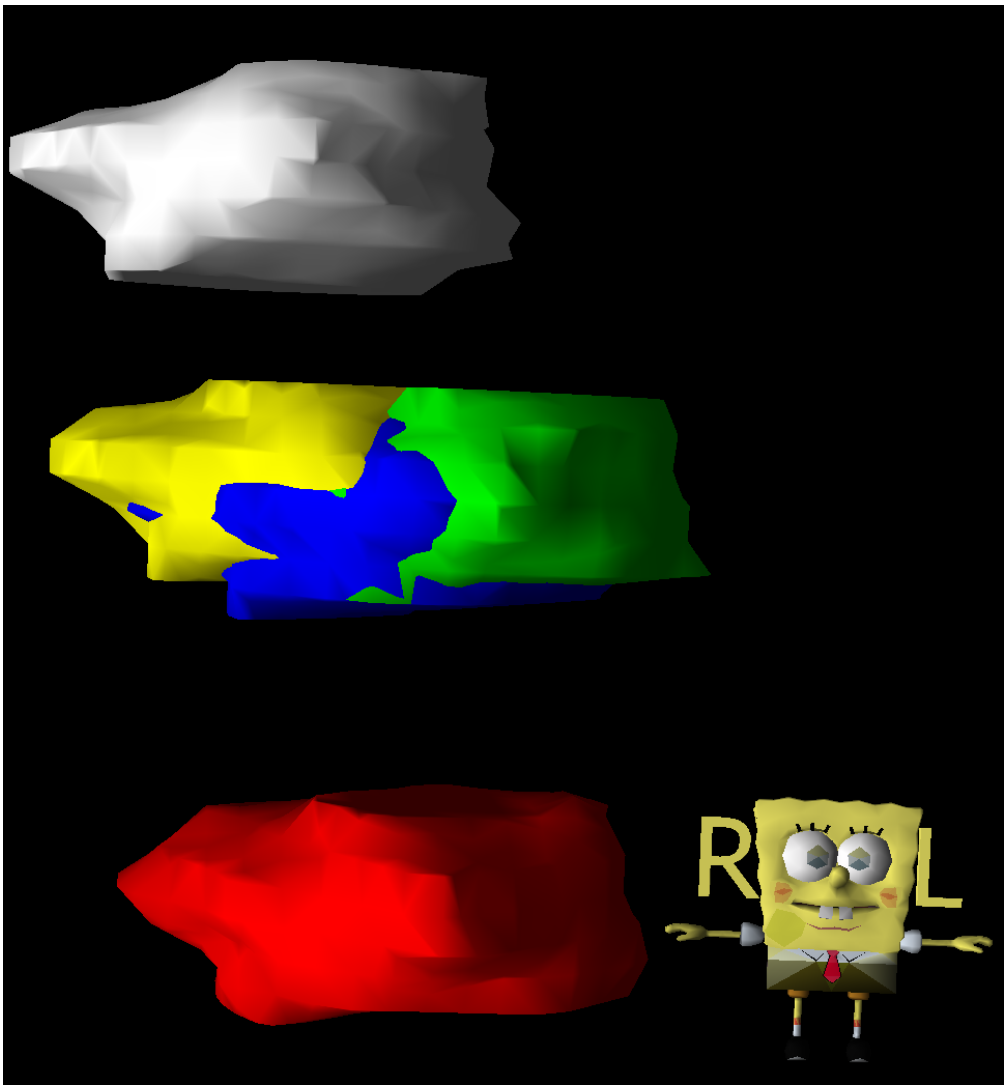

Figure 3-19: Rendering of the displacements in tumour matching between the different observers for patient 1 in coronal view. White is the original tumour location and the colours red, green, blue and yellow are the displacements of observers 1-4 respectively.

Chapter 4

Discussion

The goal of this discussion is to address the primary and secondary objectives and discuss the results. The primary objective of this study was to evaluate the feasibility of an in-house developed electromagnetic navigation system with real-time tumour tracking in rectal cancer surgery. Before the study was implemented several sub goals were addressed. The workflow and navigation setup were evaluated and adapted to the new situation, the accuracy of the window field generator (WFG) was tested and the implantation and fixation method for the tumour sensor was designed. The method is evaluated and both the ex-vivo and in-vivo results and experiences are discussed. When the study was implemented the outcome parameters of the in-vivo study were discussed and the last sub goal, verification of image registration accuracy, was addressed.

4-1 Incorporation of the field generator into the navigation setup

To ensure the field generator was incorporated in a stable and save manner, requirements for the incorporation of the field generator were determined in the methods Section 2-3. Next, the results from Section 3-1 are discussed.

The WFG was designed with straps for placement under an operating table, so this would have been the logical choice for mounting. Mounting under the table was preferred, since no changes to the table setup would have been needed and this would have been the least labour intensive and the least expensive.

However, the dedicated imaging operating room (OR) table did not allow for mounting under the table. There was only one pair of leg blades available, that could be used in this type of surgery in combination with the imaging part of the bed, and they obstructed placement under the table. Also, during surgery it should be possible to change the position of the leg blades so the surgeon is not hindered in doing his work as usual, this was not the case if the WFG had been placed under the table. A new table with an elongated carbon fibre imaging part and different leg blades is being designed, this however would probably have taken over

a year before it would be available for use. Waiting for this table to be ready for use would have taken too long, so this left placement of the field generator on the table.

Placing it on the table required the design of a new mattress. The mattress that was designed fulfils the set requirements. However, one thing was not taken into account while designing the mattress. The regular mattress needs to be on top of the imaging mattress. As a result, the measurement volume that can be used is reduced with the thickness of the regular mattress, which is approximately 5 cm. Accuracy decreases with distance from the field generator. Unfortunately the part of the Electromagnetic (EM) field with the highest accuracy, closest to the field generator, now remains unused. For this study this should not be the cause of any problems, since most sensors are close to the field generator.

In supine position two sensors were placed on the back and one in the groin. The two sensors on the back and the tumour sensor were fairly close to the base of the FG. In prone position it would therefore be wise to place two sensors on the abdomen or in the groin and one on the back to make sure enough sensors are in the EM field and close to the base of the FG (at least two reference sensors are needed for tracking). The distance of the sensor to the field generator could potentially cause problems in other navigation studies. For liver surgery for instance it could cause problems. The liver is located high up in the abdomen, far from the field generator. It is possible the tumour sensor will be out of reach from the field generator and cannot be detected.

4-2 Accuracy of the window field generator

The second sub goal was to evaluate the accuracy of the field generator in test and OR setting. The results from Section 3-2 are discussed.

It was found that both position jitter and root-mean-square error (RMSE) are dependent on the distance to the field generator. The vector jitter was approximately 0.02 cm within 45 cm from the WFG in both the test and OR setup as seen in Figure 3-5 and Figure 3-11. There was no literature found about the NDI WFG, but position RMSE and jitter for the table top field generator (TTFG) were determined in a paper by Nijkamp et al., [37]. According to this paper the position jitter was 0.1 cm standard deviation (SD) within 45 cm distance from the TTFG. The jitter found in this study was a factor 5 smaller compared to the values found in literature. Also, the maximum jitter that was found did not rise above 0.1 cm SD. This gives enough reason to believe that jitter will be of little influence.

According to Northern Digital Inc. (NDI), the absolute accuracy of the WFG is similar to the TTFG. However, the results of this study showed something different. In the test setup, the RMSE was approximately 0.36 cm at 30 cm from the WFG increasing to 1.10 cm at 45 cm distance from the WFG (see Figure 3-6 and Table 3-1). The RMSE for the WFG is approximately two to three times as high as for the TTFG. The paper of Nijkamp et al. shows that position RMSE was approximately 0.1 cm up to 32 cm distance, increasing to 0.4 cm at 52 cm distance, [37]. An error of more than 1 cm at 45 cm from the field generator is quite large. During surgery this error could result in damaging critical structures.

Though, in test setting the measurements with the WFG were compared to optical tracking measurements and in the OR the relative distances between sensors on the sensor plate were measured making the results not exactly comparable, the error in the OR seems a lot higher

than in test setting. To be able to compare these measurements better, measurements with the optical tracker as a reference should still be performed in the OR. The incorporation of the field generator into the mattress prohibits the placement of optical reflective spheres on the field generator. To do these measurements the field generator could be tested in the OR without being placed inside the mattress, this was not done during this study however.

The relative distance measurements show that up to 30 cm from the WFG, the difference between sensors 1 and 4 varied between 14.8-15.6 cm. This is a difference of 0.8 cm between the highest and the lowest measurement value, where the distance between the sensors is actually 15 cm. This is quite a large deviation, showing that the accuracy in the OR is not quite as good as we had expected. To be able to rely on the navigation it needs to be more accurate.

Results showed that part of the inaccuracy seemed to have a systematic nature which could be corrected with an exponential function. Differences in the values measured by the WFG and by the optical system occur mainly in the Z-direction, however a slight deviation in the x- and y-direction is also seen. Potentially, three functions could be fitted to describe the errors in the x- y- and z-direction separately, and these can be used to correct for the systemic error. Results from other literature support this idea, [37], [50]. Calibration of the device by the manufacturer might also reduce the systemic error. However, we already worked with two window field generators and both showed the same problems, so it could also be possible that calibration is not a solution for this problem, but that the development of the device should be improved. In the OR environment there are also dynamic errors present, which cannot be corrected for with a calibration of the field generator.

For tracking of mobile tumours both position and orientation information is important. In this study only the positional accuracy of the WFG is tested. The reason for accuracy testing was to be able to compare the accuracy of the TTFG and the WFG. It was thought that testing the positional accuracy would be enough to compare both field generators.

The surgeons in our hospital would like to have a 1 mm and 1° accuracy, [37]. The WFG does not comply in this first criterion and the second has yet to be tested. The WFG obviously has a lower accuracy, however for tracking of mobile tumours the image quality of the TTFG is insufficient and this field generator cannot be used in this study. The better image quality in the WFG is a large advantage and necessary for coupling of the tumour delineation to the tumour sensor. The TTFG has the large advantage that it is able to shield the magnetic field above from the table below. The WFG does not have a shielding mechanism. This could explain the difference in accuracy between both field generators. To be able to rely on the tumour tracking device as a surgical tool, tracking accuracy has to be improved. Currently, the accuracy is too low and can cause more damage than when it is not used at all. Possibly, the TTFG generator could be used if it would be removed during imaging and put back after imaging. This would require a matrass where the TTFG could slide in and out. The downside is that you cannot assess the sensor positions directly after imaging, since the field generator is removed during imaging. This could pose a problem if the tumour moves in the meantime.

4-3 Sensor implantation and fixation

The third sub-goal was to design a sensor implantation and fixation method. The results from Section 3-3 and corresponding in-vivo results from Section 3-5-1. are discussed. To deliver the sensor a proctoscope was chosen as the best device. For rectal tumours up to 10 cm from the anus this device suffices. It is easy to use and is not a risk for failure of the sensor placement. If the study should be taken to another level and sensors would be implanted in other parts of the bowel as well, a proctoscope will not be sufficient. In the future, an endoscope would be more useful to deliver a sensor. However, this would also require wireless sensors and for now this is not possible. The design of the fixation method and the ex-vivo and in-vivo results are discussed in the following sections.

4-3-1 Ex-vivo sensor implantation and fixation

For sensor fixation, previous research showed that anchoring, plugging or gluing the sensor to the rectum wall or tumour are the most valid fixation methods, [46]. In this study we decided that gluing would be the most easy and least invasive method for sensor fixation. This method will probably not suffice in the future, yet, in the future these wired sensor will probably be exchanged for wireless sensors. As the goal of this study is to evaluate the feasibility of the tracking system, this sensor fixation method was expected to be sufficient to reach this goal.

In choosing the glue, several things were taken into account. There are many types of glue available on the market. For budgetary reasons it was chosen to focus on only 3 glues at first instance. If these glues would prove to be insufficient, more glues would be looked into. Blue Histoacryl and Dermabond were already available in the hospital and are topical skin adhesives. Since both are skin adhesives and need quite dry surface to glue on, another type of glue was sought. The bowel wall contains a mucosal layer and the glue should be compatible with this type of surface. In literature was found that PeriAcryl90, which is often used in orthodontic procedures, was used to glue sensors to the surface of the tongue, [51].

Since the glue agglutinates on the mucosa of the oral cavity, it was expected it would also function properly on the mucosa of the rectal wall. Blue Histoacryl and PeriAcryl90 showed many similar characteristics. The disadvantage of blue Histoacryl was that it is very fluid and flew down the tissue quickly before polymerisation had taken place, so this glue was eliminated after the first test.

Since the delay before starting the surgery should be limited as much as possible, Dermabond had the advantage of a quick polymerisation time. However this quick polymerisation time for Dermabond is also a pitfall. Polymerisation starts directly when it is out of the applicator, so quick application is needed. This could result in poor fixation. The easiness of gluing was better for PeriAcryl90, since it only polymerises when in contact with physiological fluids. The hardness of Dermabond caused the glue not to adapt to the shape of the bowel, as PeryAcryl90 does, this resulted in the glue to detach quite quickly. Though PeriAcryl90 has a longer polymerisation time, the benefits of this glue with respect to Dermabond, and the disadvantages of Dermabond, resulted in choosing PeriAcryl90 for fixation of the sensor.

4-3-2 In-vivo sensor implantation and fixation

The sensor implantation and fixation method with PeriAcryl90 was successful in ex-vivo research, so it was decided that the method was ready for in-vivo use. To receive successful interpretable navigation data, the successful implantation of the sensor is vital. So far, successful sensor fixation, and therefore obtained data, has succeeded in only one of three patients. Extra time needed for the navigation procedure was within the set limits. The main issue in the navigation procedure was fixating the sensor to the tumour, directly influencing the successful delivery of interpretable data.

Results from ex-vivo experiments gave reason to believe that gluing the sensor is a sufficient fixation method. In the OR however, it proved very difficult to glue the sensor to the bowel. There were several factors different between the in- and ex-vivo setting and that could have contributed to failed sensor fixation. First there are differences between in- and ex-vivo tissue. Where in-vivo tissue is well perfused and at body temperature, the specimen that is tested is out of the body for about 15-30 minutes before sensor fixation. The temperature of the specimen has probably lowered a few degrees and perfusion is obviously absent.

Second, for proper fixation the surface of the bowel should be as dry and clean as possible. In in-vivo tissue, mucus forming or the cleanliness of the bowel might be of impact on the fixation. Even though PeriAcryl90 is designed for mucous tissue, too much fluid might deteriorate the fixation strength. Third, the distance from the anus to the tumour might be of influence on the ease of sensor placement. Further, the experience with handling the tools, of the person who places the sensor, is probably of influence on the quality of sensor placement.

In the first patient that was operated the tumour was located very deep, on the outer reach of the proctoscope. Also the placement of the sensor was done by a not surgically educated researcher (the author of this report). With little experience in this field, placing the sensor without assistance from an experienced surgeon proved to be a challenge. It was quite difficult to glue the sensor, since the glue kept hardening quite fast. The glue actually hardened in the needle, disabling it. The glue also stuck to the proctoscope and the surgical forceps, such that the sensor came out of the rectum when removing the surgical tools.

Since gluing did not work, clipping the sensor to the tumour was attempted. The clipping device was easy to use through the proctoscope, however the hold on the tissue was not easy to accomplish. Finally clipping succeeded and one clip was placed on the wire and one was on the sensor itself. However, the navigation system was not able to detect the sensor and the navigation procedure could not proceed.

After the procedure, the sensor was taken for testing. It appeared that the sensor could be detected by the navigation system, but could not give reliable data. This most likely means that the wire was still intact, but that the clip on the sensor probably twisted the sensor out of shape. After trying to straighten the sensor, it was broken.

For the second patient it was decided that the sensor would be clipped to the tissue. Clipping directly on the sensor or wire directly is not recommended. To be able to clip the sensor to the tissue without damaging the sensor, it was sewn into a vicryl mesh. In the OR clipping proved to be difficult once again, so it was decided to stitch the vicryl mesh to the tissue. Apparently the clips do not result in a strong hold on the tissue so this method should be rejected. Stitching is also not a solution to the problem. It was only possible since the tumour

was 3 cm from the anus and it could easily be reached. In many patients this is not the case and stitching the sensor into the depth through the proctoscope will probably be too difficult and time-consuming and is dissuaded.

After the second patient was operated on, another ex-vivo specimen was available for fixation tests. The tests were performed with an experienced surgeon. The change in approach, using a pipette instead of a needle, was very successful. It was very easy to glue the sensor to the tissue and the glue did not harden into the pipette. It was quite easy to scrape of the abundant amount of glue from the pipette so it could be used multiple times. This resulted in the decision to use this approach in the following procedure with the requirement that the surgeon would be present to place the sensor.

For, the next patient the same experienced surgeon was present to perform the sensor fixation. The change of approach was successful in terms of being able to glue the sensor to the tissue without the glue sticking to the pipette, surgical forceps or the proctoscope. The sensor, however, came out with an excrement after several minutes. The patient did not receive proper bowel preparation before the surgery and his intestines were quite dirty, so this could be a reason for the failed fixation. The patient kept excreting faeces and at one point it was quite a large excrement that pulled the sensor along with it. Secondly, the waiting time of 5 minutes for the glue to dry was not abided. After a few minutes the proctoscope was retracted, this might have had an influence on the strength of the fixation.

Finally, to make sure the sensor cannot be pulled loose accidentally, the wire was stitched to the patient's bottom. To distribute the forces on the wire, the first part of the sensor wire (0.5 - 1 cm) could be glued to the bowel as well. Caution is needed when the sensor wire is glued to the tissue. More glue on a larger surface is used, so the risk of glue sticking to the proctoscope is higher and this should be prevented. Second, in LAR procedures an anastomosis is made, so the sensor and the first part of the wire should not be glued too far from the tumour.

After all these fixation difficulties in every single patient, it is strongly advised to evaluate the method of sensor fixation. The fixation could be attempted one more time, but the patient should have received had proper bowel preparation and the sensor should be placed by the same experienced surgeon. Keeping the time restraint of 5 minutes is strictly advised. In this study the focus was on gluing, since it would have been the least invasive option. If gluing were successful that would have been superior, however there are strong indications that this is not the case. If sensor fixation fails again, when all the circumstantial problems are minimised, it is very likely that gluing in general is not the right approach. It is recommended that other options besides gluing are explored.

In previous research, a design for anchoring the sensor was proposed, [46]. It is recommended that this approach is reconsidered as a fixation method. Further, the use of wireless sensors in the future could be an immense improvement. The calypso transponder tracking system (Varian Medical Systems Inc., Palo Alto, California, USA) might be one of those potentially valuable wireless tracking systems. It is developed for tumour tracking in radiation therapy and not for computer assisted interventions. Franz et al. applied the standardized assessment protocol by Hummel et al. to the calypso system to test the accuracy of the system. In an ideal environment the accuracy is below 1 mm, which is comparable to other tracking systems, [50], [52].

4-4 Outcome parameters in-vivo study

The main study parameter was to evaluate the feasibility of the navigation system during real-time tumour tracking in rectal surgery. Feasibility is primarily evaluated by judging the successful delivery of interpretable navigation data per procedure. This is discussed in Section 4-3-1. Next results from Section 3-5-2 are discussed. Secondary study parameters were the determination of the accuracy of the navigation towards anatomical landmarks and the correlation of the navigation data with ultrasound.

Also the position RMSE of the sensor registration accuracy was continually calculated while the navigation program was running. The mean RMSE was 0.515 cm. This was slightly higher than the results in the chain test, but the RMSE stayed under the set boundary of 0.8 cm. Though this value is stated as acceptable, the accuracy is not quite as good as the results from the TTFG, which is around 0.1-0.2 cm. The WFG field generator does not have shielding, which is highly likely the cause of this lower sensor registration accuracy.

4-4-1 Accuracy towards anatomical landmarks

During the procedure, adaptations can be done manually to improve the accuracy. By hovering the blunt tip probe over the landmarks, the discrepancy between the location of the pointer tip in reality and the location seen in the 3D image can be corrected. So far, we were able to do the navigation procedure in only one patient. In abdominal navigation there are several landmarks that can be used for verification of the accuracy. In prone position this is not the case. The coccyx is about the only structure we were able to do the navigation accuracy verification on.

The navigation procedure in patient 2 was done in prone position and it proved to be quite difficult to provide proper tracking accuracy with only one landmark to evaluate this on. The coccyx is the most rigid structure to do the registration on, unfortunately, the actual rigidity of the coccyx is questionable.

Besides that, in patient 2 the coccyx was not properly segmented making the registration even less reliable. The segmentation was done automatically and not checked properly, so for the next patients the coccyx should be segmented manually to have a delineation that is as accurate as possible. After manual adaptations the accuracy was visually within 3 mm of the coccyx, however with the unreliable segmentation this result is also unreliable.

In retrospect, the coccyx was delineated manually and the adaptations were checked. At first there was quite a large difference between the actual location of the pointer tip on the coccygeal bone and were it was seen in the 3D model. When the coccyx was delineated properly it was seen that this difference was much smaller. During surgery the pointer tip location was adapted in anteroposterior (AP) direction mostly. It was moved about a centimetre in posterior direction and a few millimetres in left-right (LR) and craniocaudal (CC) direction. After manually delineating the coccyx it showed that the adaptation should have moved a few millimetres in anterior direction instead. So with the adaptations the accuracy was decreased even more, since they were in the wrong direction.

4-4-2 Correlation with ultrasound

The correlation of navigation with ultrasound is not possible, so we were not able to gather useful data.

It was possible to determine the distance from the pointer tip location to the tumour sensor. This data could easily be extracted from the navigation data that was recorded continuously. The sensor however cannot be recognised on ultrasound. Though the tip of the pointer can be fairly accurately found by placing a stitch on the specimen and placing the ultrasound device on the stitch, it is not possible to exactly know where the sensor is located with respect to the tumour based on ultrasound. The tumour is, but since we do not know where the sensor is exactly with respect to the tumour, there is inaccuracy in the outcome.

It would be possible to locate the tumour sensor in other imaging modalities, the preferred choice would be computed tomography (CT). This would be a good option instead of ultrasound as a reference method. We should then place a clip on the pointer location, since this could also be easily identified on the CT scan. In this manner we could directly correlate the distance from the pointer tip to the sensor location and determine the accuracy of the navigation system.

4-5 Verification of image registration accuracy

The last sub-goal is to verify the image registration accuracy during surgery. Results from section Section 3-5-3 are discussed.

The tumour can almost never be distinguished on CT, so the tumour cannot be used for matching. Preferably the structure used for matching is properly distinguished on CT and the position of the tumour with respect to this structure should not change. Therefore tumours were matched based on the delineated rectum. This means that the rectum should always be delineated and added to the 3D model.

The tumours of two included patients, were matched by 4 different observers to determine the reproducibility of the registration. The difference between the original and the new position of the tumour between the observers was compared. What could be seen in Figure 3-19 and in the data and figures shown in Appendix H, as well as the data shown in Table 3-5 and Appendix G is that there is a fairly large inter-observer variation. For patient 1, there was even one observer that did not have any overlap in the tumour registration compared to the other observers.

The mean displacement was calculated and it can be seen that in some directions (LR, CC or AP) the standard deviation of the displacement is of similar size or even higher than the mean displacement value. Meaning that the variation between the observers is quite large.

The Dice similarity coefficient (DICE) can be used as a statistical validation metric to evaluate the performance of the reproducibility of manual segmentations between observers. However, it is not robust in terms of target size, [53]. This makes it difficult to compare the DICE values for both patients, since the tumour of patient 1 was 0.5 cc and the tumour of patient 2 was 5 cc, a factor 10 larger. In both patients the DICE is quite low, ranging between 0.33-0.60 in patient 1 and 0.19-0.63 in patient 2. Before the navigation system can be used to make clinical decisions, the image registration should be much more accurate.

Chapter 5

Conclusions and recommendations

5-1 General conclusions

This section gives an overview of the general conclusions about the primary and secondary objectives. First the secondary objectives will be elaborated on and finally the conclusions on the primary objective will be noted.

5-1-1 Evaluation of the workflow and setup of the navigation procedure

The current setup of the navigation procedure and workflow is adapted to the new navigation situation. To place the window field generator (WFG) on the table a custom made matrass that incorporates the WFG was successfully designed. The addition of the top mattress was not taken into account in the design process but this should not cause any problems in this navigation study. The workflow in the operating room (OR) is feasible in terms of extra time needed.

5-1-2 Accuracy of the window field generator

The WFG improves the image quality so the soft tissue in the abdomen can be recognized and used for registration. Both position jitter and root-mean-square error (RMSE) are dependent on the distance to the field generator. The largest error occurred in the z-direction. The jitter found in this study was a factor 5 smaller compared to the values found in literature. This gives enough reason to believe that jitter will be of little influence.

The RMSE for the WFG is approximately two to three times as high as for the table top field generator (TTFG) in test setting and the error in the OR seems a lot higher than in test setting. Calibration of the device by the manufacturer might reduce the systemic error, this however does not account for the dynamic errors in the OR. It is more likely that the WFG needs further development.

The surgeons in our hospital would like to have a 1 mm and 1° accuracy. The WFG does not comply in this first criterion and the second has yet to be tested. To be able to rely on the tumour tracking device as a surgical tool, tracking accuracy has to be improved. Currently, the accuracy is too low and can cause more damage than when it is not used at all.

5-1-3 Sensor implantation and fixation method design

To place a sensor on rectal tumours up to 10 cm from the anus a proctoscope suffices. PeriAcryl90 worked in ex-vivo experiments, it can be kept outside the original container until applied and it is easy to apply. After in-vivo fixation difficulties in every single patient, it is strongly advised to evaluate the method of sensor fixation. The fixation could be attempted once more, if the patient is properly prepared, the sensor is placed by the same experienced surgeon and the time restraint of 5 minutes is strictly advised. If sensor fixation fails again it should be evaluated and other options besides gluing should be explored.

5-1-4 Image registration accuracy

The tumour itself cannot be used for matching. The rectum can properly be distinguished on computed tomography (CT) and the position of the tumour with respect to rectum does not change. Therefore the tumour should be matched based on the delineated rectum. Further, the inter-observer variation is too large, making the registration method not yet accurate enough for clinical use.

5-1-5 Feasibility of the in-house developed electromagnetic navigation system with real-time tumour tracking in rectal cancer surgery

Feasibility can only be determined after finishing the study, and is defined as the successful completion of the whole investigational workflow resulting in continuous delivery of interpretable navigation data for rectal surgery.

However, preliminary conclusions could be drawn. The workflow seems feasible in terms of extra time needed. The navigation system in the current setup is not accurate enough for clinical use. The field generator itself is not accurate enough and the current sensor implantation method does not deliver interpretable data. Further, the image registration method is not yet accurate enough for clinical use.

5-2 Future recommendations

Real-time electromagnetic tracking in general is a very promising technique. The clinical challenge in cancer surgery is to find a balance between radicality of surgery and preservation of function and the knowledge of the exact tumour location during surgery would be a large advantage. Though the technique is very promising there are many challenges ahead.

5-2-1 Accuracy of the field generator

Even though the window field generator is a large improvement in terms of image quality, necessary for tumour matching, this field generator is not accurate enough to be used in a clinical setting where surgeons depend on the tracking system for guidance. For this study, the accuracy sufficed to be able to assess the feasibility of the navigation system. However, the system needs more development by the manufacturer or another company that will take the job of improving the accuracy. If the system is not being developed further, the use of this system should not be prolonged and the tumour matching should be achieved in another manner.

The most promising way would be to implant a sensor before the preoperative CT scan is acquired. The sensor can also be added to the 3D model. In this way the match can be done on the sensor itself and the location of the sensor with respect to the tumour can be determined exactly. If a sensor is implanted before the CT scan, this would preferably a wireless sensor. For one, it would not be comfortable for a patient to have a wire hanging out of their anus for a day or more. Second, wireless sensors could also be implanted more than a day before surgery and also in other locations than the rectum, providing a whole new range of tumour locations for real-time tracking.

5-2-2 Sensor fixation

Proper sensor fixation is a key issue for the success of the study and this method should be evaluated. This study showed that gluing the sensor, even though the ex-vivo tests showed differently, is not the best method for fixation. The development of a device that can inject the sensor and anchor the sensor in place is probably the best direction to take in this research. A method was already designed by de Jonge in 2014, [46]. It should be taken into account that, with the high probability of wireless sensors being available in the near future, the wired sensors will not be needed any more. So both the method for sensor fixation by de Jonge and the introduction of wireless sensors could be explored. The first method would only have added value if the latter would take too much time before it can be introduced into the clinical setting.

5-2-3 Correlation of navigation with another imaging modality

Correlation of the navigation accuracy with US in this study was not successful. The sensor was not visible on the US images, making it impossible correlate the data properly. To be able to correlate the accuracy, another imaging modality that is able to recognize the sensor should be used. CT would be the most obvious choice. The sensor could be recognized on CT images and if the pointer location is marked with a clip that is recognizable on CT, this data could be correlated.

5-2-4 Wireless tracking sensors

The most important recommendation that can be given is to implement wireless sensors as soon as possible. With the introduction of wireless sensors that can be implanted before the

Figure 5-1: Calypso transponder tracking system beacons, adopted from [55].

CT scan is acquired and that are visible on the scan, the need for the WFG is eliminated. Instead of matching the tumour location on the soft tissue of the bowel, the match can be performed on the implanted sensors. This would most likely also improve image registration accuracy. As long as image registration is based on soft tissue structures, the variability between observers will probably not improve much. For one, the observers are not experts in judging the images and this will take a lot of time and practice. Asking experts, the radiologists, would be difficult to implement.

The calypso transponder tracking system (Varian Medical Systems Inc., Palo Alto, California, USA) might be one of those potentially valuable wireless tracking systems. Franz et al. showed that, in an ideal environment, the accuracy is below 1 mm, which is comparable to other tracking systems, [52]. The tracking sensors are very small (less than 1 cm) and there is an implantation device to place the sensors (Figure 33). The sensors are clearly visible on CT scans as seen in Figure 34. This system is currently approved by the Food and Drug Administration (FDA) for use in prostate and post-prostatectomy prostate bed radiation therapy in America, [54]. Unpublished in-house research shows very promising results in a breast cancer phantom study.

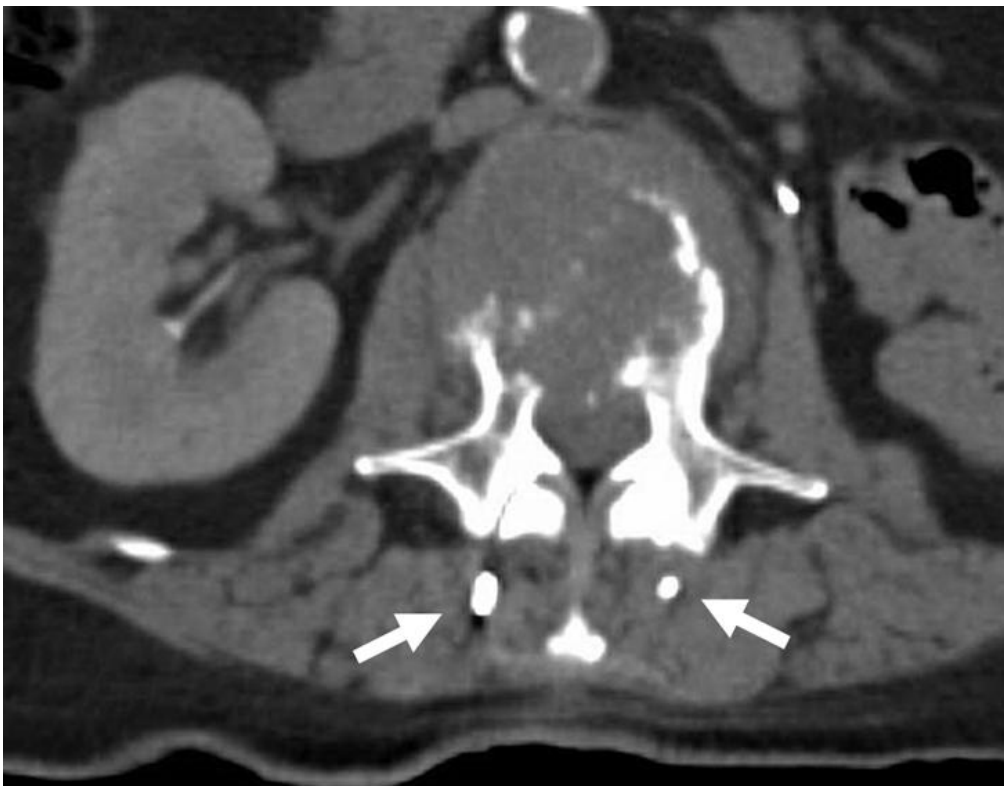

Figure 5-2: Calypso beacons seen in CT scan (white arrows), adopted from [54].

Bibliography

[1] L. A. Torre, F. Bray, R. L. Siegel, J. Ferlay, J. Lortet-Tieulent, and A. Jemal, "Global Cancer Statistics," 2012. doi:10.3322/caac.21262.

[2] J. Ferlay, I. Soerjomataram, M. Ervik, R. Dikshit, S. Eser, C. Mathers, M. Rebelo, D. Parkin, D. Forman, and F. Bray, "GLOBOCAN 2012 v1.0, Cancer Incidence and Mortality Worldwide: IARC CancerBase No. 11." http://globocan.iarc.fr, 2013.

[3] IKNL, "Cijfers over Kanker." http://www.cijfersoverkanker.nl/selecties/, 2016.

[4] RIVM, "Bevolkingsonderzoek Darmkanker - Rapportage 2014," tech. rep., Erasmus MC and NKI/AvL, 2015.

[5] IKNL, "Colorectaalcarcinoom, Landelijke richtlijn versie 3.0," tech. rep., Integraal Kankercentrum Nederland (IKNL), 2014.

[6] DeMerck, "deMerck Manual Medisch Handboek." http://www.merckmanual.nl/mmhenl/print/sec09/ch131/ch131i.html, 2003.

[7] K. Moore and A. Dalley, *Clinically Oriented Anatomy*. LippincottWilliams&Wilkins, 5th ed., 2005.

[8] SEER, "SEER Training Modules, Colorectal.." http://training.seer.cancer.gov/colorectal/. US National Institutes of Health, National Cancer Institute.

[9] OpenStax CNX, "Overview of the Digestive System. Anatomy and Physiology," in *Anatomy and Physiology*, ch. 23, 2013.

[10] R. Rubin and D. Strayer, *Rubin's Pathology*. Lippincott Williams and Wilkins, 5 ed., 2008.

[11] P. Kumar and M. Clarke, *Clinical Medicine*. Elsevier Saunders, 6 ed., 2005.

[12] S. Hamza, V. Cottet, N. Touillon, V. Dancourt, C. Bonithon-Kopp, C. Lepage, and J. Faivre, "Long-term effect of faecal occult blood screening on incidence and mortality

from colorectal cancer," *Digestive and Liver Disease*, vol. 46, no. 12, pp. 1121–1125, 2014. doi:10.1016/j.dld.2014.08.041.

[13] A. G. Zauber, "The impact of screening on colorectal cancer mortality and incidence: has it really made a difference?," *Digestive diseases and sciences*, vol. 60, no. 3, pp. 681–691, 2015. doi:10.1007/s10620-015-3600-5.

[14] R. Heald and B. Moran, "Embriology and anatomy of the rectum," *Semin Surg Oncol*, vol. 15, pp. 66–71, 1998.

[15] F.-Y. Li and M.-D. Lai, "Colorectal cancer, one entity or three," *Journal of Zhejiang University SCIENCE B*, vol. 10, no. 3, pp. 219–229, 2009. doi:10.1631/jzus.B0820273.

[16] K. Tamas, A. M. E. Walenkamp, E. G. E. de Vries, M. A. T. M. van Vugt, R. G. Beets-Tan, B. van Etten, D. J. A. de Groot, and G. A. P. Hospers, "Rectal and colon cancer: Not just a different anatomic site," *Cancer Treatment Reviews*, vol. 41, no. 8, pp. 671–679, 2015. doi:10.1016/j.ctrv.2015.06.007.

[17] R. Bleday and D. Shibata, "Surgical resection of primary rectal adenocarcinoma." http://www.uptodate.com/contents/surgical-resection-of-primary-rectal-adenocarcinoma, 2015.

[18] K. C. Peeters, C. a.M. Marijnen, I. D. Nagtegaal, E. K. Kranenbarg, H. Putter, T. Wiggers, H. Rutten, L. Pahlman, B. Glimelius, J. W. Leer, and C. J. van de Velde, "The TME Trial After a Median Follow-up of 6 Years," *Annals of Surgery*, vol. 246, no. 5, pp. 693–701, 2007. doi: 10.1097/01.sla.0000257358.56863.ce.

[19] J. K. MacFarlane, R. D. Ryall, and R. J. Heald, "Mesorectal excision for rectal cancer.," *Lancet (London, England)*, vol. 341, no. 8843, pp. 457–60, 1993.

[20] A. L. Martling, T. Holm, L.-E. Rutqvist, B. Moran, R. Heald, and B. Cedermark, "Effect of a surgical training programme on outcome of rectal cancer in the County of Stockholm," *The Lancet*, vol. 356, no. 9224, pp. 93–96, 2000. doi:10.1016/S0140-6736(00)02469-7.

[21] E. Kapiteijn, H. Putter, and C. J. H. Van de Velde, "Impact of the introduction and training of total mesorectal excision on recurrence and survival in rectal cancer in the Netherlands. The cooperative investigators of the Dutch ColoRectal Cancer Group.," *British Journal of Surgery*, vol. 89, pp. 1142–1149, 2002.

[22] R. J. Heald, E. M. Husband, and R. D. Ryall, "The mesorectum in rectal cancer surgery–the clue to pelvic recurrence?," *The British journal of surgery*, vol. 69, no. 10, pp. 613–616, 1982. doi:10.1007/s11725-008-0110-z.

[23] Netherlands Cancer Institute - Antoni van Leeuwenhoek Hospital, "Radiotherapie bij rectumkanker." https://www.avl.nl/behandelingen/radiotherapie-bij-rectumkanker/.

[24] I. D. Nagtegaal and P. Quirke, "What is the role for the circumferential margin in the modern treatment of rectal cancer?," *Journal of Clinical Oncology*, vol. 26, no. 2, pp. 303–312, 2008. doi:10.1200/JCO.2007.12.7027.

[25] Dica, "DSCA darmkanker, Jaarrapportage 2014." https://www.dica.nl/jaarrapportage-2014/dsca.html, 2014.

[26] L. Bordeianou, L. H. Maguire, K. Alavi, R. Sudan, P. E. Wise, and A. M. Kaiser, "Sphincter-Sparing Surgery in Patients with Low-Lying Rectal Cancer: Techniques, Oncologic Outcomes, and Functional Results," *Journal of Gastrointestinal Surgery*, vol. 18, no. 7, pp. 1358–1372, 2014. doi:10.1007/s11605-014-2528-y.

[27] A. Alves, Y. Panis, P. Mathieu, F. Kwiatkowski, K. Slim, and G. Mantion, "Mortality and morbidity after surgery of mid and low rectal cancer. Results of a French prospective multicentric study," *Gastroenterologie clinique et biologique*, vol. 29, no. 0399-8320; 5, pp. 509–514, 2005.

[28] S. Atallah, B. Martin-Perez, and S. Larach, "Image-guided real-time navigation for transanal total mesorectal excision: a pilot study," *Techniques in Coloproctology*, vol. 19, no. 11, pp. 679–684, 2015. doi:10.1007/s10151-015-1329-y.

[29] S. Atallah, G. Nassif, and S. Larach, "Stereotactic navigation for TAMIS-TME: opening the gateway to frameless, image-guided abdominal and pelvic surgery," *Surgical Endoscopy and Other Interventional Techniques*, vol. 29, no. 1, pp. 207–211, 2014. doi:10.1007/s00464-014-3655-y.

[30] P. W. A. Willems, J. W. B. Van Der Sprenkel, C. A. F. Tulleken, M. A. Viergever, and M. J. B. Taphoorn, "Neuronavigation and surgery of intracerebral tumours," *Journal of Neurology*, vol. 253, no. 9, pp. 1123–1136, 2006.

[31] G. Eggers, J. Mühling, and R. Marmulla, "Image-to-patient registration techniques in head surgery," *International Journal of Oral and Maxillofacial Surgery*, vol. 35, no. 12, pp. 1081–1095, 2006. doi:10.1016/j.ijom.2006.09.015.

[32] U. Mezger, C. Jendrewski, and M. Bartels, "Navigation in surgery," *Langenbeck's Archives of Surgery*, vol. 398, no. 4, pp. 501–514, 2013. doi:10.1007/s00423-013-1059-4.

[33] J. Zwingmann, G. Konrad, E. Kotter, N. P. Südkamp, and M. Oberst, "Computer-navigated iliosacral screw insertion reduces malposition rate and radiation exposure," *Clinical Orthopaedics and Related Research*, vol. 467, no. 7, pp. 1833–1838, 2009. doi:10.1007/s11999-008-0632-6.

[34] T. Y. C. So, Y. L. Lam, and K. L. Mak, "Computer-assisted navigation in bone tumor surgery: Seamless workflow model and evolution of technique," *Clinical Orthopaedics and Related Research*, vol. 468, no. 11, pp. 2985–2991, 2010.

[35] R. Elfring, M. De La Fuente, and K. Radermacher, "Accuracy of optical localizers for computer aided surgery," *IFMBE Proceedings*, vol. 25, no. 6, pp. 328–330, 2009. doi:10.1007/978-3-642-03906-5-90.

[36] A. M. Franz, T. Haidegger, W. Birkfellner, K. Cleary, T. M. Peters, and L. Maier-Hein, "Electromagnetic tracking in medicine -A review of technology, validation, and applications," *IEEE Transactions on Medical Imaging*, vol. 33, no. 8, pp. 1702–1725, 2014. doi:10.1109/TMI.2014.2321777.

[37] J. Nijkamp, B. Schermers, S. Schmitz, S. de Jonge, K. Kuhlmann, F. van der Heijden, J.-J. Sonke, and T. Ruers, "Comparing position and orientation accuracy of different electromagnetic sensors for tracking during interventions," *International Journal of Computer Assisted Radiology and Surgery*, 2016. doi:10.1007/s11548-015-1348-1.

[38] M. Wagner, M. Gondan, C. Zöllner, J. J. Wünscher, F. Nickel, L. Albala, A. Groch, S. Suwelack, S. Speidel, L. Maier-Hein, B. P. Müller-Stich, and H. G. Kenngott, "Electromagnetic organ tracking allows for real-time compensation of tissue shift in image-guided laparoscopic rectal surgery: results of a phantom study," *Surgical Endoscopy and Other Interventional Techniques*, vol. 30, no. 2, pp. 495–503, 2016.

[39] W. Birkfellner, J. Hummel, and E. Wilson, "Chapter 2 Tracking Devices," *Business*, pp. 23–45, 2008.

[40] V. V. Kindratenko, "A survey of electromagnetic position tracker calibration techniques," *Virtual Reality*, vol. 5, no. 3, pp. 169–182, 2000. doi:10.1007/BF01409422.

[41] NDI, "Aurora V3 User Guide with Window FG." 2014.

[42] L. Maier-Hein, A. M. Franz, W. Birkfellner, J. Hummel, I. Gergel, I. Wegner, and H. P. Meinzer, "Standardized assessment of new electromagnetic field generators in an interventional radiology setting," *Med Phys*, vol. 39, no. 6, pp. 3424–3434, 2012. doi:10.1118/1.4712222.

[43] C. S. D. Jonge, "Clinical preparation , dynamic accuracy assessment and preoperative sensor placement for image-guided rectal surgery using electromagnetic navigation," Tech. Rep. July 2013, Antoni van Leeuwenhoek Hostpital, Amsterdam, 2014.

[44] J. Yoo, S. Schafer, A. Uneri, Y. Otake, A. Khanna, and J. H. Siewerdsen, "An electromagnetic âĂIJ Tracker-in-Table âĂİ configuration for X-ray fluoroscopy and cone-beam CT-guided surgery," no. 8, pp. 1–13, 2013. doi:10.1007/s11548-012-0744-z.

[45] A. Lasso, T. Heffter, A. Rankin, C. Pinter, T. Ungi, and G. Fichtinger, "PLUS: open-source toolkit for ultrasound-guided intervention systems," vol. 61, no. 10, pp. 2527–2537, 2015.

[46] C. S. D. Jonge, "Clinical preparation , dynamic accuracy assessment and preoperative sensor placement for image-guided rectal surgery using electromagnetic navigation," Tech. Rep. July 2013, Amsterdam, 2014.

[47] GluStitch, "PeriAcryl®90 Oral Tissue Adhesive."

[48] Braun, "B . Braun Closure Technologies Clinical Evidence for Histoacryl ® Clinical Evidence for Histoacryl ®," tech. rep., B. Braun Medical B.V., Oss.

[49] Ethicon, "DERMABOND ADVANCED® Topical Skin Adhesive."

[50] J. Hummel, M. Figl, W. Birkfellner, M. R. Bax, R. Shahidi, C. R. Maurer Jr, and H. Bergmann, "Evaluation of a new electromagnetic tracking system using a standardized assessment protocol," *PHYSICS IN MEDICINE AND BIOLOGY*, vol. 205, pp. N205–N210, 2006. doi:10.1088/0031-9155/51/10/N01.

[51] M. Wieling, F. Tomaschek, D. Arnold, M. Tiede, F. Bröker, S. Thiele, S. N. Wood, and R. H. Baayen, "Investigating dialectal differences using articulography," *Journal of Phonetics*, vol. 59, pp. 122–143, 2016.

[52] a. M. Franz, D. Schmitt, A. Seitel, M. Chatrasingh, G. Echner, U. Oelfke, S. Nill, W. Birkfellner, and L. Maier-Hein, "Standardized accuracy assessment of the calypso wireless transponder tracking system," *Physics in Medicine and Biology*, vol. 59, no. 22, p. 6797, 2014. doi:10.1088/0031-9155/59/22/6797.

[53] K. H. Zou, S. K. Warfield, A. Bharatha, C. M. C. Tempany, M. R. Kaus, S. J. Haker, W. M. Wells, F. A. Jolesz, and R. Kikinis, "Statistical Validation of Image Segmentation Quality Based on a Spatial Overlap Index," *Academic Radiology*, vol. 11, no. 2, pp. 178–189, 2004. doi:10.1016/S1076-6332(03)00671-8.

[54] A. P. Shah, P. A. Kupelian, T. R. Willoughby, and S. L. Meeks, "Expanding the use of real-time electromagnetic tracking in radiation oncology.," *Journal of applied clinical medical physics / American College of Medical Physics*, vol. 12, no. 4, p. 3590, 2011. doi:10.1120/jacmp.v12i4.3590.

[55] Medgadget, "Dynamic Edge Automatic Gating Technology from Calypso Preserves Organs from Radiation Exposure." http://www.medgadget.com/2010/10/dynamic_edge_automatic_gating_technology_from_calypso_preserves_organs_from_radiation_exposure.html, 2010.

Appendix A

Mattress design: dimensions of all components

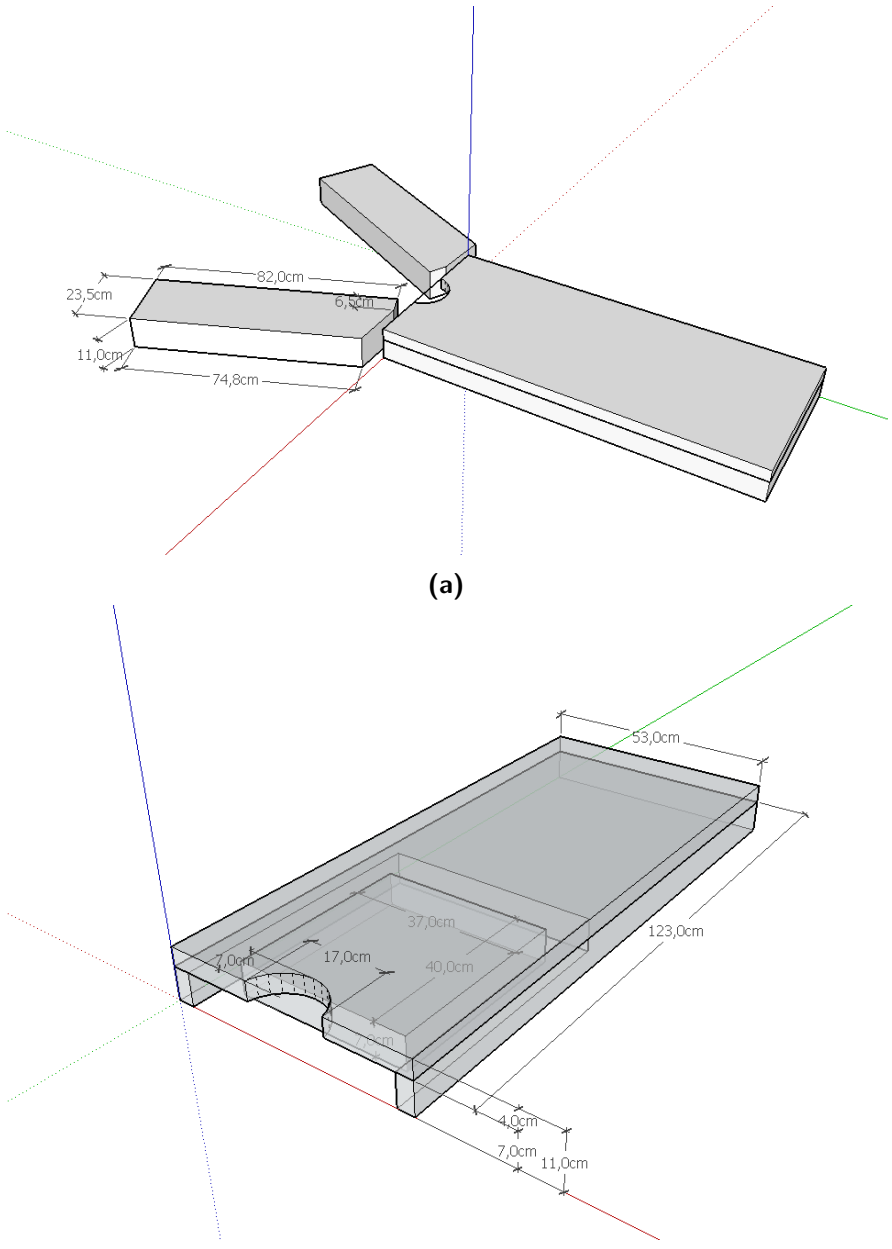

Figure A-1: Mattress design: dimensions of all components from different views.

Appendix B

The chain test to validate the workflow of the navigation procedure

Table B-1: The chain test to validate the workflow of the navigation procedure, part 1.

Test ID:	**SurgNav003**	Created by:	**N. Versteeg + J. Nijkamp**
Version:	**V1.0**	Date:	**2016-05-27**
Purpose:	**Chain test from imaging to navigation**		

PRECONDITIONS:

Hardware: NDI Aurora Navigation system
Wired reference sensors
Wired tumour sensor
Navigation PC (64 bits windows)
Software: SurgNav.exe
Plusserver.exe
Worldmatch.exe (or something similar)
Tools: Crate with a wax phantom inside

Preceding actions: SurgNav001, SurgNav002
Options required to be installed/selected: none

TEST REQUIREMENTS:

All the actual results should be according to the expected results.

Any occurring problem during the test steps should be described.

TEST SPECIFICATION:

This chain test has the purpose to validate the entire workflow of surgical navigation as a black box. The combination of software and hardware is validated in one go. To cover the entire chain, the test will start at acquiring a CT scan, providing RTSTRUCTS in DICOM format, loading the data into SurgNav.exe and end at assessing the navigation accuracy.

Table B-2: The chain test to validate the workflow of the navigation procedure, part 2.

TEST DESCRIPTION: Test steps: 1. Acquire an axial CT scan of the crate with the phantom inside and reconstruct at a slice thickness of less than 2 mm. Make sure the entire crate is visible. 2. Store the CT data in the DICOM server (Carestream PACS). 3. Load the CT data into Worldmatch (or something similar), automatically segment the BONES, and manually segment at least one tumour in the phantom. Store the RTSTRUCT's in the DICOM server (Carestream PACS) 4. Position the phantom on the Aurora field generator that is embedded in the navigation matrass. 5. Connect the reference sensors on port 1-3, connect the tumour sensor on port 4 and connect a navigation pointer on port 5 and evaluate if the sensors are visible in the NDI-Track software. 6. Attach a tumour sensor to the phantom inside the crate. 7. Place the reference sensors on the outside of the crate. 8. Acquire one or two XperCT scans with the Philips Allura system, make sure that the reference sensors on the outside of the crate and the tumour sensor inside the crate are visible. 9. Load the CT data and RTSTRUCT's into SurgNav.exe 10. Visually validate the visualized RTSTRUCT's with respect to the CT scan (report visual findings) 11. Load the acquired XPerCT scans into SurgNav, and do a bone registration to the planning CT scan. If more than 1 scan is loaded, merge them. 12. Mark all the reference sensors in the XperCT scan. 13. Now register the XPerCT to the planning CT on the tumour. Use this registration to link the tumour sensor to the tumour segmentation. 14. Store the navigation settings in the database 15. Make connection with the navigation system using configuration Treat.xml (report connection established) 16. After connection is established, register the sensors (between actual position and scanned position) (report RMSE from the screen) 17. Use the pointer to visually validate navigation accuracy. Point at a visual landmark on the phantom. Point out a sensor. (result: store the navigation data for every location) 18. Move the tumour to a new location within the crate, and visually assess the navigations update (report your findings) 19. Now use the pointer again to localize the new tumour location (result: store the navigation data for every location
POSSIBLE TEST VARIANTS: **None**

Table B-3: The chain test to validate the workflow of the navigation procedure, part 3.

<table>
<tr><td colspan="2">EXPECTED RESULTS:

10. The RTSTRUCTS nicely fit the CT data
15. Connection established within 1 minute
16. RMSE should be within 0.8 cm
17. Each pointed position should visually be within 3 mm of the expected position
18. The tumour position on the navigation screen is updated according to the actual situation
19. Each pointed position should visually be within 3 mm of the expected position</td></tr>
<tr><td colspan="2">ACTUAL RESULTS:

Write your results here. As expected is not enough, specify the actual deviations.

10.

15.

16.

17.

18.

19.</td></tr>
<tr><td>PASS
/ FAIL</td><td>PROBLEM
REPORT(S)</td></tr>
<tr><td>HARDWARE
TESTED:

PC WS0021
NDI Aurora window field generator

Labled as NaviOne: ID0024519</td><td rowspan="2">SOFTWARE
TESTED:

[version numbers]
SurgNav.exe [V2.30]
PlusServer.exe [V1.00]</td></tr>
<tr><td>TESTED
BY:</td></tr>
<tr><td>TESTED
ON (DATE):</td><td>APPROVED
BY:</td></tr>
</table>

Appendix C

Detailed manual navigation software N16TRS

Before OR:

1. Open SurgNav
2. Select local server, load patient, load scans, load delineations *(see pre-procedural navigation manual for detailed information about making planning images)*

3. Scans in de viewer are the P (primary) and S(secondary) scan selected in small window right.

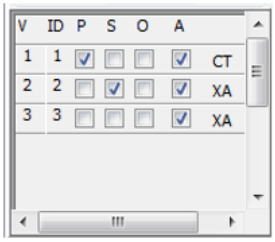

4. Match scans
5. Show delineations, render only
6. Save start_OK

In the OR:

1. Load start_OK
2. Start server and start tracking
3. Make CBCT
4. After CBCT save positions of the markers
5. Stop tracking

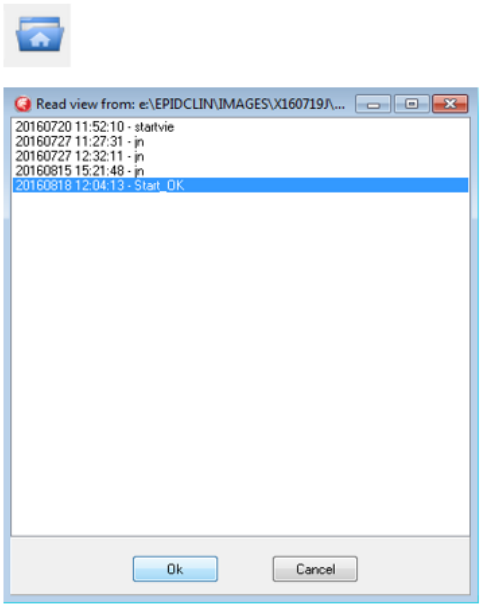

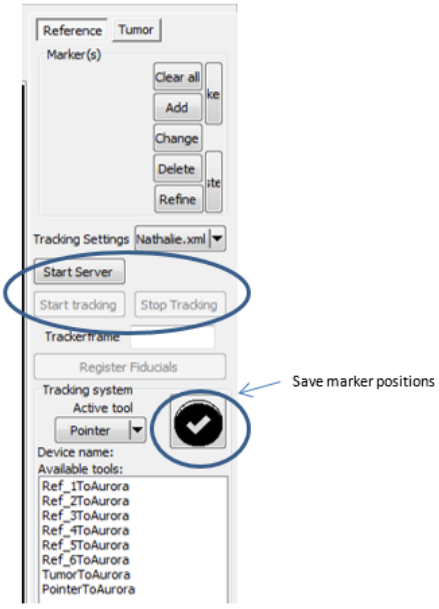

Match CBCT scan to planning CT

6. Go to matching tab
7. Add CBCT scans one by one and match to bones

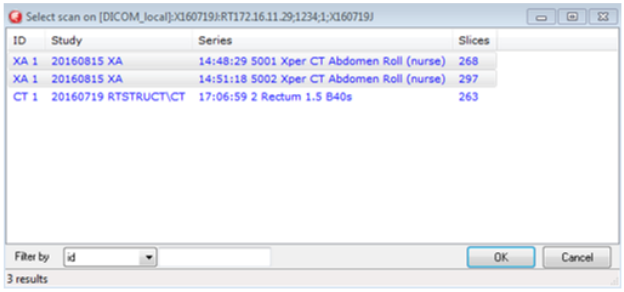

a. Set planning CT as primary and CBCT as secondary
b. Display mode = GreenPurple.
c. Pre-match, tick manual matching and match scans manually as good as possible, than untick manual matching.

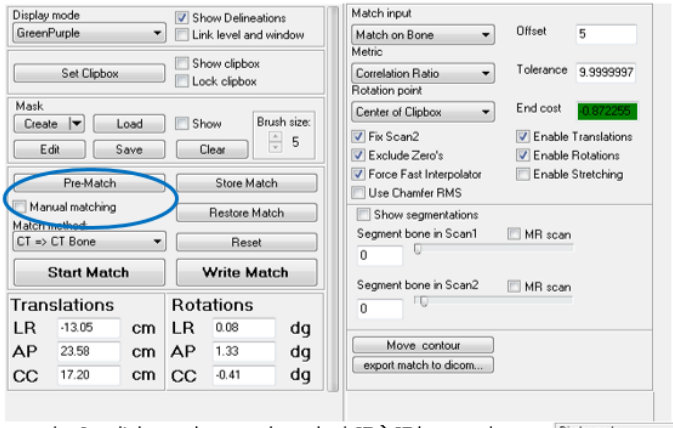

d. Set clipbox, select match method CT→CT bone and start match
e. Store match
f. If there is a second CBCT set planning CT as primary and second CBCT as secondary
g. Restore-match, tick manual matching and match scans manually as good as possible, than untick manual matching.
h. Start match
i. Merge CBCT scans → Set CBCT 1 as primary and CBCT 2 as secondary
j. Merged scans are saved under CBCT 1
k. Store match

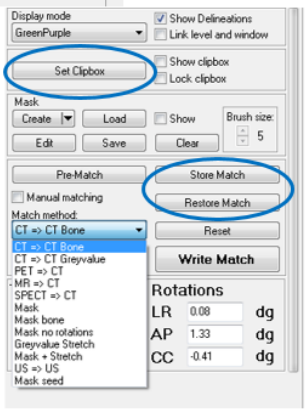

Match CBCT scan to planning CT

6. Go to matching tab
7. Add CBCT scans one by one and match to bones

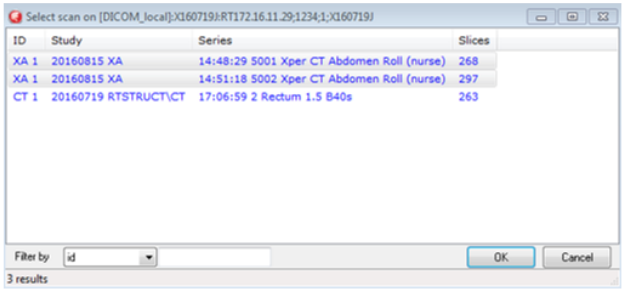

a. Set planning CT as primary and CBCT as secondary
b. Display mode = GreenPurple.
c. Pre-match, tick manual matching and match scans manually as good as possible, than untick manual matching.

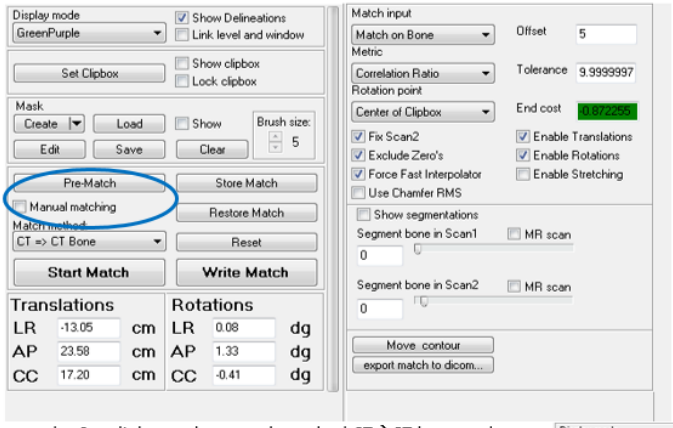

d. Set clipbox, select match method CT→CT bone and start match
e. Store match
f. If there is a second CBCT set planning CT as primary and second CBCT as secondary
g. Restore-match, tick manual matching and match scans manually as good as possible, than untick manual matching.
h. Start match
i. Merge CBCT scans → Set CBCT 1 as primary and CBCT 2 as secondary
j. Merged scans are saved under CBCT 1
k. Store match

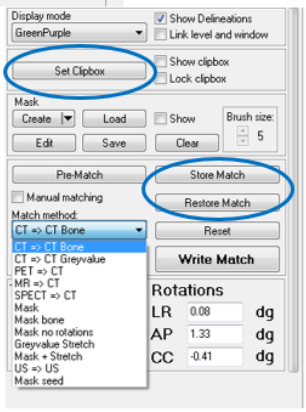

Appendix D

Test setting measurements: Results of accuracy measurements in x- and y-directions

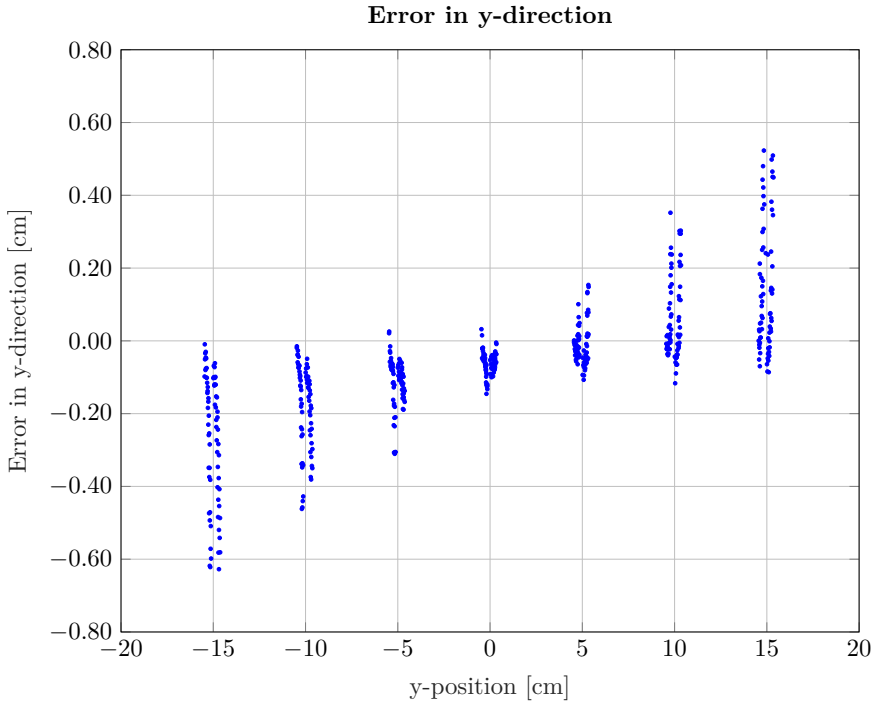

Figure D-1: Test setting measurements: results of accuracy measurements in y-directions.

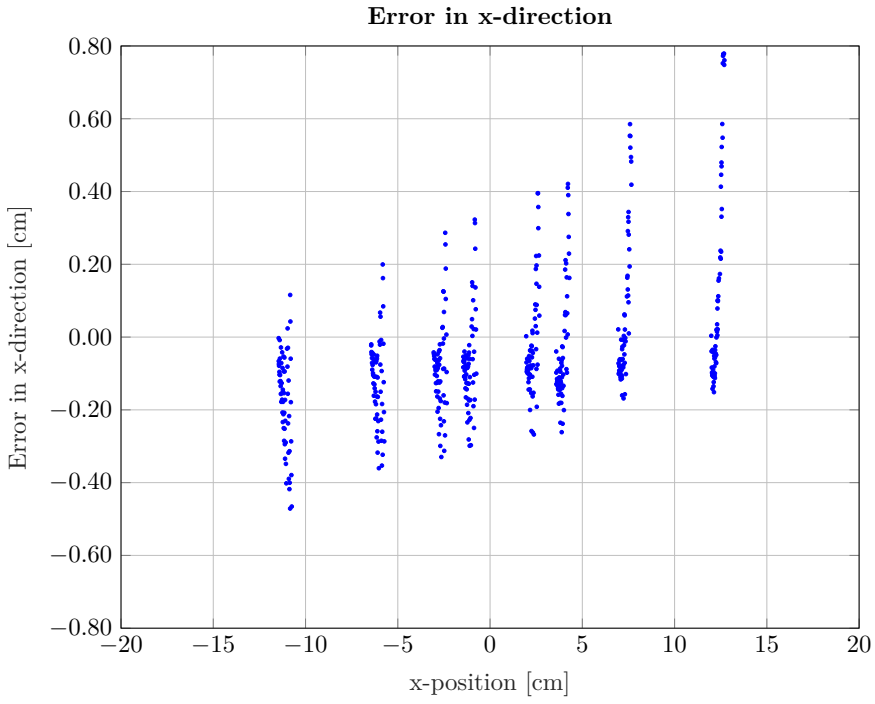

Figure D-2: Test setting measurements: results of accuracy measurements in x-directions.

Appendix E

Measurements operating room (OR) setting: distance measurements between sensors 1 and 2, and 1 and 3

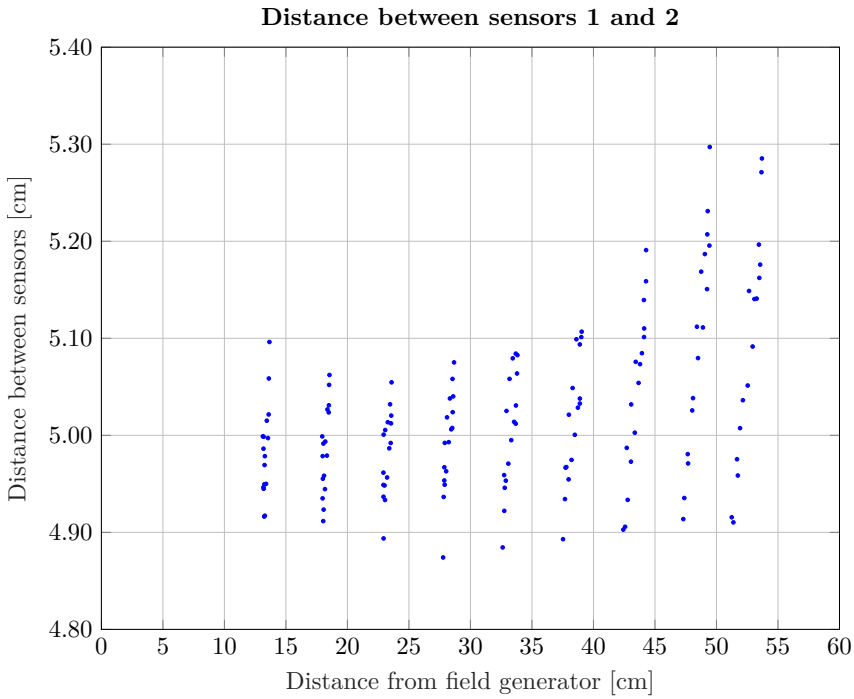

Figure E-1: Measurements OR setting: distance measurements between sensors 1 and 2.

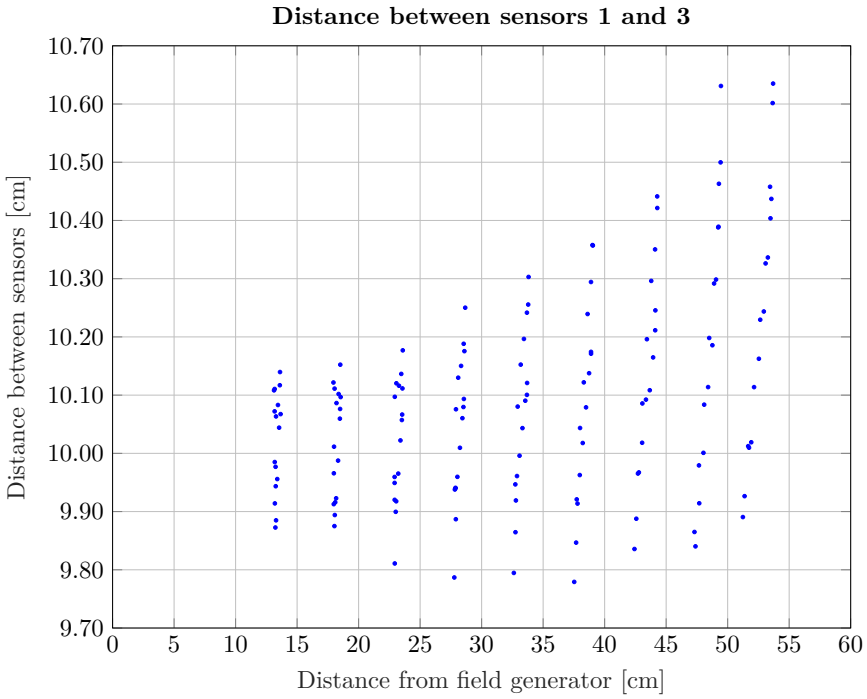

Figure E-2: Measurements OR setting: distance measurements between sensors 1 and 3.

Appendix F

3D model of patients 1 - 3 respectively

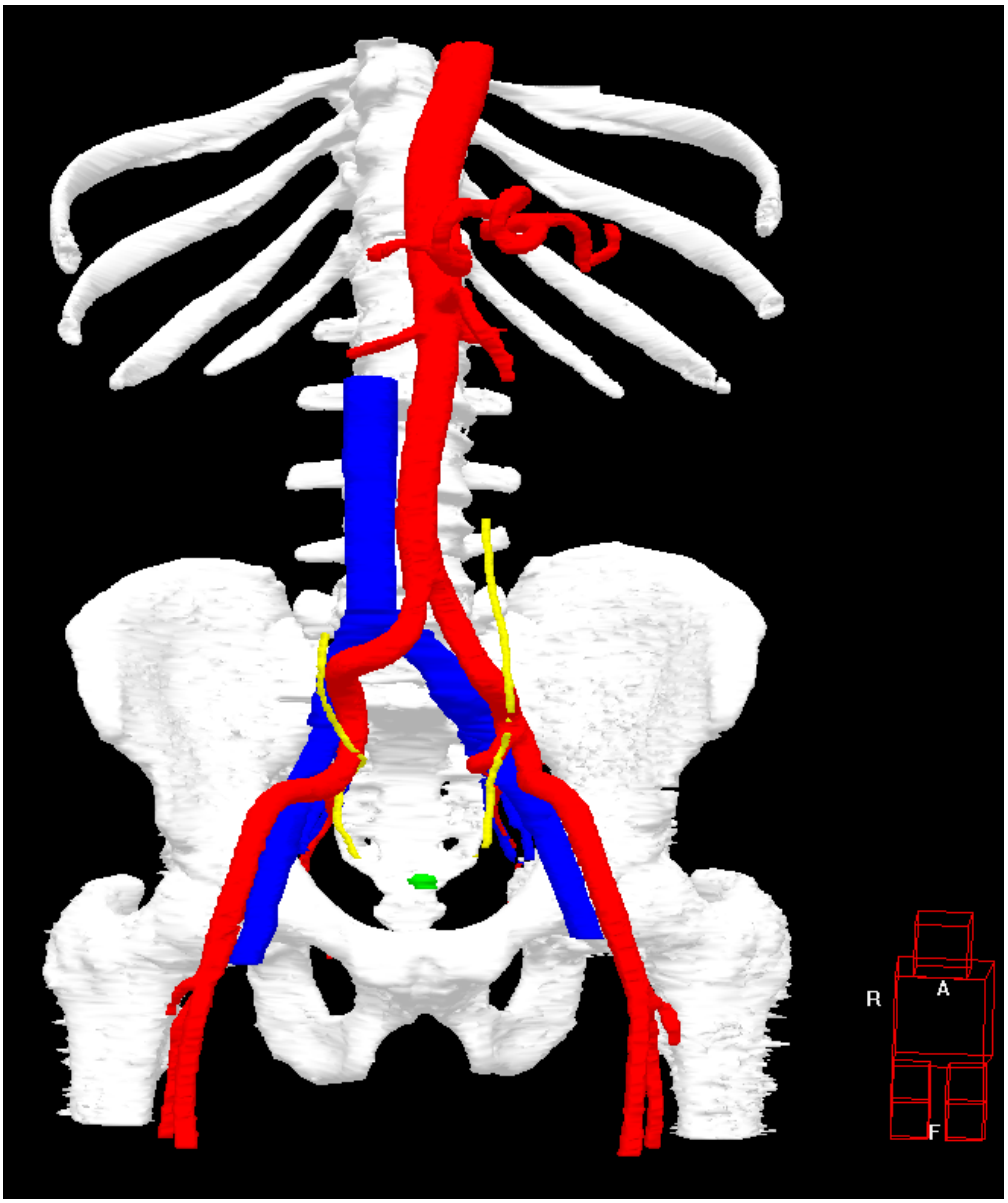

Figure F-1: 3D model of patient 1.

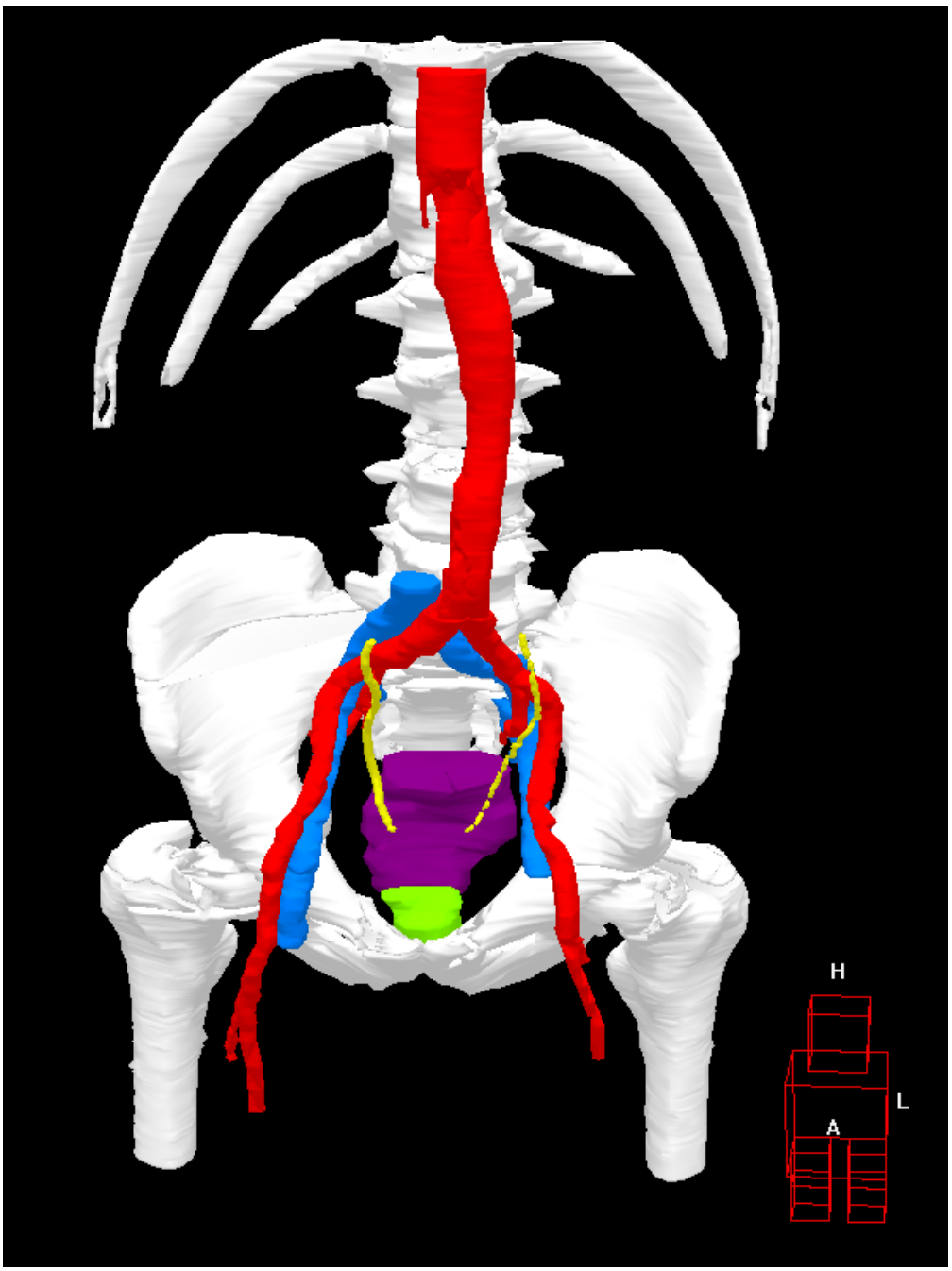

Figure F-2: 3D model of patient 2.

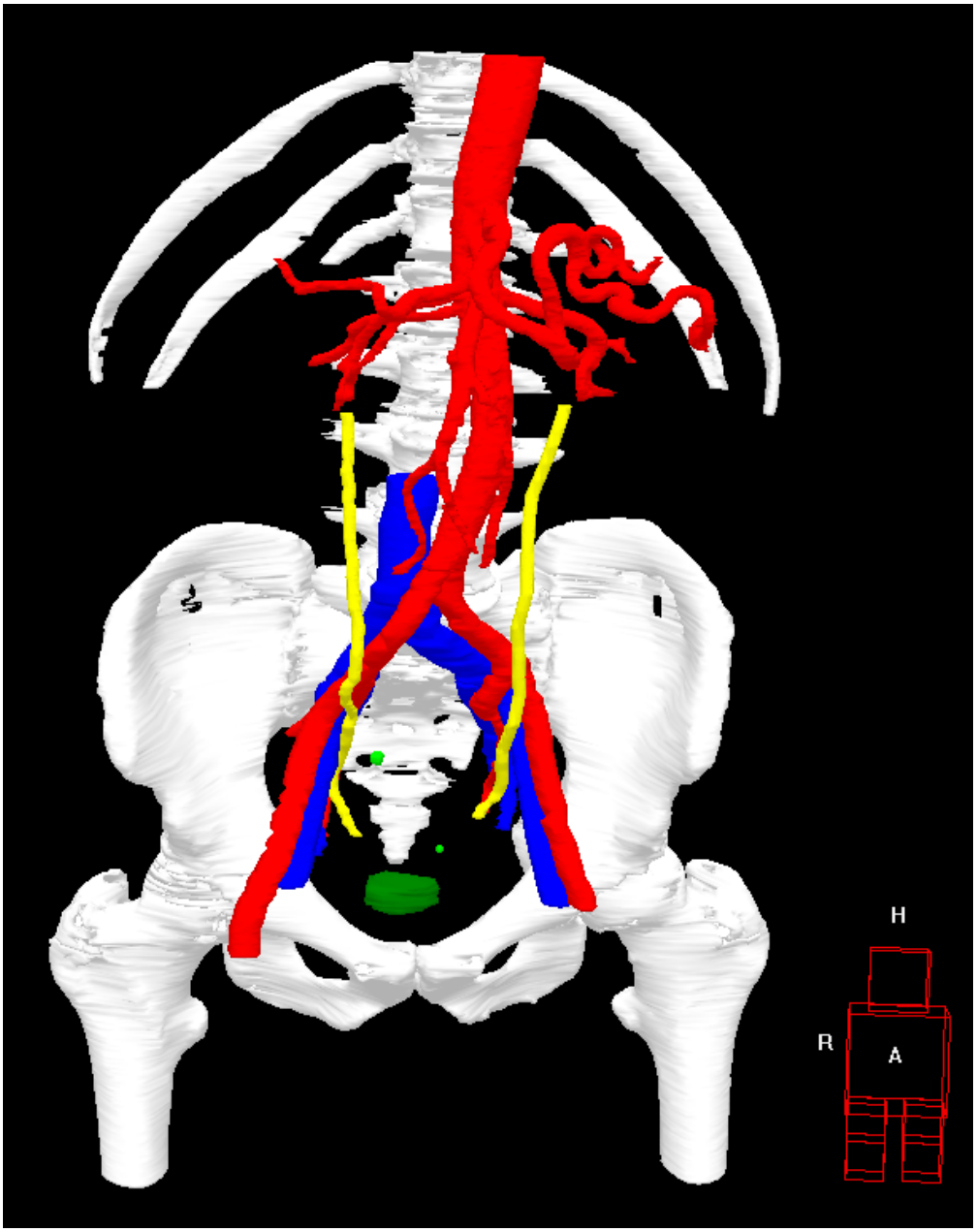

Figure F-3: 3D model of patient 3.

Appendix G

Table with values of common area, encompass and DICE for patients 1 and 2 for all observers

Table G-1: The common area, encompass and the resulting overlap (common divided by encompass) for patients 1 and 2 for all observers.

		Patient 1			**Patient 2**		
		Observer 2	**Observer 3**	**Observer 4**	**Observer 2**	**Observer 3**	**Observer 4**
Common	Observer 1	0.00	0.00	0.00	2.52	3.97	1.62
	Observer 2		0.45	0.30		2.89	3.28
	Observer 3			0.34			1.92
Encompass	Observer 1	0.00	0.00	0.00	8.10	6.30	8.55
	Observer 2		0.75	0.90		7.69	7.35
	Observer 3			0.85			8.22
DICE	Observer 1	0.00	0.00	0.00	0.31	0.63	0.19
	Observer 2		0.60	0.33		0.38	0.45
	Observer 3			0.40			0.23

Appendix H

Rendering of the tumour match between the different observers for patients 1 and 2

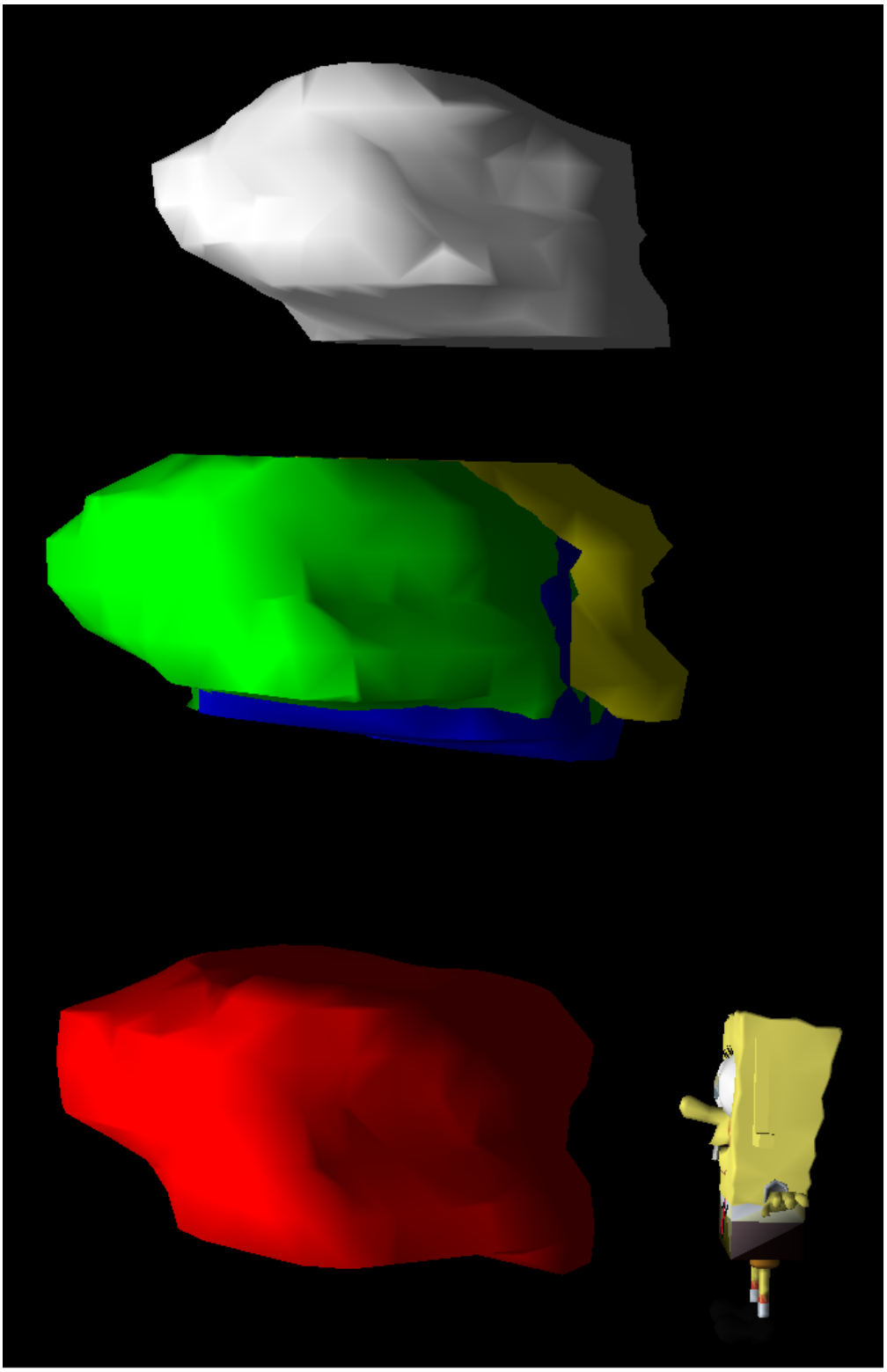

Figure H-1: Rendering of the displacements in tumour matching between the different observers for patient 1 in sagittal view. White is the original tumour location and the colours red, green, blue and yellow are the displacements of observers 1-4 respectively.

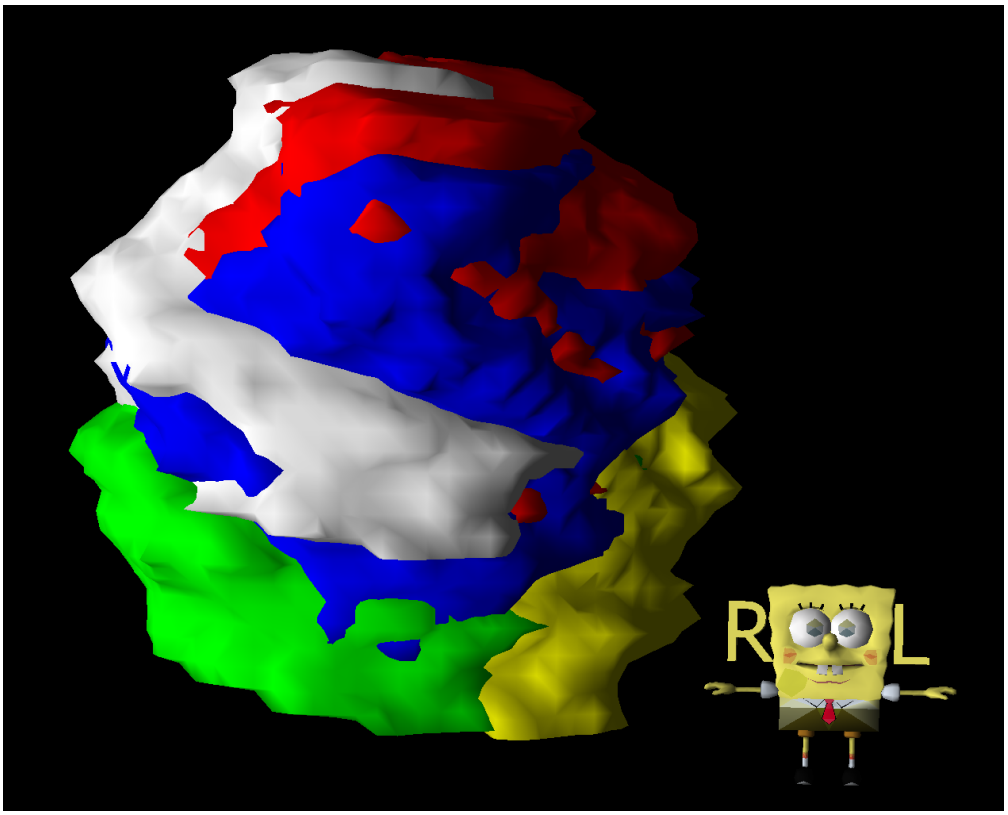

Figure H-2: Rendering of the displacements in tumour matching between the different observers for patient 2 in coronal view. White is the original tumour location and the colours red, green, blue and yellow are the displacements of observers 1-4 respectively.

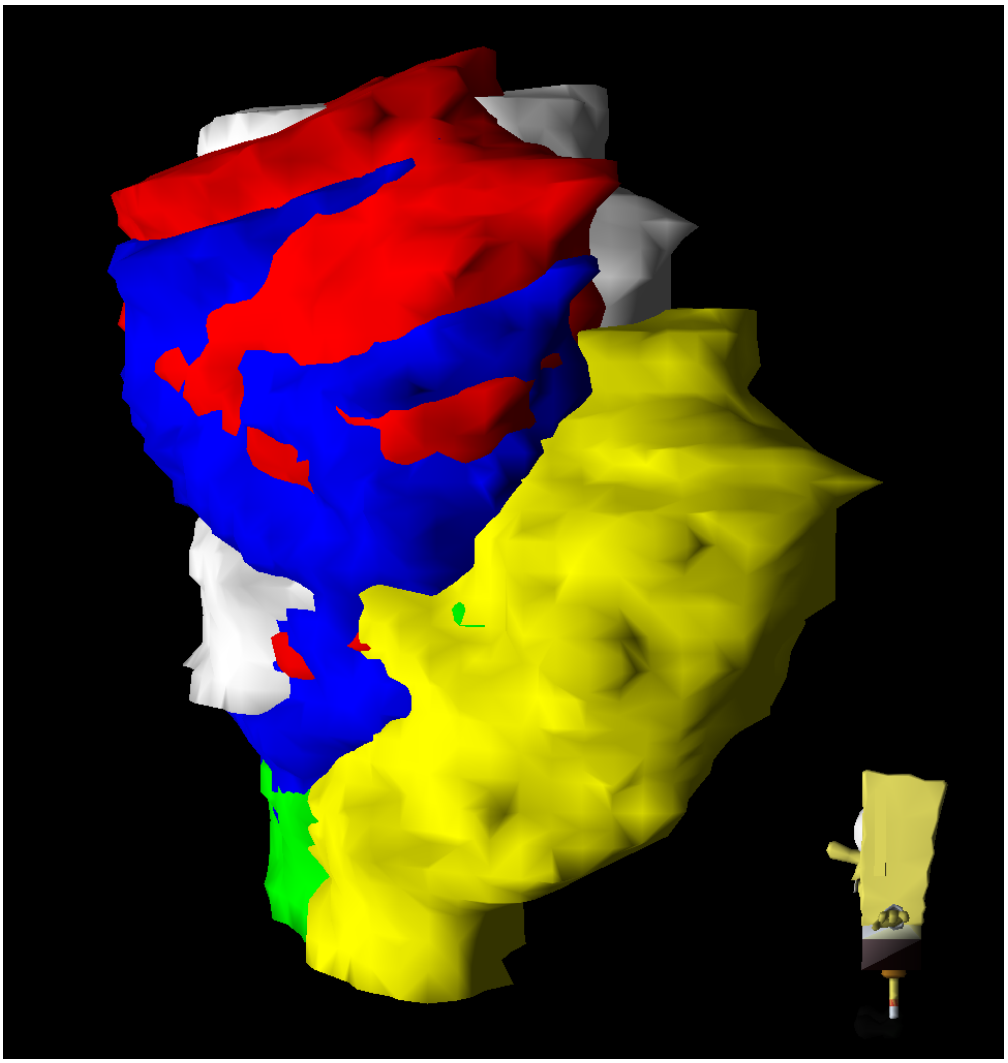

Figure H-3: Rendering of the displacements in tumour matching between the different observers for patient 2 in sagittal view. White is the original tumour location and the colours red, green, blue and yellow are the displacements of observers 1-4 respectively.

Glossary

List of Acronyms

AC	alternating current
APR	abdominoperineal resection
CBCT	cone-beam CT
CRC	Colorectal carcinoma
CRM	circumferential resection margin
CT	computed tomography
DC	direct current
DICE	Dice similarity coefficient
DICOM	Digital Imaging and Communications in Medicine
DLL	dynamic link libraries
DOF	degrees of freedom
EM	Electromagnetic
EMTS	Electromagnetic tracking system
FDA	Food and Drug Administration
FOBT	faecal occult blood test
IARC	International Agency for Research on Cancer
LAR	low anterior resection
MEC	Medical Ethics Committee
MRI	magnetic resonance image

N13NAV	Navigation 1 study
NDI	Northern Digital Inc.
NKI-AvL	Netherlands Cancer Institute
OR	operating room
PACS	Picture Archiving and Communication System
RMSE	root-mean-square error
SD	standard deviation
SIU	sensor interface unit
SCU	system control unit
TME	total mesorectal excision
TTFG	table top field generator
WFG	window field generator